# Symmetry and Localized Control of Extended Chaotic Systems

Thesis by
Roman O. Grigoriev

In Partial Fulfillment of the Requirements
for the Degree of
Doctor of Philosophy


Caltech
Pasadena, California

1999
(Defended July 14, 1998)

# Acknowledgements

This thesis would not have been written without help and mentorship of my advisor, Professor Michael Cross, whose broad knowledge and scientific intuition were my guiding light during the years I spent at Caltech. I am indebted to Dr. Heinz Schuster who introduced me to the exciting subject of chaos control for all the help and moral support. I am grateful to Professor Noel Corngold for many enlightening and stimulating discussions. I am also grateful to Professor John Doyle who always managed to provide me with an alternative point of view on every topic we touched.

Financial support for the research that lead to this thesis has been partially provided by the National Science Foundation through grant No. DMR-9013984.

# Abstract

The present study is prompted by the failure of conventional chaos control theory to provide a practically sound algorithm for controlling the chaos in general spatially extended experimental systems. The primary reason for this failure is the presence of symmetry, which is a feature of most extended dynamical systems and which violates a number of assumptions of genericity made by conventional control theory. These assumptions can be relaxed, but at a price that increases with increasing symmetry of the target state. This price includes the larger number of independent control parameters that must be adjusted to steer the system towards the target trajectory, as well as the larger number of independent observables required to reconstruct the dynamics of an experimental system with symmetries.

We show that spatially extended chaotic systems can be controlled by monitoring and perturbing them at multiple spatial locations, or pinning sites, with separations determined by the noise in the system. We show that the arrangement of pinning sites must comply with constraints determined by the symmetry of the system in order to achieve control. We determine how the system can be forced from the spatiotemporally chaotic state into the controllable target state. Finally, we determine the maximal distance between pinning sites and the maximal level of noise tolerated by a given arrangement of pinning sites for a model extended system.

# Contents

# List of Figures

# Chapter 1 Introduction

## 1.1 Motivation

The desire to improve performance of many practically important systems and devices often calls for shifting their operating range into a highly nonlinear area, which after a series of bifurcations usually leads to irregular chaotic behavior. This kind of behavior, however, is rarely desired, while substantial benefits could be obtained by making the dynamics regular. This goal can typically be achieved by applying small preprogrammed perturbations to steer the system towards a periodic orbit with desired properties, which is broadly referred to as chaos control.

The most difficult type of chaos to control, the spatiotemporal chaos is ubiquitous in spatially extended nonlinear systems and manifests itself in phenomena such as turbulence [1], plasma [2] and combustion [3] instabilities, cardiac arrhythmia [4], and brain epilepsy [5]. The majority of spatiotemporally chaotic systems are continuous and are properly described by partial differential equations, but some are spatially discrete and as such admit a description in terms of coupled ordinary differential equations (or sometimes delay differential equations). Nevertheless, all these systems share enough common features, especially in their spatial structure, to be treated in a unifying framework.

The list of practically important systems and devices displaying spatiotemporal chaos which could benefit from application of control is rather long, so we mention just a few characteristic examples. For instance, stabilization permits the operation of chemical reactors [6] beyond the normal limit of their stability, which may be desirable for increased thermodynamic efficiency, product yield, or product purity. Wide aperture semiconductor lasers [7] display uncontrolled random beam steering and loss of spatial coherence at high pumping levels needed to achieve desired output. Neural networks [8] require control in order to be placed in an adequate (intrinsically unstable) state for information processing. Finally, power grids are unstable to certain

types of electrical instabilities, which in the absence of control could lead to power surges, overload and failure of constituent components.

Unfortunately, despite all the success achieved in recent years in controlling relatively simple low-dimensional chaotic systems, most high-dimensional systems (with tens or more effective degrees of freedom), those just mentioned included, remain notoriously difficult to control and little progress has been made so far in the implementation of existing control techniques. In fact, discounting stirred chemical reactors, whose evolution has no spatial dependence [6; 9], there have been no reports of successful control achieved in experimental spatially extended chaotic systems up to date. This situation is not very surprising given the absence of a general theory for control of spatiotemporal chaos.

Spatially extended homogeneous systems can, in principle, be treated as a special case of high-dimensional chaotic systems [10; 11; 12]. However, some of the practical issues that arise in the control problem are quite specific and are probably best handled by taking into account the spatiotemporal structure of the system and the target state in general, and their symmetry properties in particular [13]. More important from the theoretical point of view, the spatiotemporal structure with common characteristic features possessed by various extended systems provides the natural context for analysis and reevaluation of the existing techniques and results.

Although spatially extended chaotic systems are the primary focus of our attention, arbitrary symmetric systems are, arguably, as interesting and important. Hence, by making our analysis as general as possible, we can hope to obtain many results whose range of applicability far exceeds the class of systems that motivated the present study. Therefore, our goal can be summarized as an attempt to correct some of the shortcomings of the existing theory and make the first step towards developing a general, thorough and consistent control formalism applicable to symmetric chaotic systems, in general, and spatially extended chaotic systems, in particular. Such formalism requires collection, systematization and development of the fragmentary results and methods of data analysis, deterministic chaos, linear systems and control, and group theory.

## 1.2 Outline

The outline of the thesis is as follows. In chapter 2 we begin with an overview of the theoretical advances in the area of controlling spatiotemporal chaos. We review and compare the techniques proposed by various authors to suppress chaos and target unstable steady and periodic states with desired properties in systems described by partial differential equations, coupled ordinary differential equations and coupled map lattices. We also formulate a number of defining questions to be answered by the rest of this study.

In chapter 3 we proceed with an overview of the data analysis techniques used to reconstruct the spatiotemporal dynamics of an experimental system displaying chaotic behavior using a time series measurement of an output signal. We review the major results concerning the continuous-time reconstruction of the global system dynamics and discrete-time reduction using the Poincaré section technique. We then turn to the question of local reconstruction and identification of recurring points and propose a generalized algorithm applicable to periodic orbits of arbitrary periodicity. Finally, we give a brief overview of noise reduction techniques proposed in the literature.

In chapter 4 we provide an expanded discussion of the results concerning the effects of symmetry on the dynamics and control previously reported in [13]. We discuss why the conventional control approach fails when applied to symmetric systems and show how it should be modified in order to achieve control. In particular, we show that when nontrivial symmetries are present one has to use multi-parameter control as opposed to the single-parameter control used in the conventional approach. We compare the results obtained for continuous- and discrete-time systems and study the effects of weak symmetry violation. In the conclusion of the chapter we show that the problem of phase space reconstruction is affected by symmetries in a manner similar to the control problem. We discuss how the data collection and analysis have to be modified to permit the reconstruction of symmetric chaotic attractors preserving their symmetries.

In chapter 5 we turn to the problem of feedback control. We review and compare the most widely used feedback control techniques developed on the foundations of

nonlinear dynamics and control theory. We analyze two single-parameter generalizations of the OGY control method and show how they can be extended for the multi-parameter case. We also show that these methods, being derived in the assumption of deterministic dynamics, become severely handicapped when applied to a certain class of stochastic systems. This has profound effect on the problem of control of extended chaotic systems, which is the primary focus of our attention. We also review two general stochastic control methods which provide a systematic treatment of the problem of feedback control as well as dynamic state reconstruction in the presence of external noise and measurement errors.

In chapter 6 we apply the results of the preceding chapters to the problem of controlling extended spatiotemporally chaotic systems. Following the previous study [14], we introduce a stochastic generalization of the one-dimensional coupled map lattice as our model, and argue that it is generic in the class of general extended systems. We show that our model cannot be controlled by perturbing the global system parameters and, therefore, calls for localized control. We analyze the method of pinning control introduced by Hu and Qu [15] and show how it can be modified to achieve greater flexibility, at the same time drastically reducing the density of pinning sites. This brings us to the method of control using adjustable boundary conditions, which proves to be extremely versatile and effective, allowing control of arbitrary target states in a variety of conditions. Our results are illustrated with a number of numerical experiments. We also discuss how the methods of pinning control and control at the boundaries can be combined to obtain a scalable distributed control approach applicable to systems of arbitrary size. In the conclusion we show how the combination of the nonlinearity and stochasticity in our model leads to the blowup of noise and loss of control and derive theoretical estimates on the size of the system at which this happens.

Finally, we summarize our results in chapter 7 and discuss their implications for the problem of controlling continuous (in space as well as time) extended chaotic dynamical systems in an arbitrary number of dimensions.

# Chapter 2 Overview

## 2.1 Selective Targeting

In order to determine the missing components of a general theory for control of spatiotemporal chaos we proceed with the analysis of theoretical advances in the area. We begin by considering the class of methods designed not just to suppress chaos, but more specifically, to target and stabilize a chosen unstable steady state or periodic trajectory with desired properties. Historically the first to address the issue of controlling spatiotemporal chaos, Hu and He [16] considered a one-dimensional periodically driven system described by a nonlinear drift-wave partial differential equation of the form

$$\frac{\partial \phi}{\partial t} + \alpha \frac{\partial^3 \phi}{\partial t \partial x^2} + \beta \frac{\partial \phi}{\partial x} + \mu \phi \frac{\partial \phi}{\partial x} + \gamma \phi = \epsilon \sin(x - \Omega t). \tag{2.1}$$

Upon transforming into the moving frame $z = x - \Omega t$, this partial differential equation becomes autonomous and (as any other similar autonomous PDE) can be converted into an equivalent system of ordinary differential equations expanding the solution $\phi(z,t)$ in the basis of normal modes $\psi_k(z)$ (which coincide with Fourier modes due to the translational symmetry of equation (2.1), so index $k$ is just a wave vector):

$$\phi(z,t) = \lim_{N \to \infty} \sum_{k=0}^{N} s_k(t) \psi_k(z). \tag{2.2}$$

Constructing an infinite-dimensional vector $\mathbf{s}(t) = [s_1(t), s_2(t), \cdots]^T$ from the coefficients $s_k(t)$, and defining the vector of parameters $\mathbf{u} = [\alpha, \beta, \mu, \gamma, \epsilon]^T$, one can write the system of ODEs in the form

$$\dot{\mathbf{s}}(t) = \mathbf{\Phi}(\mathbf{s}(t), \mathbf{u}), \tag{2.3}$$

where $\mathbf{\Phi}$ is some nonlinear function of coefficients $s_k(t)$ and parameters of the system.

Hu and He suggested two ways to stabilize a prescribed unstable periodic solution $\bar{\phi}(x,t) = \bar{\phi}(x - \Omega t)$ of (2.1). One can perturb an appropriately chosen normal mode $\psi_i(z)$ by adding a damping term $\Psi_i(t) = -\lambda s_i(t)$ to the $i$th component of equation (2.3), which can be interpreted as localized control in the Fourier space. Alternatively, one can apply localized damping at a single point of the real space, adding a term such as $\Psi_i(x,t) = -\lambda\delta(x - x_0)[\phi(x,t) - \bar{\phi}(x - \Omega t)]$ to the right-hand side of equation (2.1). The first type of feedback is somewhat more difficult to implement experimentally than the second one, because the system has to be perturbed at every point of the real space, but it can, in principle, be implemented for the majority of spatially extended systems. In addition, the first type of feedback requires the knowledge of the dynamical equations, while the second one does not.

As a result of a series of numerical experiments, it was determined that, when the first type of feedback was used, for some choices of the mode number $i$, the values of damping $\lambda$ and system parameters $\mathbf{u}$ the stabilization of the target state $\bar{\phi}(x - \Omega t)$ succeeded; for other choices it failed. Instead, the stabilization of a variety of other periodic and quaziperiodic states was achieved, which can be traced to the poor selectivity of this type of feedback. When the second type of feedback was used, however, the target solution was stabilized more effectively, especially for large damping $\lambda$.

We will make two comments regarding this control technique. First of all, although the number of degrees of freedom is infinite, due to small size ($x \in [0, 2\pi]$) the system is only *weakly chaotic* (the number of excited normal modes was estimated to be of order $N = 13$) and, therefore, is rather *highly correlated* spatially. Second, although the nondriven system is highly symmetric, the target state $\bar{\phi}(x - \Omega t)$ has a rather *low* symmetry. It can be shown that both of these factors contribute to the success of this technique (and are prerequisites of almost every other existing technique for control of spatiotemporal chaos).

Another version of control in Fourier space (applicable to systems described by PDEs as well as coupled ODEs) was proposed by Lourenco and Babloyantz [8]. They suggested using the Poincaré surface of section to reduce a continuous-time evolution

equation of the type (2.3) to a discrete-time map of the type

$$\mathbf{s}^{n+1} = \mathbf{F}(\mathbf{s}^n, u), \tag{2.4}$$

where $\mathbf{s}^n$ represents the value of the vector $\mathbf{s}(t)$ at the $n$th crossing of the surface and $u$ is a scalar system parameter. Assuming that only a small number of modes are excited near the target state (the system is again weakly chaotic), the effective dimensionality of the map (2.4) can be made finite (and small), thus reducing the problem to the standard form used in conventional chaos control theory [10; 17]. The effectiveness of this approach was demonstrated numerically by stabilizing a number of unstable periodic orbits of the small one-dimensional array of coupled delay differential equations with different (but supposedly low) spatiotemporal symmetries. This method differs from the one proposed in [16] in that the perturbation of the system parameter $u$ is used instead of direct perturbation of the state of the system, which can also be relatively easily achieved experimentally. In either case, however, a *single* control parameter is used.

Petrov *et al.* used the Poincaré surface of section technique to derive a control law without using the dynamical equations. In a series of paper [3; 18] the authors considered the spatially extended combustion model described by a Kuramoto-Sivashinsky equation

$$\frac{\partial \phi}{\partial t} = \left(\frac{\partial \phi}{\partial x}\right)^2 - \frac{\partial^2 \phi}{\partial x^2} - \frac{\partial^4 \phi}{\partial x^4}, \tag{2.5}$$

where the variable $\phi(x,t)$ represents the planar front of a premixed flame. However, instead of a map of the type (2.4) describing the evolution of the system between successive crossings of the Poincaré section in the Fourier space, a similar map in real space was constructed using the measurement of a scalar function $\xi(t)$ of the state $\phi(x,t)$ of the system in the vicinity of the targeted orbit $\bar{\phi}(x,t)$. There is a single parameter in the model, the length $l$. The system was considered for the values of $l$ where the dynamics are weakly chaotic, i.e., only a few normal modes are excited and, as consequence, the constructed map is effectively low-dimensional, so that the system could again be treated using the tools of conventional chaos control theory. It was demonstrated numerically that control can be achieved by perturbing one of the

boundary conditions. A very similar approach was used by Tziperman *et al.* [19] in order to control spatiotemporal chaos in a model used for weather prediction.

As an alternative to the above approach Petrov *et al.* suggested using the method of transfer functions borrowed from control theory [20]. This method combines the two steps of the control problem, construction of the Poincaré map and calculation of feedback into a single step, which simplifies the analysis of the data obtained from an experimental system to a certain degree. This method was used to stabilize steady and periodic unstable flame profiles of the model (2.5) [18] as well as unstable Turing patterns in a reaction-diffusion system described by the Gray-Scott model [21]. In both cases the symmetry of the targeted states was relatively low and the systems where rather highly correlated spatially.

## 2.2 Suppression of Chaos

In addition to the three control techniques already described, a number of other, much less sophisticated, techniques based on incorporating preset time delays in the feedback law have been proposed. Despite being conceptually simple, techniques of this type, as a rule, provide very poor selectivity and thus should be regarded as methods to suppress spatiotemporal chaos in favor of some sort of periodic behavior, rather than methods to stabilize a chosen unstable periodic trajectory. One of the simplest such methods was suggested by Battogtokh *et al.* [22], who considered the complex Ginzburg-Landau equation

$$\frac{\partial \phi}{\partial t} = (1 - i\omega)\phi + (1 + i\alpha)\frac{\partial^2 \phi}{\partial x^2} - (1 - i\beta)|\phi|^2\phi, \tag{2.6}$$

describing a large class of (very weakly chaotic, again!) systems undergoing a bifurcation from regular oscillations to spatiotemporal chaos. One can use a time delayed *global* feedback proportional to the spatial average of the field $\phi(x,t)$, which corresponds to adding to the right-hand side of equation (2.6) a term

$$\Psi(x,t) = -\lambda e^{i\chi}\langle\phi(x,t-T)\rangle_x, \tag{2.7}$$

where $T$ is the time delay. Parameters $\lambda$ and $\chi$ are the magnitude and phase of the feedback, which depending on the phase can act as either damping or amplification of the spatially uniform mode $\psi_0(x) = const$. This type of feedback obviously favors uniform time-periodic states with period $T$, i.e., states with very high spatial symmetry. In the numerical experiments it was established that the uniform *steady* state was indeed stabilized for $\chi = 0$ (damping) and certain choices of the delay $T$, while choosing $\chi \neq 0$ resulted in the stabilization of oscillating cellular patterns. Similar type of feedback was used to suppress chaos in coupled ODEs [8], and coupled map lattices [23].

In order to facilitate the stabilization of nonuniform target states, one has to use a modification of the latter technique, which uses local values of the field $\phi(x,t)$ instead of its spatial average. This sort of generalization was used by Bleich and Socolar [24] for the stabilization of traveling wave solutions of the complex Ginzburg-Landau equation (2.6). Certain unstable periodic states can be stabilized by applying the signal constructed from the time-delayed state of the system as feedback at *every* point in space, which corresponds to adding to the right-hand side of equation (2.6) a term

$$\Psi(x,t) = \sum_{n=1}^{\infty} \lambda_n [\phi(x,t) - \phi(x,t-nT)], \tag{2.8}$$

where $T$ is the period of the targeted unstable state (e.g., traveling wave) and $\{\lambda_n\}$ is a sequence of damping coefficients (one should obviously have $\sum_n |\lambda_n| = \lambda < \infty$). This type of feedback is known as *extended time-delay auto synchronization*, and it has been successfully applied to a number of low-dimensional chaotic systems [25]. Similar types of feedback were suggested to control spatiotemporal chaos in systems described by coupled ODEs [8] and coupled map lattices [23]. Stabilization of a variety of unstable periodic orbits was demonstrated numerically.

Similarly to the case of delayed global feedback, this type of control does not require the knowledge of dynamical equations and has rather poor selectivity with respect to target states with desired properties. Since one can only adjust the time delay to match the period $T$ of the targeted state, the stabilization is a matter of luck rather than choice. Besides, the area of practical applicability of this approach

is *extremely* limited. Apart from optical systems, implementing this type of feedback in continuous systems borders on the impossible due to the fact that it uses a number of control parameters equal to the number of degrees of freedom, which is infinite. Even in application to spatially discrete systems the complexity of this method will likely prevent it from ever being used in practice.

The selectivity of the latter method can be improved by introducing spatial filtering of the field $\phi(x,t)$. The methods proposed by Lu *et al.* [26] and Bleich *et al.* [7] can be represented in the same general form by writing the feedback term as

$$\Psi(x,t) = \sum_{n=1}^{\infty} \lambda_n \left[ \phi(x,t) - \int K(x,x')\phi(x',t-nT)dx' \right], \tag{2.9}$$

where $K(x,x')$ is the kernel of the filtering operator, which is assumed to be chosen appropriately for each target state. The global and local delayed feedback discussed above clearly correspond to choosing $K(x,x') = const$ and $K(x,x') = \delta(x-x')$, respectively. This type of feedback is again effectively equivalent to using an infinite number of control parameters in continuous extended systems and thus is limited to applications for optical systems. Control of unstable traveling wave states was achieved in the numerical model of a single longitudinal mode laser [7]. A version of this technique for coupled ODEs [8] also exists.

## 2.3 Pinning Control

We have seen a number of times that successful control of spatiotemporal chaos by applying feedback at a single spatial location was achieved only in systems which possessed a high degree of spatial correlation. This, however, does not imply that weakly correlated systems require application of feedback at *every* point in space. A more economical and flexible approach is to monitor and perturb the system at multiple locations separated by the characteristic length which depends on the strength of noise and other system parameters. This approach was called *pinning control* [15], and spatial locations used for feedback were respectively termed *pinning sites* or *pinnings*.

A number of relatively successful attempts were made to employ pinning control for stabilizing unstable states in spatially discrete systems such as coupled ODEs [27] and coupled map lattices with symmetric coupling [15]

$$\phi_i^{t+1} = \epsilon f(\phi_{i-1}^t) + (1-2\epsilon) f(\phi_i^t) + \epsilon f(\phi_{i+1}^t). \tag{2.10}$$

The results can be summarized as follows. It was numerically demonstrated that a variety of unstable steady states and periodic trajectories could be successfully stabilized. This, however, required an extremely high density of pinnings, with the distance between adjacent pinnings no larger than four and three lattice spacings in the case of the coupled map lattice and coupled ODEs, respectively.

Significantly lower density of pinnings can be used in the case of coupled map lattice with broken symmetry

$$\phi_i^{t+1} = \epsilon_1 f(\phi_{i-1}^t) + (1-\epsilon_1-\epsilon_2) f(\phi_i^t) + \epsilon_2 f(\phi_{i+1}^t), \tag{2.11}$$

where $\epsilon_1 \neq \epsilon_2$. This surprising, at first sight, result has nothing to do with the spatial correlations in the system. On the contrary, as we will see below, it can be explained by the difference in symmetry properties of equations (2.10) and (2.11). Successful control of the steady uniform target state of the model (2.11) has been achieved [28] with the distance between pinnings of up to 14 sites, in the presence of noise of relative magnitude $\sigma = 10^{-10}$.

Bleich and Socolar [24] formulated three questions which should be answered by a consistent general theory of controlling spatiotemporal chaos: *What is the minimum density of discrete controllers* (actuators) *needed in situations where spatially continuous processing in the feedback loop is not possible* (i.e., almost always)*? What level of noise can be tolerated? How can one force the system from the spatiotemporally chaotic state into the desired controllable state?* Detailed examination of the problem reveals that one more question has to be added to the above list: *How should the spatial locations at which the system is monitored and perturbed be arranged?* This last question is prompted by the intrinsic symmetries characteristic of spatially extended systems.

Even though the importance of symmetries in chaotic dynamics has been recognized by a number of authors [29; 30; 31; 32], symmetric systems did not receive adequate treatment in the general framework of chaos control primarily because the question of symmetry is largely ignored by the theory of deterministic chaos as well as data analysis and control theory. All three disciplines regard symmetric systems as nongeneric and, therefore, not very interesting and important. However, many practically important dynamical systems, such as spatially extended chaotic ones, are intrinsically nongeneric, and thus cannot be successfully treated using the formalism developed for generic systems.

# Chapter 3 System Identification

## 3.1 Time Delay Embedding

The primary challenge one faces when presented with an objective to defeat the chaotic behavior in a real continuous-time experimental system is to determine the laws governing the dynamics or, in other words, construct a mathematical model of that system using the experimental data. For now, we will assume that the system under consideration is deterministic, and defer the treatment of stochastic systems until chapter 5. We will also assume that the evolution takes place on a finite-dimensional chaotic attractor $\mathcal{A}$ and the actual dynamical equations can be written in the form

$$\dot{\mathbf{s}}(t) = \mathbf{\Phi}(\mathbf{s}(t), \mathbf{u}, t), \tag{3.1}$$

where $\mathbf{s}(t) \in \mathcal{Q}$ is the $n_s$-dimensional state of the system, $\mathbf{u} \in \mathbb{R}^{n_u}$ is the $n_u$-dimensional vector of system parameters, and $\mathbf{\Phi}$ denotes an unknown vector field on the phase space manifold $\mathcal{Q}$. For generality we will assume that $n_s$ is arbitrary (or even infinite) and $n_u \geq 1$. Although the particular form (3.1) of the dynamical equations limits the generality of the proposed approach by excluding the systems described by differential algebraic equations, it directly bears on the validity of the following results, and thus is essential here.

We are primarily interested in the two special cases of the dynamical equation (3.1), which represent the two classes of systems most often encountered in practice, autonomous and periodically driven. First, consider an autonomous system for which $\partial_t \mathbf{\Phi}(\mathbf{s}(t), \mathbf{u}, t) = \mathbf{0}$ and, therefore,

$$\dot{\mathbf{s}}(t) = \mathbf{\Phi}(\mathbf{s}(t), \mathbf{u}). \tag{3.2}$$

The complete information about the state of an experimental system is rarely available, so one typically has to contend with having a measurement of a single scalar

output of the system (sometimes called an *observable*) for the description of the dynamics. The output is, in general, a function of the (unknown) internal state of the system $\mathbf{s}(t)$:

$$y(t) = G(\mathbf{s}(t)). \tag{3.3}$$

It turns out that it is possible to reconstruct both the internal state of the system *and* its dynamics based on the time series measurement of the output $y(t)$ using the procedure originally proposed by Packard *et al.* [33]. The easiest way to obtain several signals from a single one is to use time delays. Let us choose different delay times $T_1, T_2, \cdots, T_{n_z}$ and construct an $n_z$-dimensional delay coordinate vector

$$\mathbf{z}(t) = \begin{bmatrix} y(t+T_1) \\ y(t+T_2) \\ \vdots \\ y(t+T_{n_z}) \end{bmatrix}. \tag{3.4}$$

Takens showed [34] that for a scalar output (3.3) and conveniently chosen delay times $T_i$, if the dimension $n_z$ of the embedding space is such that $n_z \geq 2n_s^h + 1$, where $n_s^h$ is the Hausdorff dimension of the attractor $\mathcal{A}$, the map $\mathbf{P} : \mathbf{s}(t) \to \mathbf{z}(t)$ generically provides a global one-to-one representation of the attractor and, hence, the system state. As we will see below, the genericity assumption in the Takens' embedding theorem is not satisfied for most of the extended systems due to the symmetry-related degeneracy of the evolution operators. However, since the rest of the algorithm only depends on the existence of the global embedding $\mathbf{P}$, we proceed with the discussion assuming that the theorem holds and consider the modifications required for nongeneric systems in section 4.5.

Since the Hausdorff dimension of the chaotic attractor is often much smaller than the number of degrees of freedom, $n_s^h \ll n_s$, even for systems of high dimensionality an unambiguous representation of the system state can usually be obtained in an embedding space of rather low dimensionality. For instance, Roux *et al.* [35] have shown that the state of the Belousov-Zhabotinskii system, which is described by more than 30 independent variables, can be represented nicely in $\mathbb{R}^3$. Even more important, as long as $n_s^h < \infty$, the reconstruction technique can be successfully applied to infinite-

dimensional systems, such as those described by partial differential equations. Several authors, including Romeiras *et al.* [17], further suggested that, if only a local one-to-one representation of the state in the vicinity of some periodic trajectory is needed, $n_z = n_s^h$ is typically sufficient, decreasing the dimensionality of the embedding space even further.

The next step in the procedure allows one to recreate the dynamical equations. In principle, it is possible to extract the necessary information about the dynamics using the continuous-time measurement of the reconstructed state $\mathbf{z}(t)$. However, the trajectory generated by $\mathbf{z}(t)$ is usually very complicated and may be difficult to interpret. A small number of methods exist [36; 37], which allow one to recreate the system of ordinary differential equations of the form (3.2) using the reconstructed trajectory, but they are neither general nor precise enough for the control purposes. In the conclusion of this section we mention that in cases where the mathematical model of an infinite-dimensional extended system is available, the trajectory $\mathbf{z}(t)$ and the finite-dimensional representation of the dynamical equations can be obtained using the Galerkin method [38].

## 3.2 Discrete-Time Reduction

The problem of reconstructing the dynamical equations can be simplified substantially by using the Poincaré section technique [33], which reduces the continuous trajectory $\mathbf{z}(t)$ in the $n_z$-dimensional embedding space to a set of points in its $(n_z-1)$-dimensional subspace. Let us define the Poincaré surface of section by the equation $\phi(\mathbf{z}(t)) = 0$. The crossings of the surface by the trajectory of the system generate a sequence of times $t_0, t_1, t_2, \cdots$, which subsequently define a sequence of points $\mathbf{z}^k = \mathbf{z}(t_k)$ through the delay embedding. The choice of delay times $T_i$ is, in principle, arbitrary, but most often a sequence of delay times $T_i = (i-1)T_D$ is used, where $T_D < 0$ is a negative basic delay (see, for example, [12; 17]). This choice is not always convenient for the purpose of real-time data acquisition, since it requires an *a priori* knowledge of the reference times $t_k$. To correct the situation we take $T_D > 0$ instead. For instance, if one sets $\phi(\mathbf{z}(t)) = z_1(t) - c$, where $c$ is a constant, one can extract the components of the

vectors $\mathbf{z}^k$ from the measured signal $y(t)$ in real-time mode by testing the condition $y(t_k) = c$ to determine $t_k$ and then measure $z_i^k = y(t_k + (i-1)T_D)$ for $i = 2, \cdots, n_z$.

The reconstruction of periodically driven systems can be handled in a very similar manner. If we denote the period of the driving signal $T_F$, then we should have $\mathbf{\Phi}(\mathbf{s}(t), \mathbf{u}, t + T_F) = \mathbf{\Phi}(\mathbf{s}(t), \mathbf{u}, t)$. Since the driving defines a natural frequency in the system, one can use the stroboscopic technique to define a sequence of reference times $t_0, t_1, t_2, \cdots$ using the period of driving instead of the Poincaré section. Specifically, one takes $t_k = t_0 + kT_F$. A sequence of points $\mathbf{z}^k = \mathbf{z}(t_k)$ is then determined identically to the case of an autonomous system.

Since the dynamics is deterministic, if the system parameters are fixed, $\mathbf{u} = \bar{\mathbf{u}}$, then $\mathbf{z}^k$ determines $\mathbf{z}^{k+1}$, hence defining the first return map $\tilde{\mathbf{F}} : \mathbb{R}^{n_z} \times \mathbb{R}^{n_u} \to \mathbb{R}^{n_z}$

$$\mathbf{z}^{k+1} = \tilde{\mathbf{F}}(\mathbf{z}^k, \bar{\mathbf{u}}). \tag{3.5}$$

In the control problem system parameters are kept constant during the intervals $t \in [t_k, t_{k+1}]$, but they are changed discontinuously at the times $t_k$, so equation (3.5) has to be modified. In general, $\mathbf{z}^{k+1}$ would depend on $\mathbf{z}^k$ as well as the history of change in $\mathbf{u}(t)$ during the time interval $t \in [t_k, t_{k+1} + T_{n_z}]$. Assuming that the largest delay $T_{n_z}$ is chosen small enough, such that $t_{k+1} + T_{n_z} < t_{k+2}$ for every $k$, and denoting $\mathbf{u}^k$ the value of the parameter vector $\mathbf{u}(t)$ in the interval $t \in [t_{k+1}, t_{k+2}]$, one concludes that the state of the system at time $t_{k+1}$ depends on the values of parameters during two successive intervals:

$$\mathbf{z}^{k+1} = \tilde{\mathbf{F}}(\mathbf{z}^k, \mathbf{u}^k, \mathbf{u}^{k-1}), \tag{3.6}$$

which coincides with the equation obtained for negative basic delays [39].

Finally, let us introduce an expanded state-plus-parameter vector

$$\mathbf{x}^k = \begin{bmatrix} \mathbf{x}_s^k \\ \mathbf{x}_u^k \end{bmatrix} = \begin{bmatrix} \mathbf{z}^k \\ \mathbf{u}^{k-1} \end{bmatrix} \tag{3.7}$$

and define a new map $\mathbf{F} : \mathbb{R}^{n_x} \times \mathbb{R}^{n_u} \to \mathbb{R}^{n_x}$

$$\mathbf{F}(\mathbf{x}, \mathbf{u}) = \begin{bmatrix} \tilde{\mathbf{F}}(\mathbf{x}_s, \mathbf{u}, \mathbf{x}_u) \\ \mathbf{u} \end{bmatrix}, \tag{3.8}$$

where $n_x = n_z + n_u$. This allows equation (3.6) to be rewritten in a more conventional form

$$\mathbf{x}^{k+1} = \mathbf{F}(\mathbf{x}^k, \mathbf{u}^k). \tag{3.9}$$

It is important to realize that the maps (3.6) and (3.9) represent nothing but two completely equivalent descriptions of the same dynamics in two different spaces and either description can be used depending on the circumstances. We will predominantly use the map (3.9), since it has the form required by conventional control theory.

When the sequence of states $\mathbf{x}^k$ and the map (3.9) are reconstructed from the output $y(t)$ of the experimental system, it can be claimed that the dynamics of the system is essentially understood. However, even though in certain cases (such as the Belousov-Zhabotinskii system [35]) finding the nonlinear map $\mathbf{F}$ that fits the data well enough is relatively easy, this can rarely be achieved for typical high-dimensional systems. One, therefore, has to look for a more practical and economical way to describe the system.

## 3.3 Periodic Trajectories

Fortunately, the problem can be simplified even further by stripping the redundant information about the global structure of the chaotic attractor $\mathcal{A}$ contained in the dynamical equation (3.1). Indeed, the closure of the attractor, $\bar{\mathcal{A}}$, can be thought of as a union of an infinite number of unstable periodic orbits and thus the vector field $\mathbf{\Phi}$ contains the information about all these orbits. For the purpose of control just one such orbit $\bar{\mathbf{s}}(t)$ is selected as the target state. It turns out that one only needs to know the local properties of the equation (3.1) in the vicinity of the target state in order to drive the system towards it using the method of linear feedback control.

As a result of the equivalence between the full description of the system in terms of the differential equation (3.1) and its reduced description in terms of the map (3.6), continuous-time periodic trajectories are mapped to discrete-time periodic trajectories. Indeed, consider the projection $\mathbf{P} : \bar{\mathbf{s}}(t) \to \bar{\mathbf{z}}(t)$ of the target trajectory into the embedding space. As discussed above, the crossing of the Poincaré section by the reconstructed trajectory $\bar{\mathbf{z}}(t)$ generates a sequence of points $\bar{\mathbf{z}}^0, \bar{\mathbf{z}}^1, \cdots$. On the one

hand, if the target trajectory $\bar{\mathbf{s}}(t)$ is time-invariant, so is $\bar{\mathbf{z}}(t)$ and, therefore, $\bar{\mathbf{z}}^{k+1} = \bar{\mathbf{z}}^k$ for every $k$, which corresponds to a fixed point of the map (3.6). On the other hand, if $\bar{\mathbf{s}}(t)$ is time-periodic, $\bar{\mathbf{s}}(t+T) = \bar{\mathbf{s}}(t)$, then $\bar{\mathbf{z}}(t)$ is also time-periodic with the same period $T$. Obviously, if $\bar{\mathbf{z}}(t)$ crosses the Poincaré surface of section $\tau$ times during the first period $t \in [0, T]$, it will do so during each of the consecutive periods, thus generating the discrete-time trajectory $\bar{\mathbf{z}}^k$ with period $\tau$, $\bar{\mathbf{z}}^{k+\tau} = \bar{\mathbf{z}}^k$. Defining

$$\bar{\mathbf{x}}^k = \begin{bmatrix} \bar{\mathbf{z}}^k \\ \\ \bar{\mathbf{u}} \end{bmatrix}, \tag{3.10}$$

we can conclude that each periodic trajectory $\bar{\mathbf{s}}(t)$ of the original system can be represented either by a periodic trajectory $\bar{\mathbf{z}}^1, \cdots, \bar{\mathbf{z}}^\tau$ of the map (3.6) or by an equivalent periodic trajectory $\bar{\mathbf{x}}^1, \cdots, \bar{\mathbf{x}}^\tau$ of the map (3.9) with $\tau \geq 1$. From now on we can, in principle, assume that the dynamics of the experimental system is described by the discrete-time evolution equation (3.9) and its target states are represented by the periodic trajectories of the map $\mathbf{F}$.

In addition, one can claim that the local properties of the differential equation (3.1) in the vicinity of the target state $\bar{\mathbf{s}}(t)$ are completely described by the linearization of the map (3.9) about the respective periodic trajectory $\bar{\mathbf{x}}^k$. Denoting the displacement from the target trajectory $\bar{\mathbf{x}}^k$ as $\Delta\mathbf{x}^k = \mathbf{x}^k - \bar{\mathbf{x}}^k$ and the perturbation of the control parameters relative to the equilibrium values of parameters $\bar{\mathbf{u}}$ as $\Delta\mathbf{u}^k = \mathbf{u}^k - \bar{\mathbf{u}}$, one obtains the following linearized evolution equation in the tangent space $\mathbb{R}^{n_x}$:

$$\Delta\mathbf{x}^{k+1} = A^k \Delta\mathbf{x}^k + B^k \Delta\mathbf{u}^k. \tag{3.11}$$

Here we introduced the notations

$$A^k = \mathbf{D}_\mathbf{x}\mathbf{F}(\bar{\mathbf{x}}^k, \bar{\mathbf{u}}) \tag{3.12}$$

for the *Jacobian* of the transformation (3.9) and

$$B^k = \mathbf{D}_\mathbf{u}\mathbf{F}(\bar{\mathbf{x}}^k, \bar{\mathbf{u}}) \tag{3.13}$$

for the linear response of the system to changes in the control parameters, which we

call the *control matrix*. Clearly, the matrices $A^k$ and $B^k$ are periodic in the index $k$ with the same period $\tau$ as the target trajectory, $A^{k+\tau} = A^k$ and $B^{k+\tau} = B^k$.

For practical purposes, however, it is often more convenient to use a similar linearization constructed for the map (3.6). Denoting $\Delta\mathbf{z}^k = \mathbf{z}^k - \bar{\mathbf{z}}^k$, one obtains:

$$\Delta\mathbf{z}^{k+1} = \tilde{A}^k\Delta\mathbf{x}^k + \tilde{B}_1^k\Delta\mathbf{u}^k + \tilde{B}_2^k\Delta\mathbf{u}^{k-1}. \tag{3.14}$$

The matrices $A^k$ and $B^k$ can be trivially reexpressed in terms of $\tilde{A}^k$, $\tilde{B}_1^k$, and $\tilde{B}_2^k$ using the definition (3.8):

$$A^k = \begin{bmatrix} \tilde{A}^k & \tilde{B}_2^k \\ 0 & 0 \end{bmatrix}, \qquad B^k = \begin{bmatrix} \tilde{B}_1^k \\ I \end{bmatrix}. \tag{3.15}$$

(This equation itself is often taken as the definition of $A^k$ and $B^k$, e.g., in Ding *et al.* [10].) The set of matrices $\{A^k, B^k\}$ (or $\{\tilde{A}^k, \tilde{B}_1^k, \tilde{B}_2^k\}$) completely determines the local dynamics of the system in the tangent space and, therefore, provides all the essential information needed for the solution of the control problem. The only difficulty is neither the map (3.9) nor the periodic trajectory $\bar{\mathbf{x}}^1, \cdots, \bar{\mathbf{x}}^\tau$, which we used to formally define the Jacobian and the control matrix, are known.

## 3.4 Local Reconstruction

In fact, it is much easier to extract the periodic trajectory *and* the matrices $\tilde{A}^k$, $\tilde{B}_1^k$ and $\tilde{B}_2^k$ directly from the experimental data using the well-known technique of recurring points [40; 41] than it is to find the map (3.9) and then use it to calculate $A^k$ and $B^k$ from the definitions (3.12), (3.13). The additional benefit of using the linearized form of the dynamical equations is that the maximal dimension of the embedding space required for the reconstruction is reduced from $2n_s^h + 1$ to $n_s^h$.

Since the Hausdorff dimension of the attractor is unlikely to be known for an experimental system, the choice of the embedding dimension $n_z$ will typically have to be made using trial and error. One then needs to generate, for the fixed system parameters, $\mathbf{u} = \bar{\mathbf{u}}$, a sequence of points $\mathbf{z}^0, \mathbf{z}^1, \cdots, \mathbf{z}^N$ and select from it $n$, $1 \ll n \ll$

$N$, recurring points $\mathbf{z}^{r_1}, \cdots, \mathbf{z}^{r_n}$ such that

$$|\mathbf{z}^{r_1} - \mathbf{z}^{r_1+\tau}| \leq \cdots \leq |\mathbf{z}^{r_n} - \mathbf{z}^{r_n+\tau}| \leq \min_{k \neq r_j} |\mathbf{z}^k - \mathbf{z}^{k+\tau}|. \tag{3.16}$$

A number $\epsilon$ is then chosen, and the recurring points $\mathbf{z}^{r_j}$ are sorted into classes $\mathcal{K}_m$ according to the following rule. The point $\mathbf{z}^{r_1}$ always defines (becomes the center of) the first class $\mathcal{K}_1$. The next recurring point $\mathbf{z}^{r_2}$ is then attached to $\mathcal{K}_1$, if the distance $|\mathbf{z}^{r_1} - \mathbf{z}^{r_2}| < \epsilon$. Otherwise $\mathbf{z}^{r_2}$ defines the new class $\mathcal{K}_2$. The rest of the recurring points are then tested, and each is either attached to an existing class $\mathcal{K}_j$, if the distance to its center is smaller than $\epsilon$, or defines a new class. As one increases $\epsilon$ from zero the number of classes decreases from $n$ to one. If $n$ is large enough, one expects the number of classes to have a plateau at intermediate values of $\epsilon$ defining the natural partitioning of the set of recurring points into classes. Each class determines the neighborhood of either a fixed point of the map (3.6) or a point of a periodic trajectory with period $\tau$ or less (the period should be a factor of $\tau$, though).

Once a class $\mathcal{K} = \mathcal{K}_j$ is found corresponding to a point of periodic trajectory with period $\tau$, one can use the same sequence of data points $\mathbf{z}^0, \mathbf{z}^1, \cdots, \mathbf{z}^N$ to simultaneously determine the points $\bar{\mathbf{z}}^k$ of the target trajectory and the sequence of Jacobian matrices $\tilde{A}^k$. This is achieved using the least squares method to iteratively find the best fit for the linear approximation

$$\mathbf{z}^{k+1} = \bar{\mathbf{z}}^{k+1} + \tilde{A}^k(\mathbf{z}^k - \bar{\mathbf{z}}^k) \tag{3.17}$$

for each $k = 1, \cdots, \tau$. The $\chi^2$ function should be constructed to incorporate the information about the trajectories of length $\tau$ generated by each element of the class $\mathcal{K}$. For instance, one can take

$$\chi^2 = \sum_{\mathbf{z}^{r_i} \in \mathcal{K}} \sum_{k=1}^{\tau} \rho\left(\left|\mathbf{z}^{r_i} - \bar{\mathbf{z}}^1_{(p-1)}\right|\right) \left|\bar{\mathbf{z}}^{k+1}_{(p)} - \mathbf{z}^{r_i+k} + \tilde{A}^k_{(p)}\left(\mathbf{z}^{r_i+k-1} - \bar{\mathbf{z}}^k_{(p)}\right)\right|^2, \tag{3.18}$$

where the subscript denotes the level of approximation. The 0th level approximation $\bar{\mathbf{z}}^1_{(0)}$ is assumed to be given by the center of the class and the least squares procedure is repeated until the estimates $\tilde{A}^k_{(p)}$ and $\bar{\mathbf{z}}^k_{(p)}$ converge. Nonuniform weights $\rho(d)$ can

be chosen to compensate for the lack of data points in the vicinity of the target trajectory. Assigning a lower weight to trajectories which are farther from the target trajectory reduces the error caused by the nonlinearity of the original map (3.6). For instance, one can take $\rho(d) = \exp(-d^2/a^2)$, where $a$ is an adjustable parameter of order the radius $\epsilon$ of the class $\mathcal{K}$.

The optimal embedding dimension $n_z$ is not known *a priori*, but can be determined using the adaptive method similar to the one suggested by Petrov *et al.* [18]. The idea is rather simple. One starts with the original sequence of points $\mathbf{z}^0, \mathbf{z}^1, \cdots, \mathbf{z}^N$ and calculates the value of the $\chi^2$ function as described above. One then decreases the embedding dimension by one, discarding the last component of all data points, yielding a new sequence $\mathbf{z}_1^0, \mathbf{z}_1^1, \cdots, \mathbf{z}_1^N$. Calculating the value of the $\chi^2$ function once again and repeating the process until the dimension $n_z$ is exhausted or poor convergence of the estimates $\tilde{A}^k_{(p)}$ and $\bar{\mathbf{z}}^k_{(p)}$ is observed, one obtains a series of values $\chi^2(n_z)$. The optimal embedding dimension is then chosen as the minimal value of $n_z$ for which the function $\chi^2(n_z)$ is close to its minimal value.

Finally, the control matrices $\tilde{B}_1^k$ and $\tilde{B}_2^k$ can be found by generating a new sequence of points $\mathbf{z}^0, \mathbf{z}^1, \cdots, \mathbf{z}^N$, but now with system parameters that are slightly perturbed, and the perturbations recorded as a separate data sequence $\Delta\mathbf{u}^0, \Delta\mathbf{u}^1, \cdots, \Delta\mathbf{u}^N$. One then forms a new class of points $\mathcal{K}'$ by taking $\bar{\mathbf{z}}^1$ as the master point and either rejecting or attaching the points $\mathbf{z}^i$ to $\mathcal{K}'$ based on whether the distance $|\mathbf{z}^i - \bar{\mathbf{z}}^1|$ is larger or smaller than the radius $\epsilon$ (the same as the one used to construct the class $\mathcal{K}$). The least squares method is then used once again to find the best fit for the linear approximation

$$\mathbf{z}^{k+1} = \bar{\mathbf{z}}^{k+1} + \tilde{A}^k(\mathbf{z}^k - \bar{\mathbf{z}}^k) + \tilde{B}_1^k\Delta\mathbf{u}^k + \tilde{B}_2^k\Delta\mathbf{u}^{k-1} \tag{3.19}$$

for each $k = 1, \cdots, \tau$. The $\chi^2$ function is constructed similarly to the previous case, with $\tilde{A}^k$ and $\bar{\mathbf{z}}^k$ fixed at their optimal values calculated previously,

$$\begin{aligned} \chi^2 &= \sum_{\mathbf{z}^i \in \mathcal{K}'} \sum_{k=1}^{\tau} \rho\left(\left|\mathbf{z}^i - \bar{\mathbf{z}}^1\right|\right) \\ &\times \left|\bar{\mathbf{z}}^{k+1} - \mathbf{z}^{i+k} + \tilde{A}^k\left(\mathbf{z}^{i+k-1} - \bar{\mathbf{z}}^k\right) + \tilde{B}_1^k\Delta\mathbf{u}^{i+k-1} + \tilde{B}_2^k\Delta\mathbf{u}^{i+k-2}\right|^2. \end{aligned} \tag{3.20}$$

Minimizing $\chi^2$ with respect to $\tilde{B}_1^k$ and $\tilde{B}_2^k$ yields the sequence of control matrices and gives us the last bit of information required to reconstruct the local dynamics of the experimental system.

As pointed out by Petrov *et al.* [18], the control perturbations $\Delta\mathbf{u}^k$ may shift the system away from the attracting manifold and thus excite additional degrees of freedom effectively absent in the unperturbed dynamics on the attractor $\mathcal{A}$. For spatiotemporal systems most (but not all) of the normal modes will decay rapidly compared to the time $t_{k+1} - t_k$ between successive crossings of the Poincaré section, so that the corresponding degrees of freedom can still be ignored in the linearization (3.14). The embedding dimension in this case should be increased to describe the slowly decaying excited modes. The new value $n_z'$ can be adaptively found as in the unperturbed case, with one modification. The function $\chi^2$ should be defined by (3.20) with variable $\bar{\mathbf{z}}^k$, $\tilde{A}^k$, $\tilde{B}_1^k$ and $\tilde{B}_2^k$ instead of (3.18). Finally, the matrices $A^k$ and $B^k$ and the target trajectory $\bar{\mathbf{x}}^k$ in the extended state-plus-parameter space are obtained using (3.15) and (3.10).

Of course, this whole scenario is highly idealized, because in practice the measurements are of finite duration and noisy, which can lead to excessive errors in the determination of both the dynamical equations and the periodic trajectories. We are not going to discuss the techniques used to reduce the effects of noise in detail and instead just give a few references. The two most popular methods are the Karhunen-Loève decomposition [42; 43] and the wavelet transform [44]. The Karhunen-Loève decomposition (also called singular system analysis, bi-orthogonal decomposition, etc.) is based on choosing an appropriate basis of vectors to represent the time series. The vectors are determined as a set of eigenvectors of the two-point correlation matrix computed using the experimental data. The wavelet transform is a generalization of the Fourier transform which represents the translation and the scaling of components of a signal. Both methods are extremely useful and are used rather extensively to reconstruct the dynamics of high-dimensional, and especially spatially extended, dynamical systems. The range of applications to the control problem is rather limited so far (see, e.g., the work by Triandaf and Schwartz [45]), but is expected to grow rapidly.

Summarizing the results of this chapter, we conclude that even when no mathematical model for the system is available, the dynamical equations describing its evolution can be extracted from the experimental data. Besides, the control problem only requires the knowledge of the linearization of these equations about the selected target state, which can be obtained even easier, and with better precision, than the full nonlinear equations. We can, therefore, proceed with the analysis of the control problem assuming that the dynamical equations *are known*.

# Chapter 4 Symmetric Systems

Despite the recent wave of interest towards controlling chaotic dynamics an interesting and important question of controlling systems with symmetries received surprisingly little attention in the physics literature. The importance of symmetries in controlling, for instance, spatiotemporal chaos is evident, since the systems typically show rotational and translational symmetries. Such phenomena as fluid flows, convection or chemical reactions often take place inside symmetric containers — cylinders, spheres, pipes and annuli. Even the dynamics of unbounded systems is often influenced by the symmetries of the physical space. Although the presence of symmetries usually significantly simplifies the analysis of the dynamics, it also makes system identification and control more complicated due to the inherent degeneracies of the evolution operators. In fact, the presence of symmetries, explicit or implicit, makes a number of single-control-parameter methods fail [10; 17; 18], calling for multi-parameter control [11; 14; 46; 47].

In order to see how the control problem is affected by symmetries, we consider (following the analysis conducted in [13]) a general discrete-time system (the arguments for continuous-time systems are very similar), whose evolution is described by the map (3.9). If the target trajectory $\bar{\mathbf{x}}^t$ of the system is unstable, it can be stabilized by an appropriate feedback through the time-dependent control perturbation $\Delta\mathbf{u}^t$, provided the matrices $A^t$ and $B^t$ in the linearization (3.11) satisfy certain conditions. In the present chapter we concentrate on selecting from the complete set of available *system* parameters a minimal set of *control* parameters whose perturbation allows the stabilization of the target state, i.e., making an appropriate choice of the control matrix $B^t$, given the Jacobian $A^t$. The discussion of the problem of actually finding a stabilizing feedback is deferred until chapter 5. We will see below that the constraints affecting the choice of control parameters can be easily obtained from the symmetry properties of the system and the controlled state. What is more interesting, symmetry allows one to determine the minimal number of control parameters even when the

Jacobian $A^t$ describing the local dynamics is unknown.

As we have seen in the previous chapter, discrete-time evolution equations of type (3.9) are often obtained as a result of phase space reconstruction of a continuous-time system when the dynamical equations describing its evolution are unknown. Generically, such reconstruction is possible when the measurement of a single scalar time-dependent signal $y(t)$, which is a function of the system state $\mathbf{s}(t)$, is available. Many practically interesting systems, symmetric ones in particular, are, however, extremely nongeneric and require a number of independent scalar signals for the complete reconstruction. Eckmann and Ruelle [48] acknowledged that the choice of signals has to be made carefully by trial and error. Certain general rules concerning this choice, however, can be established on purely theoretical grounds, since this problem too can be effectively treated based on the knowledge of underlying symmetries [49].

## 4.1 Time-Invariant States

### 4.1.1 Stabilizability and Controllability

Although our analysis is applicable to time-varying systems, we start for simplicity by assuming that the controlled state is time-invariant, $\bar{\mathbf{x}}^t = \bar{\mathbf{x}}$. Then the matrices $A^t$ and $B^t$ become constant, and we can drop the time index in (3.11) to obtain

$$\Delta\mathbf{x}^{t+1} = A\Delta\mathbf{x}^t + B\Delta\mathbf{u}^t. \tag{4.1}$$

It is useful to introduce and compare two characterizations of the linearized evolution equation (4.1), which extremely simplify the analysis of feedback control algorithms: *stabilizability* and *controllability*.

The dynamical system (4.1) or the pair $(A, B)$ is said to be *stabilizable*, if there exists a *state feedback*

$$\Delta\mathbf{u}^t = -K\Delta\mathbf{x}^t, \tag{4.2}$$

making the system (4.1) stable, i.e., it is possible to find a *feedback gain matrix* $K$, such that all eigenvalues $\lambda'_k$ of the matrix $A' = A - BK$ lie within a unit circle of the complex plane, $|\lambda'_k| < 1$, $\forall k$. Otherwise the system or the pair $(A, B)$ is

called *unstabilizable*. Indeed, substituting the feedback (4.2) into (4.1) one obtains the linearized evolution equation for the *closed-loop* system

$$\Delta\mathbf{x}^{t+1} = (A - BK)\Delta\mathbf{x}^t, \tag{4.3}$$

with $\Delta\mathbf{x} = \mathbf{0}$ becoming the stable fixed point of the map (4.3), if and only if $A - BK$ is stable.

Since the magnitude of the control perturbation $\Delta\mathbf{u}^t$ is proportional to the deviation $\Delta\mathbf{x}^t$ of the system from the target state, feedback of the form (4.2) is often called *proportional* in the physics literature, although there are a number of other terms used to denote this type of feedback. Control theory uses the term *state* feedback to refer to the fact that the state of the system is used to determine the control perturbation. At first sight equation (4.2) seems to impose strict limitations on the allowed form of the feedback law. However, this is precisely the form demanded by a number of widely used control algorithms [10; 12; 17].

Stabilizability is a property, which usually sensitively depends on the values of system parameters. In the majority of practical applications, however, it is preferable to have an adaptive control that would stabilize a given steady state $\bar{\mathbf{x}}(\bar{\mathbf{u}})$ for arbitrary values of system parameters. This is especially important, if one is to track the trajectory $\bar{\mathbf{x}}$ as parameters slowly vary, which might be advantageous in many applications, e.g., for moving the operating point of a nonlinear device across a bifurcation, from the stable region to the chaotic region. Such a control scheme can be obtained, if the more restrictive condition of controllability, which is essentially parameter-independent, is imposed on the matrices $A$ and $B$. On the other hand, it can be demonstrated [50] that the controllability condition guarantees that the eigenvalues of the matrix $A - BK$ can be freely assigned (with complex ones in conjugate pairs) by an appropriate choice of the matrix $K$. Therefore, if the system is controllable, it is stabilizable as well, and by requiring controllability we satisfy both conditions at once.

The $n_x$-dimensional linear system (4.1) or the pair $(A, B)$ is said to be *controllable* if, for any initial state $\Delta\mathbf{x}^{t_i} = \Delta\mathbf{x}_i$, times $t_f - t_i \geq n_x$, and final state $\Delta\mathbf{x}_f$, there

exists a sequence of control perturbations $\Delta\mathbf{u}^{t_i}, \cdots, \Delta\mathbf{u}^{t_f-1}$ such that the solution of equation (4.1) satisfies $\Delta\mathbf{x}^{t_f} = \Delta\mathbf{x}_f$. Otherwise, the system or the pair $(A, B)$ is called *uncontrollable*.

The controllability condition can be represented in a number of different equivalent forms. To obtain one particularly convenient form, we make the trivial observation that, if it is possible to drive the linear system from an arbitrary initial state $\Delta\mathbf{x}_i$ to an arbitrary final state $\Delta\mathbf{x}_f$ in $n_x$ steps, it is possible to do the same in any number of steps $n$ exceeding $n_x$. Suppose we let the system evolve under control for $n_x$ steps from the initial state $\Delta\mathbf{x}^t$. The final state will be given by[1]

$$\Delta\mathbf{x}^{t+n_x} = (A)^{n_x}\Delta\mathbf{x}^t + \sum_{k=1}^{n_x}(A)^{n_x-k}B\Delta\mathbf{u}^{t+k-1}. \tag{4.4}$$

Denote $\mathbf{b}_m$ the $m$th column of the matrix $B$:

$$B = [\,\mathbf{b}_1 \quad \mathbf{b}_2 \quad \cdots \quad \mathbf{b}_{n_u}\,]. \tag{4.5}$$

Regarding the terms $(A)^{n_x-k}\mathbf{b}_m$ as vectors in the tangent space $\mathbb{R}^{n_x}$,

$$\mathbf{h}_m^k = (A)^{n_x-k}\mathbf{b}_m, \quad k = 1, \cdots, n_x,\ m = 1, \cdots, n_u, \tag{4.6}$$

and the control perturbations $\Delta u_m^{t+k-1}$ as coordinates, we immediately conclude that equation (4.4) rewritten as

$$\Delta\mathbf{x}_f - (A)^{n_x}\Delta\mathbf{x}_i = \sum_{k=1}^{n_x}\sum_{m=1}^{n_u}\Delta u_m^{t+k-1}\mathbf{h}_m^k \tag{4.7}$$

can only be satisfied, if and only if there are $n_x$ linearly independent vectors in the set (4.6), i.e., the set $\{\mathbf{h}_m^k\}$ spans the tangent space $\mathbb{R}^{n_x}$. This is equivalent to requiring that

$$\mathrm{rank}(\mathcal{C}) = n_x, \tag{4.8}$$

where the matrix

$$\mathcal{C} \equiv [\,B \quad AB \quad (A)^2B \quad \cdots \quad (A)^{n_x-1}B\,] \tag{4.9}$$

[1]Here and below in the text we use the notation $(A)^n$ to indicate that $A$ is taken to the power of $n$ to differentiate it from the notation $A^t$, where index $t$ defines the time dependence.

is called the *controllability matrix*. Condition (4.8) was introduced into the physics literature from linear systems theory by Romeiras *et al.* [17] as a simple, but practical test of the controllability.

In contrast, the stabilizability condition requires that the set (4.6) spans only the unstable subspace $L^u \subseteq \mathbb{R}^{n_x}$ of the Jacobian $A$, instead of the whole tangent space $\mathbb{R}^{n_x}$. Stabilizability can be formally expressed in the form identical to (4.8). Let us define the number of stable and unstable[2] eigenvalues of the Jacobian $n_x^s$ and $n_x^u$, respectively (one obviously has $n_x^s + n_x^u = n_x$). For instance, if $A$ is a diagonalizable matrix, it has $n_x^s$ linearly independent stable eigenvectors which we denote $\mathbf{e}_i^s$, $i = 1, \cdots, n_x^s$. It can, therefore, be shown using an appropriate coordinate transformation that the pair $(A, B)$ is stabilizable if and only if

$$\mathrm{rank}(\mathcal{S}) = n_x, \tag{4.10}$$

where the matrix

$$\mathcal{S} \equiv [\, \mathbf{e}_1^s \quad \cdots \quad \mathbf{e}_{n_x^s}^s \quad B \quad AB \quad \cdots \quad (A)^{n_x^u - 1} B \,] \tag{4.11}$$

can be called the *stabilizability matrix* by analogy with the controllability matrix.

In order to better understand the restrictions imposed on the control scheme by symmetries, it is beneficial to look at the controllability condition from the geometrical point of view, assuming $n_u = 1$ and, consequently, $B = \mathbf{b}$. The controllability in this context is equivalent to the vectors $\mathbf{h}^1, \mathbf{h}^2, \cdots, \mathbf{h}^{n_x}$ spanning the tangent space $\mathbb{R}^{n_x}$. Generically, the matrix $A$ is nondegenerate (has a nondegenerate spectrum), so one can always find a vector $\mathbf{b}$, such that the resulting set (4.6) forms a basis. However, if $A$ is degenerate, which is a usual consequence of symmetry, there will exist an eigenspace of the Jacobian, $L^r \subset \mathbb{R}^{n_x}$, such that $\mathbf{x}^\dagger A = \lambda_r \mathbf{x}^\dagger$, $\forall \mathbf{x} \in L^r$ with the dimension $d_r = \dim(L^r) > 1$, where $\dagger$ denotes (complex conjugate) transpose of a matrix or vector. The dynamics of the system in such an eigenspace cannot be controlled with just one control parameter (see [17] for an example of such a situation), because the vectors $\mathbf{h}^k$ only span a one-dimensional subspace of $L^r$. Indeed, since

[2] For the purpose of control we regard the central directions, defined by the eigenvalues $\lambda$ such that $|\lambda| = 1$ ($\mathrm{Re}(\lambda) = 0$ in the continuous-time case), as unstable.

$d_r > 1$ there will exist $d_r - 1$ adjoint eigenvectors $\mathbf{f}_j \in L^r$ orthogonal to $\mathbf{b}$ and each other. Then

$$(\mathbf{f}_j \cdot \mathbf{h}^k) = \mathbf{f}_j^\dagger (A)^{n_x - k} \mathbf{b} = \lambda_r^{n_x - k} \mathbf{f}_j^\dagger \mathbf{b} = \lambda_r^{n_x - k} (\mathbf{f}_j \cdot \mathbf{b}) = 0, \tag{4.12}$$

so every basis vector $\mathbf{h}^k$ is orthogonal to every eigenvector $\mathbf{f}_j$, $j = 1, \cdots, d_r - 1$.

It is often convenient to define the notion of controllability for individual eigenvectors. We will say that the adjoint eigenvector $\mathbf{f}$ of the Jacobian $A$ is controllable, if there exists $m$, $1 \leq m \leq n_u$, such that $(\mathbf{f} \cdot \mathbf{b}_m) \neq 0$. Respectively, the eigenvector that is orthogonal to every column of the control matrix $B$ is called uncontrollable. Using these definitions we can, therefore, conclude that the controllability of the linearized system is equivalent to the controllability of each and every adjoint eigenvector of the Jacobian matrix (also see [51]). Similarly, the stabilizability is equivalent to the controllability of each and every *unstable* adjoint eigenvector.

If the system dynamics in $L^r$ happens to be stable (e.g., when the system is stabilizable, but uncontrollable), the system can still be stabilized similarly to the nondegenerate case, but we have to ensure the controllability in case the dynamics in this eigenspace is unstable. This can be achieved by increasing the number of control parameters $n_u$, which extends the set (4.6), until it spans every eigenspace of $\mathbb{R}^{n_x}$. This would lead one to assume that the minimal value of $n_u$ should be defined by the highest degeneracy of the Jacobian matrix $A$. We will see, however, that various kinds of degeneracy have a somewhat different effect on the controllability of the system.

### 4.1.2 Symmetries of the System

Symmetries usually significantly simplify the analysis of system dynamics, and the control problem is no exception. In particular, even when the exact form of the Jacobian matrix is unknown, the structure of the symmetry group describing the symmetries of the system allows one to reduce the controllability condition (4.8) to a set of much simpler conditions, which provide a number of system-independent results. The discussion below is based on bifurcation theory [31] and closely parallels the treatment of degeneracy in quantum mechanics and spontaneous symmetry breaking

in quantum field theory and phase transitions.

In general we call the system symmetric, if the nonlinear evolution equation preserves its form under a set of linear transformations $g : \mathbf{x} \to \mathbf{x}' = g(\mathbf{x})$ of the phase space. More formally, we say that the evolution equation (3.9) possesses a *structural* symmetry described by a symmetry group $\mathcal{G}$, if the map $\mathbf{F}$ commutes with all group actions:

$$\mathbf{F}(g(\mathbf{x}), \mathbf{u}) = g(\mathbf{F}(\mathbf{x}, \mathbf{u})), \quad \forall g \in \mathcal{G},\ \forall \mathbf{x} \in \mathbb{R}^{n_x} \tag{4.13}$$

or, in other words, if the function $\mathbf{F}(\mathbf{x}, \mathbf{u})$ is $\mathcal{G}$-equivariant with respect to its first argument. The group $\mathcal{G}$ is usually a byproduct of symmetries of the underlying physical space, such as rotational and translational symmetry (domain symmetry), and symmetries of the phase space, such as phase symmetry $\phi \to \phi + 2\pi$ (range symmetry). Since all interesting physical symmetries are unitary (such rare exceptions as the Lorentz group are hardly relevant in the context of control problem), we will assume that $\mathcal{G}$ is a unitary group.

Usually, the symmetry demonstrates itself in more than just one way: often steady (as well as time-periodic) states $\bar{\mathbf{x}}$ of symmetric systems too will be symmetric with respect to transformations $g \in \mathcal{H}_{\bar{\mathbf{x}}}$, where $\mathcal{H}_{\bar{\mathbf{x}}} \subseteq \mathcal{G}$ is an *isotropy* subgroup of $\bar{\mathbf{x}}$. In general, the target state $\bar{\mathbf{x}}$ might also be symmetric with respect to transformations which do not belong to $\mathcal{G}$ (we will see an example in section 4.3.1). However, considering those does not provide any additional information, so we assume that

$$g(\bar{\mathbf{x}}) = \bar{\mathbf{x}}, \quad \forall g \in \mathcal{H}_{\bar{\mathbf{x}}}. \tag{4.14}$$

For the purpose of control it is important to observe that upon linearization about the target state $\bar{\mathbf{x}}$ the structural symmetry of the evolution equation (3.9) does not disappear, but is replaced with a related *dynamical* symmetry. Indeed, using the definitions (4.13), (4.14) and the fact that symmetry transformations are linear, one

obtains in the linear approximation for an arbitrary $g \in \mathcal{H}_{\bar{\mathbf{x}}}$:

$$\begin{aligned} \bar{\mathbf{x}} + g(A\Delta\mathbf{x}) &= g(\bar{\mathbf{x}}) + g(A\Delta\mathbf{x}) = g(\bar{\mathbf{x}} + A\Delta\mathbf{x}) \\ &= g(\mathbf{F}(\bar{\mathbf{x}}, \bar{\mathbf{u}}) + A\Delta\mathbf{x}) = g(\mathbf{F}(\bar{\mathbf{x}} + \Delta\mathbf{x}, \bar{\mathbf{u}})) \\ &= \mathbf{F}(g(\bar{\mathbf{x}} + \Delta\mathbf{x}), \bar{\mathbf{u}}) = \mathbf{F}(g(\bar{\mathbf{x}}) + g(\Delta\mathbf{x}), \bar{\mathbf{u}}) \\ &= \mathbf{F}(\bar{\mathbf{x}} + g(\Delta\mathbf{x}), \bar{\mathbf{u}}) = \mathbf{F}(\bar{\mathbf{x}}, \bar{\mathbf{u}}) + Ag(\Delta\mathbf{x}) \\ &= \bar{\mathbf{x}} + Ag(\Delta\mathbf{x}). \end{aligned} \tag{4.15}$$

Defining $\mathcal{L}$ the full symmetry group of the linearized equation (4.1) in the absence of control ($\Delta\mathbf{u}^t = \mathbf{0}$):

$$g(A\Delta\mathbf{x}) = Ag(\Delta\mathbf{x}), \quad \forall g \in \mathcal{L}, \tag{4.16}$$

one concludes that the group $\mathcal{L}$ describing the dynamical symmetry of the system in the vicinity of the target state $\bar{\mathbf{x}}$ includes all transformations $g \in \mathcal{H}_{\bar{\mathbf{x}}}$, and therefore:

$$\mathcal{H}_{\bar{\mathbf{x}}} \subseteq \mathcal{L}. \tag{4.17}$$

One can speculate that typically $\mathcal{L}$ will coincide with $\mathcal{H}_{\bar{\mathbf{x}}}$. As a consequence, if the target state $\bar{\mathbf{x}}$ has low symmetry, the symmetry of the evolution equation will be reduced upon linearization to a subgroup of $\mathcal{G}$. However, as we will see in section 4.3.1, $\mathcal{L}$ might be equal to $\mathcal{G}$, or even include $\mathcal{G}$ as a subgroup for highly symmetric target states, with the apparent symmetry increased by linearization.

It turns out that with the help of group representation theory one can substantially simplify the controllability condition (4.8) and, as a result, obtain a number of useful restrictions on the set of control parameters. Consider the matrix representation $T$ generated in the tangent space $\mathbb{R}^{n_x}$ by the action of transformations $g$ from an arbitrary subgroup $\mathcal{L}'$ of the full dynamical symmetry group $\mathcal{L}$:

$$(g(\mathbf{x}))_i = (T(g)\mathbf{x})_i = \sum_{j=1}^{n_x} T_{ij}(g)x_j, \quad \forall \mathbf{x} \in \mathbb{R}^{n_x}, \tag{4.18}$$

where, according to (4.16), all matrices $T(g)$ commute with the Jacobian

$$T(g)A = AT(g), \quad \forall g \in \mathcal{L}' \subseteq \mathcal{L}. \tag{4.19}$$

The knowledge of the representation $T$ is enough to derive a very simple criterion for the admissibility of the control matrix. Observe that, if $T(g)B = B$ for an arbitrary transformation $g \in \mathcal{L}'$, then

$$\begin{aligned} \mathcal{C} &= [\,T(g)B \quad AT(g)B \quad \cdots \quad (A)^{n_x-1}T(g)B\,] \\ &= [\,T(g)B \quad T(g)AB \quad \cdots \quad T(g)(A)^{n_x-1}B\,] = T(g)\mathcal{C}. \end{aligned} \tag{4.20}$$

As a result, since $T_{ij}(g) \neq \delta_{i,j}$ for any $g \neq e$ (where we defined $e$ as the identity transformation: $e(\mathbf{x}) = \mathbf{x}$), the rows $\tilde{\mathbf{c}}_j$ of the controllability matrix become linearly dependent,

$$\sum_{j=1}^{n_x} (T_{ij}(g) - \delta_{i,j})\tilde{\mathbf{c}}_j = \mathbf{0}, \tag{4.21}$$

and the controllability condition (4.8) is violated. Therefore, we obtain a necessary condition on the control matrix:

$$T(g)B \neq B, \quad \forall g \in \mathcal{L}' \setminus \{e\}. \tag{4.22}$$

In other words, the control arrangement should be chosen such that the symmetry of the linearized evolution equation (4.1) is completely broken for (almost all) nonzero control perturbations $\Delta\mathbf{u} \neq \mathbf{0}$.

### 4.1.3 Group Coordinates

Though simple and general, criterion (4.22) is not very helpful for finding the minimal set of control parameters satisfying the controllability condition. In order to derive a more practically useful criterion one has to make a few more steps. We begin with the reduction of the controllability condition to a set of simpler conditions which can be performed [50] be constructing the Jordan block decomposition of the Jacobian matrix. The task of constructing this decomposition can be greatly simplified by transforming to the "group coordinates," defined with respect to the basis set composed of vectors which transform according to different irreducible representations contained in $T$, in which the Jacobian is block-diagonal. In practice, it is usually impossible to determine whether the isotropy group $\mathcal{H}_{\bar{\mathbf{x}}}$ exhausts the dynamical sym-

metries of the system or the group $\mathcal{L}$ contains some hidden symmetries as well. It is, therefore, important to show that a number of restrictions on the set of control parameters can be obtained using an arbitrary unitary subgroup $\mathcal{L}'$ of $\mathcal{L}$.

Decomposing the representation $T$ into a sum of irreducible representations $T^r$ of the group $\mathcal{L}'$ with respective dimensionalities $d_r$, we obtain:

$$T = p_1 T^1 \oplus p_2 T^2 \oplus \cdots \oplus p_q T^q \tag{4.23}$$

with

$$n_x = p_1 d_1 + p_2 d_2 + \cdots + p_q d_q, \tag{4.24}$$

where $p_r$ denotes the number of equivalent representations $T^r$ present in the decomposition (4.23), and $q$ is the total number of nonequivalent irreducible representations. Since $\mathcal{L}'$ is unitary, all irreducible representations $T^r$ in (4.23) can be chosen as unitary [52].

The tangent space $\mathbb{R}^{n_x}$ is similarly decomposed into a sum of invariant subspaces $L^{r\alpha}_{\mathcal{L}'}$ such that $T(g)\mathbf{x} \in L^{r\alpha}_{\mathcal{L}'}$, $\forall \mathbf{x} \in L^{r\alpha}_{\mathcal{L}'}$ and $\forall g \in \mathcal{L}'$:

$$\mathbb{R}^{n_x} = L^1_{\mathcal{L}'} \oplus L^2_{\mathcal{L}'} \oplus \cdots \oplus L^q_{\mathcal{L}'}, \tag{4.25}$$

where

$$L^r_{\mathcal{L}'} = L^{r1}_{\mathcal{L}'} \oplus L^{r2}_{\mathcal{L}'} \oplus \cdots \oplus L^{rp_r}_{\mathcal{L}'} \tag{4.26}$$

and $\alpha = 1, \cdots, p_r$ indexes different invariant subspaces, which correspond to the same group of equivalent irreducible representations $T^r$. It should be noted that even though the decomposition (4.25) is unique, the decomposition (4.26) is not, unless $p_r = 1$. Let us introduce a basis in each invariant subspace $L^{r\alpha}_{\mathcal{L}'}$ and denote the basis vectors $\mathbf{e}^{r\alpha}_i$, $i = 1, \cdots, d_r$. We choose the basis vectors such that they transform according to the irreducible representation $T^r$, i.e.,

$$T(g)\,\mathbf{e}^{r\alpha}_i = \sum_{j=1}^{d_r} T^r_{ij}(g)\,\mathbf{e}^{r\alpha}_j, \quad \forall g \in \mathcal{L}'. \tag{4.27}$$

For unitary $T^r$ a generalized orthogonality condition between basis vectors $\mathbf{e}^{r\alpha}_i$ can

be established [52] as a consequence of (4.27):

$$(\mathbf{e}_i^{r\beta} \cdot \mathbf{e}_j^{s\alpha}) = \delta_{r,s}\delta_{i,j}(\mathbf{e}_i^{r\beta} \cdot \mathbf{e}_i^{r\alpha}). \tag{4.28}$$

In addition, for $p_r > 1$ the decomposition (4.26) can always be performed in such a way that $(\mathbf{e}_i^{r\beta} \cdot \mathbf{e}_i^{r\alpha}) = \delta_{\alpha,\beta}$ (this, however, still leaves some freedom in choosing the invariant subspaces $L^{r\alpha}_{\mathcal{L}'}$), so that the complete set of basis vectors $\{\mathbf{e}_i^{r\alpha}\}$, where $r = 1, \cdots, q$, $\alpha = 1, \cdots, p_r$, and $i = 1, \cdots, d_r$ is made orthonormal. We, therefore, conclude that the matrix $P$ defined by

$$P = \begin{bmatrix} P^1 \\ \vdots \\ P^q \end{bmatrix}, \qquad P^r = \begin{bmatrix} P^r_1 \\ \vdots \\ P^r_{d_r} \end{bmatrix}, \qquad P^r_i = \begin{bmatrix} (\mathbf{e}_i^{r1})^\dagger \\ \vdots \\ (\mathbf{e}_i^{rp_r})^\dagger \end{bmatrix}, \tag{4.29}$$

is orthogonal, $(P)^{-1} = P^\dagger$ (or, more generally, unitary).

Furthermore, according to the Wigner-Eckart theorem [52], the matrix elements of an arbitrary matrix (and the Jacobian $A$, in particular) invariant with respect to any group transformation

$$T(g)AT^{-1}(g) = A, \quad \forall g \in \mathcal{L}', \tag{4.30}$$

satisfy the following general formula:

$$(\mathbf{e}_i^{r\beta} \cdot A\mathbf{e}_j^{s\alpha}) = \delta_{r,s}\delta_{i,j}(\mathbf{e}_i^{r\beta} \cdot A\mathbf{e}_i^{r\alpha}), \tag{4.31}$$

and the scalar product

$$(\bar{\Lambda}^r)_{\alpha\beta} \equiv (\mathbf{e}_i^{r\alpha} \cdot A\mathbf{e}_i^{r\beta}) \tag{4.32}$$

is independent of the index $i = 1, \cdots, d_r$ (but depends on the decomposition (4.26)). As a result, on transformation to the group coordinates the Jacobian matrix becomes block diagonal:

$$\bar{A} = PAP^{-1} = \begin{bmatrix} \bar{A}^1 & & \\ & \ddots & \\ & & \bar{A}^q \end{bmatrix}, \tag{4.33}$$

where each block $\bar{A}^r$ is itself block-diagonal

$$\bar{A}^r = \begin{bmatrix} \bar{\Lambda}^r & & \\ & \ddots & \\ & & \bar{\Lambda}^r \end{bmatrix} \tag{4.34}$$

and consists of $d_r$ *identical* $p_r \times p_r$ blocks $\bar{\Lambda}^r$ with the matrix elements defined by the scalar product (4.32).

If no irreducible representation $T^r$ of $\mathcal{L}'$ enters the decomposition (4.23) more than once, i.e., $p_1 = \cdots = p_q = 1$, the structure of the Jacobian matrix is completely resolved: the transformed Jacobian is diagonal and its spectrum consists of eigenvalues $\lambda_r = \bar{\Lambda}^r$, $r = 1, \cdots, q$ with multiplicity $d_r$, while the basis vectors $\mathbf{e}_i^{r\alpha}$ become the corresponding eigenvectors (and, consequently, define the *normal modes* of the linearized system). In this case the invariant subspaces of the group $\mathcal{L}'$ define the eigenspaces of the Jacobian, $L^r = L^r_{\mathcal{L}'}$. Clearly, the spectrum becomes degenerate, if the symmetry is sufficiently high (such that $T$ contains at least one irreducible representation $T^r$ with dimensionality larger than one).

Degeneracy should not necessarily be associated with symmetry and might be accidental (with respect to the group $\mathcal{L}'$). For instance, it can happen that $\bar{\Lambda}^r = \bar{\Lambda}^{r'}$ for some $r \neq r'$, so that the multiplicity of the eigenvalue $\lambda_r$ is increased respectively to $d_r + d_{r'}$. Accidental degeneracies can be alternatively thought of as a consequence of hidden symmetries contained in the full symmetry group $\mathcal{L}$ of which $\mathcal{L}'$ is a subgroup. However, the degeneracies not associated with some physical symmetry are likely to disappear under a typical perturbation, such as a change of system parameters and, therefore, are most conveniently regarded as accidental. Since the full symmetry group $\mathcal{L}$, in general, depends on system parameters and cannot be directly deduced from the structural symmetry group $\mathcal{G}$, it is usually more convenient to use its parameter-independent subgroup $\mathcal{L}' = \mathcal{H}_{\bar{\mathbf{x}}}$ instead.

### 4.1.4 Jordan Decomposition

If the symmetry described by $\mathcal{L}'$ is low, a number of equivalent irreducible representations will typically be found in the decomposition (4.23), i.e., we will have $p_r > 1$

for certain $r$. In this case the knowledge of the dynamical symmetries alone is not sufficient to completely determine the structure of the Jacobian matrix, which is, in general, system-dependent. As a result, one has to solve a secular equation

$$(\bar{\Lambda}^r - \lambda_{r\alpha} I)\mathbf{e}^r_\alpha = 0, \tag{4.35}$$

for each block $\bar{\Lambda}^r$ with $p_r > 1$ in order to find the eigenvectors in the invariant subspace $L^r_{\mathcal{L}'}$ and the respective eigenvalues. Here, unlike the case of quantum mechanics, the Jacobian matrix does not have to be Hermitian and, therefore, might not be diagonalizable. However, $\bar{\Lambda}^r$ can always be reduced to the Jordan normal form by finding the coordinate transformation $\bar{Q}^r$ such that

$$\Lambda^r = \bar{Q}^r \bar{\Lambda}^r (\bar{Q}^r)^{-1} = \begin{bmatrix} \Lambda^{r1} & & \\ & \ddots & \\ & & \Lambda^{rp'_r} \end{bmatrix}, \tag{4.36}$$

where $p'_r \leq p_r$ is the number of distinct eigenvalues and the Jordan superblock

$$\Lambda^{r\alpha} = \begin{bmatrix} \Lambda^{r\alpha}_1 & & \\ & \ddots & \\ & & \Lambda^{r\alpha}_{j_{r\alpha}} \end{bmatrix} \tag{4.37}$$

corresponding to the eigenvalue $\lambda_{r\alpha}$ consists of $j_{r\alpha}$ Jordan blocks

$$\Lambda^{r\alpha}_i = \begin{bmatrix} \lambda_{r\alpha} & & & \\ 1 & \lambda_{r\alpha} & & \\ & \ddots & \ddots & \\ & & 1 & \lambda_{r\alpha} \end{bmatrix}. \tag{4.38}$$

In the absence of accidental degeneracy all eigenvalues of $\bar{\Lambda}^r$ are different, so that $p'_r = p_r$ and $j_{r\alpha} = 1$ for all $\alpha$, i.e., $\Lambda^r$ is diagonal.

Since each block $\bar{A}^r$ of the transformed Jacobian (4.33) consists of $d_r$ identical blocks $\bar{\Lambda}^r$, applying the coordinate transformation defined by the block-diagonal ma-

trix assembled from $d_r$ blocks $\bar{Q}^r$,

$$Q^r = \begin{bmatrix} \bar{Q}^r & & \\ & \ddots & \\ & & \bar{Q}^r \end{bmatrix}, \tag{4.39}$$

reduces $\bar{A}^r$ to the Jordan normal form:

$$\tilde{A}^r = Q^r \bar{A}^r (Q^r)^{-1} = \begin{bmatrix} \Lambda^r & & \\ & \ddots & \\ & & \Lambda^r \end{bmatrix}. \tag{4.40}$$

The Jordan blocks on the diagonal of $\tilde{A}^r$ will not, in general, be arranged in superblocks with the same eigenvalue. This, however, can be trivially corrected by permuting the rows and columns of $\tilde{A}^r$ to obtain the matrix

$$\hat{A}^r = R^r \tilde{A}^r (R^r)^{-1} = \begin{bmatrix} \hat{A}^{r1} & & \\ & \ddots & \\ & & \hat{A}^{rp'_r} \end{bmatrix}, \tag{4.41}$$

where $R^r$ is the permutation matrix arranging the identical Jordan blocks next to each other, and the Jordan superblock corresponding to the eigenvalue $\lambda_{r\alpha}$ has the form

$$\hat{A}^{r\alpha} = \begin{bmatrix} \hat{A}^{r\alpha}_1 & & \\ & \ddots & \\ & & \hat{A}^{r\alpha}_{j_{r\alpha}} \end{bmatrix}. \tag{4.42}$$

Each block $\hat{A}^{r\alpha}_i$ is, in turn, composed of $d_r$ identical Jordan blocks $\Lambda^{r\alpha}_i$, defined by (4.38):

$$\hat{A}^{r\alpha}_i = \begin{bmatrix} \Lambda^{r\alpha}_i & & \\ & \ddots & \\ & & \Lambda^{r\alpha}_i \end{bmatrix}. \tag{4.43}$$

Defining the block-diagonal coordinate transformation matrices $Q$ and $R$

$$Q = \begin{bmatrix} Q^1 & & \\ & \ddots & \\ & & Q^q \end{bmatrix}, \qquad R = \begin{bmatrix} R^1 & & \\ & \ddots & \\ & & R^q \end{bmatrix}, \tag{4.44}$$

we eventually obtain the sequence of coordinate transformations reducing the Jacobian matrix $A$ to the Jordan normal form:

$$\hat{A} = (RQP)A(RQP)^{-1} = \begin{bmatrix} \hat{A}^1 & & \\ & \ddots & \\ & & \hat{A}^q \end{bmatrix}, \tag{4.45}$$

where each block $\hat{A}^r$, $r = 1, \cdots, q$ is defined by (4.41).

### 4.1.5 Conditions for Controllability

Once the Jacobian is reduced to the Jordan normal form, we can turn to the problem of reducing the controllability condition to a set of simpler conditions that will give us the restrictions on the admissible set of control parameters. Since the controllability is a property of the system which does not depend on the choice of the coordinate system, condition (4.8) is invariant with respect to any (nonsingular) coordinate transformation [50], and hence is satisfied for the pair $(A, B)$, if and only if it is satisfied for the pair $(\hat{A}, \hat{B})$, where $\hat{B} = (RQP)B$ is the transformed control matrix. Let us partition the transformed control matrix $\hat{B}$ according to the block structure of $\hat{A}$:

$$\hat{B} = \begin{bmatrix} \hat{B}^1 \\ \vdots \\ \hat{B}^q \end{bmatrix}, \qquad \hat{B}^r = \begin{bmatrix} \hat{B}^{r1} \\ \vdots \\ \hat{B}^{rp'_r} \end{bmatrix}, \qquad \hat{B}^{r\alpha} = \begin{bmatrix} \hat{B}^{r\alpha}_1 \\ \vdots \\ \hat{B}^{r\alpha}_{j_{r\alpha}} \end{bmatrix}, \qquad \hat{B}^{r\alpha}_i = \begin{bmatrix} \hat{B}^{r\alpha}_{i1} \\ \vdots \\ \hat{B}^{r\alpha}_{id_r} \end{bmatrix}, \tag{4.46}$$

and denote $\hat{\mathbf{b}}^{r\alpha}_{ij}$ the first row of the matrix $\hat{B}^{r\alpha}_{ij}$. Next, define the matrix $\bar{B}^{r\alpha}$ using the relations

$$\bar{B}^{r\alpha} = \begin{bmatrix} \bar{B}^{r\alpha}_1 \\ \vdots \\ \bar{B}^{r\alpha}_{j_{r\alpha}} \end{bmatrix}, \qquad \bar{B}^{r\alpha}_i = \begin{bmatrix} \hat{\mathbf{b}}^{r\alpha}_{i1} \\ \vdots \\ \hat{\mathbf{b}}^{r\alpha}_{id_r} \end{bmatrix}. \tag{4.47}$$

In the absence of accidental degeneracy between the eigenvalues that correspond to different invariant subspaces $L^r_{\mathcal{L}'}$ equation (4.42) ensures that there are exactly $d_r j_{r\alpha}$ Jordan blocks $\Lambda^{r\alpha}_i$ with the same eigenvalue $\lambda_{r\alpha}$. If, however, there is such an accidental degeneracy involving $s$ different invariant subspaces $L^{r_1}_{\mathcal{L}'}, \cdots, L^{r_s}_{\mathcal{L}'}$, such that

for certain $\alpha_1, \cdots, \alpha_s$

$$\lambda_{r_1\alpha_1} = \cdots = \lambda_{r_s\alpha_s}, \tag{4.48}$$

the number of Jordan blocks corresponding to the eigenvalue $\lambda_{r\alpha}$ increases to

$$j'_{r\alpha} \equiv \sum_{r',\alpha':\, \lambda_{r'\alpha'}=\lambda_{r\alpha}} d_{r'} j_{r'\alpha'}. \tag{4.49}$$

The knowledge of the number of Jordan blocks is very important, since, according to the standard result of linear system theory [50], it ultimately determines the minimal number of control parameters. Specifically, it can be shown that the controllability condition for the pair of matrices $(\hat{A}, \hat{B})$ is satisfied, if and only if for every $r$ and $\alpha$ (taken equal to $r_1$ and $\alpha_1$ below)

$$\operatorname{rank} \begin{bmatrix} \bar{B}^{r_1\alpha_1} \\ \vdots \\ \bar{B}^{r_s\alpha_s} \end{bmatrix} = j'_{r\alpha} = d_{r_1} j_{r_1\alpha_1} + \cdots + d_{r_s} j_{r_s\alpha_s}, \tag{4.50}$$

where the indices $r_i$ and $\alpha_i$ are chosen according to (4.48). This, in turn, can be achieved, if and only if $n_u \geq j'_{r\alpha}$ for every $r$ and $\alpha$. Hence, in the most general case the minimal number $\bar{n}_u$ of independent control parameters should equal the maximal number of Jordan blocks with the same eigenvalue $\lambda_{r\alpha}$:

$$\bar{n}_u = \max_{r=1,\cdots,q} \max_{\alpha=1,\cdots,p'_r} j'_{r\alpha}. \tag{4.51}$$

Note that, since the block $\bar{B}^{r\alpha}$ has $d_r j_{r\alpha}$ rows, $\operatorname{rank}(\bar{B}^{r\alpha}) \leq d_r j_{r\alpha}$ for every $r$ and $\alpha$. Using this fact, the trivial matrix inequality

$$\operatorname{rank} \begin{bmatrix} \bar{B}^{r_1\alpha_1} \\ \vdots \\ \bar{B}^{r_s\alpha_s} \end{bmatrix} \leq \operatorname{rank}(\bar{B}^{r_1\alpha_1}) + \cdots + \operatorname{rank}(\bar{B}^{r_s\alpha_s}), \tag{4.52}$$

and equation (4.50) one obtains

$$\operatorname{rank}(\bar{B}^{r\alpha}) = d_r j_{r\alpha}, \quad r = 1, \cdots, q,\ \alpha = 1, \cdots, p_r. \tag{4.53}$$

Furthermore, according to the definition (4.47) of the matrix $\bar{B}^{r\alpha}$, for every $r$ and $\alpha$

$\mathrm{rank}(\hat{B}^{r\alpha}) \geq \mathrm{rank}(\bar{B}^{r\alpha})$, so one can write

$$\mathrm{rank}(\hat{B}^r) = \mathrm{rank} \begin{bmatrix} \hat{B}^{r1} \\ \vdots \\ \hat{B}^{rp_r} \end{bmatrix} \geq \max_{\alpha=1,\cdots,p_r} \mathrm{rank}(\hat{B}^{r\alpha}) \geq d_r \max_{\alpha=1,\cdots,p_r} j_{r\alpha}. \tag{4.54}$$

In addition, since $Q^r$ and $R^r$ are nonsingular coordinate transformations which do not change the rank of a matrix,

$$\mathrm{rank}(\hat{B}^r) = \mathrm{rank}(R^r Q^r P^r B) = \mathrm{rank}(P^r B), \tag{4.55}$$

where we got rid of all system-specific information, which was contained in the matrices $Q^r$ and $R^r$.

The symmetry information alone is insufficient to determine the values of either $j_{r\alpha}$ or $j'_{r\alpha}$. However, by definition one has $p_r \geq j_{r\alpha} \geq 1$ so that $j'_{r\alpha} \geq d_r$. As a consequence, we obtain two necessary conditions for controllability. First of all, equation (4.51) yields the lower bound on the minimal number of control parameters

$$\bar{n}_u \geq \max_{r=1,\cdots,q} d_r. \tag{4.56}$$

Second, inequality (4.54) combined with equality (4.55) imposes a number of restriction on the control matrix $B$,

$$\mathrm{rank}(P^r B) \geq d_r, \quad r = 1, \cdots, q, \tag{4.57}$$

which can be interpreted as the requirement of the mutual independence of control parameters. We can therefore, conclude that an arbitrary (unitary) subgroup $\mathcal{L}'$ of the full dynamical symmetry group $\mathcal{L}$ does not completely define the minimal set of control parameters. It does, however, define a set of necessary conditions required for controllability. In general, the knowledge of all dynamical symmetries, both unitary and nonunitary, described by the group $\mathcal{L}$ is required in order to completely resolve the structure of the Jacobian matrix and obtain the necessary and sufficient condition for controllability.

Nevertheless, even without knowing the full symmetry group $\mathcal{L}$ one can obtain

the necessary and sufficient conditions by making a number of assumptions. First, assume that there are no accidental degeneracies (it is usually safe to do so if, e.g., $\mathcal{L}' = \mathcal{H}_{\bar{\mathbf{x}}}$: we ensure that all physical symmetries are taken into account, and accidental degeneracies should only appear for certain special values of system parameters). Then $j_{r\alpha} = 1$, $j'_{r\alpha} = d_r$, and $\bar{B}^{r\alpha} = \hat{B}^{r\alpha}$ for all $r$ and $\alpha$, so condition (4.51) is equivalent to

$$\bar{n}_u = \max_{r=1,\cdots,q} d_r. \tag{4.58}$$

If, in addition, no irreducible representation $T^r$ of $\mathcal{L}'$ enters the decomposition (4.23) more than once, such that $p_r = 1$ for all $r$, instead of inequality (4.57) one obtains the equality:

$$\operatorname{rank}(P^r B) = d_r, \quad r = 1, \cdots, q. \tag{4.59}$$

Conditions (4.57) and (4.59) can be simplified even further by defining the projection operator $\hat{P}^r \equiv (P^r)^\dagger P^r$ onto the invariant subspace $L^r_{\mathcal{L}'} \subset \mathbb{R}^{n_x}$. This operator can be obtained directly from the matrix representation $T$ for most symmetry groups of interest. For finite discrete groups it is given by

$$\hat{P}^r = \frac{d_r}{n_g} \sum_{g \in \mathcal{L}'} \chi^r(g) T(g), \tag{4.60}$$

where $n_g$ is the number of elements of the group $\mathcal{L}'$ and $\chi^r(g)$ is the character of the group element $g$ in the representation $T^r$. Similarly, for compact continuous groups we have

$$\hat{P}^r = d_r \int_{\mathcal{L}'} \chi^r(g) T(g)\, d\mu(g), \tag{4.61}$$

where $d\mu(g)$ is the group measure [52]. Observing that $\operatorname{rank}((P^r)^\dagger P^r B) = \operatorname{rank}(P^r B)$, we can use the projection operators to rewrite the condition (4.59) in an equivalent form

$$\operatorname{rank}(\hat{P}^r B) = d_r, \quad r = 1, \cdots, q. \tag{4.62}$$

Summing up, we conclude that with the two assumptions made above the system is controllable, if and only if the two conditions are met. The first one requires the number $n_u$ of control parameters to be greater or equal to the dimensionality $d_r$ of

the largest irreducible representation $T^r$ present in the decomposition of the matrix representation $T$ of the subgroup $\mathcal{L}' \subseteq \mathcal{L}$ in the tangent space $\mathbb{R}^{n_x}$. The second one requires the control parameters to be independent: the columns $\mathbf{b}_m$ of the control matrix $B$ have to be chosen such that $d_r$ of the projections $\hat{P}^r\mathbf{b}_m$, $m = 1, \cdots, n_u$ are linearly independent (and, therefore, span the eigenspace $L^r = L^r_{\mathcal{L}'}$) for every $r = 1, \cdots, q$. The last requirement imposes a number of restrictions on the admissible form of the linear response of the system to perturbations of control parameters.

A number of comments are in order. First of all, as we have just seen, the number of control parameters is determined by the number of Jordan blocks with the same eigenvalue, not the multiplicity of that eigenvalue. It becomes intuitively clear why this is so, if one compares the action of different Jacobians already reduced to the Jordan form. For instance, the Jacobian

$$A_1 = \begin{bmatrix} \lambda & & \\ & \lambda & \\ & & \lambda \end{bmatrix} \tag{4.63}$$

generates the set of three linearly dependent vectors $\mathbf{h}^0 = \mathbf{b}$, $\mathbf{h}^1 = \lambda\mathbf{b}$, $\mathbf{h}^2 = \lambda^2\mathbf{b}$ (compare to (4.6)), that span a one-dimensional subspace of $\mathbb{R}^3$ for an arbitrary choice of $\mathbf{b}$. As a result, three control parameters and a control matrix with three linearly independent columns, $B = [\,\mathbf{b}_1 \quad \mathbf{b}_2 \quad \mathbf{b}_3\,]$, are necessary to control the system. On the contrary, the Jacobian

$$A_2 = \begin{bmatrix} \lambda & & \\ 1 & \lambda & \\ & 1 & \lambda \end{bmatrix} \tag{4.64}$$

generates a linearly independent set of basis vectors that spans $\mathbb{R}^3$, requiring just one control parameter and a control matrix with a single column $B = \mathbf{b}$.

Second, symmetry does not always make the Jacobian degenerate, and the non-degenerate case can be handled in the same way as the one with no symmetries. Neither does the degeneracy by itself imply that multi-parameter control is required: even if the eigenvalue $\lambda_{r'\alpha'}$ is degenerate, but $j'_{r\alpha} = d_r = 1$ for every $r$ and $\alpha$ (the degeneracy is accidental and limited to a single invariant subspace $L^{r'}_{\mathcal{L}'}$), one control parameter is sufficient to ensure the controllability. In both cases, however, the

dynamical symmetry should be rather low. Specifically, the decomposition (4.23) of the matrix representation $T$ should not contain any multi-dimensional irreducible representations.

Finally, the conditions on the set of control parameters that were obtained above are imposed by the *controllability* condition and guarantee that control can be achieved. However, in general, only the weaker *stabilizability* condition has to be satisfied which, according to section 4.1.1, requires that every *unstable* normal mode of the system is controllable, so that, only $r$ and $\alpha$ such that $|\lambda_{r\alpha}| \leq 1$ have to be considered in the conditions (4.50) and (4.51). As a consequence, it might be possible to stabilize highly symmetric states of compact extended systems with strong spatial correlations using a single control parameter — if only a small number of modes is excited, there is a chance that all *unstable* modes will correspond to one-dimensional irreducible representations $T^r$. In strongly chaotic systems a large number of modes will be unstable and many of them will inevitably be degenerate, calling for multi-parameter control. Similar considerations apply to weakly chaotic systems with large spatial extent.

## 4.2 Time-Varying States

The results obtained above for the time-invariant case can be generalized for the time-varying and, in particular, time-periodic case, but first we have to define the notions of controllability and dynamical symmetry in the context of time-varying trajectories. Indeed, in the time-varying case the Jacobian $A^t$ and the control matrix $B^t$ in the linearized evolution equation (3.11) are time-dependent and, as a consequence, neither the definition of controllability given in section 4.1.1 nor the condition (4.8) holds. Besides, it is not at all clear that the symmetry of the target trajectory, and hence the dynamical symmetry group $\mathcal{L}$ can be uniquely and consistently defined.

We will see that all these notions generalize in a rather straightforward way, so that the same formalism as we used in the previous sections applies here as well. To begin with, we define the controllability of a general time-varying linear system. Expanding the definition given for time-invariant target states, we call the $n_x$-dimensional linear system (3.11) or the sequences of matrices $\{A^t, B^t\}$ controllable if, for any initial

state $\Delta\mathbf{x}^{t_i} = \Delta\mathbf{x}_i$, times $t_f - t_i \geq n_x$, and final state $\Delta\mathbf{x}_f$, there exists a sequence of control perturbations $\Delta\mathbf{u}^{t_i}, \cdots, \Delta\mathbf{u}^{t_f-1}$ such that the solution of equation (3.11) satisfies $\Delta\mathbf{x}^{t_f} = \Delta\mathbf{x}_f$.

The controllability condition can be restated in terms of the matrices $A^t$ and $B^t$ conducting the analysis similar to that of section 4.1.1. Applying the map (3.11) $n_x$ times yields

$$\Delta\mathbf{x}^{t+n_x} = J_{n_x}^{t+n_x-1}\Delta\mathbf{x}^t + \sum_{k=0}^{n_x-1} J_{n_x-1-k}^{t+n_x-1} B^{t+k}\Delta\mathbf{u}^{t+k}, \tag{4.65}$$

where we have introduced a shorthand notation

$$J_k^t = A^t A^{t-1}\cdots A^{t-k+1} \tag{4.66}$$

for the product of $k$ consecutive Jacobians. Arguments identical to those used to derive the controllability condition (4.8) from equation (4.4) allow us to conclude that for time-varying states the controllability condition can again be written in the matrix form:

$$\text{rank}(\mathcal{C}_t) = n_x, \quad \forall t, \tag{4.67}$$

where the controllability matrix (4.9) is now replaced with the sequence of matrices

$$\mathcal{C}_t \equiv [\, B^t \quad J_1^t B^{t-1} \quad J_2^t B^{t-2} \quad \cdots \quad J_{n_x-1}^t B^{t-n_x+1} \,]\,. \tag{4.68}$$

Next we have to define the dynamic symmetry group $\mathcal{L}$. Suppose the target trajectory $\bar{\mathbf{x}}^1, \bar{\mathbf{x}}^2, \cdots, \bar{\mathbf{x}}^\tau$ has period $\tau$, and the symmetry of the point $\bar{\mathbf{x}}^t$ on the target trajectory is described by the group $\mathcal{H}_{\bar{\mathbf{x}}^t} \subseteq \mathcal{G}$. We can then write

$$g(\bar{\mathbf{x}}^{t+1}) = g(\mathbf{F}(\bar{\mathbf{x}}^t, \bar{\mathbf{u}})) = \mathbf{F}(g(\bar{\mathbf{x}}^t), \bar{\mathbf{u}}) = \mathbf{F}(\bar{\mathbf{x}}^t, \bar{\mathbf{u}}) = \bar{\mathbf{x}}^{t+1} \tag{4.69}$$

for every $g \in \mathcal{H}_{\bar{\mathbf{x}}^t}$. Consequently,

$$\mathcal{H}_{\bar{\mathbf{x}}^1} \subseteq \mathcal{H}_{\bar{\mathbf{x}}^2} \subseteq \cdots \subseteq \mathcal{H}_{\bar{\mathbf{x}}^\tau} \subseteq \mathcal{H}_{\bar{\mathbf{x}}^1}, \tag{4.70}$$

which means that the symmetry properties of all the points on the target trajectory

are the same and the isotropy symmetry group of the *trajectory* $\mathcal{H}_{\bar{\mathbf{x}}}$ can be uniquely defined using an arbitrary point $\bar{\mathbf{x}}^t$, $\mathcal{H}_{\bar{\mathbf{x}}} = \mathcal{H}_{\bar{\mathbf{x}}^t}$.

Using the arguments that lead to equation (4.15) we obtain for an arbitrary $g \in \mathcal{H}_{\bar{\mathbf{x}}}$:

$$\begin{aligned}
\bar{\mathbf{x}}^{t+1} + g(A^t\Delta\mathbf{x}) &= g(\bar{\mathbf{x}}^{t+1}) + g(A^t\Delta\mathbf{x}) = g(\bar{\mathbf{x}}^{t+1} + A^t\Delta\mathbf{x}) \\
&= g(\mathbf{F}(\bar{\mathbf{x}}^t, \bar{\mathbf{u}}) + A^t\Delta\mathbf{x}) = g(\mathbf{F}(\bar{\mathbf{x}}^t + \Delta\mathbf{x}, \bar{\mathbf{u}})) \\
&= \mathbf{F}(g(\bar{\mathbf{x}}^t + \Delta\mathbf{x}), \bar{\mathbf{u}}) = \mathbf{F}(g(\bar{\mathbf{x}}^t) + g(\Delta\mathbf{x}), \bar{\mathbf{u}}) \\
&= \mathbf{F}(\bar{\mathbf{x}}^t + g(\Delta\mathbf{x}), \bar{\mathbf{u}}) = \mathbf{F}(\bar{\mathbf{x}}^t, \bar{\mathbf{u}}) + A^t g(\Delta\mathbf{x}) \\
&= \bar{\mathbf{x}}^{t+1} + A^t g(\Delta\mathbf{x}). \qquad (4.71)
\end{aligned}$$

This, in turn, means that the symmetry group $\mathcal{L}_t$ of the Jacobian $A^t$ satisfies

$$\mathcal{H}_{\bar{\mathbf{x}}} \subseteq \mathcal{L}_t, \quad t = 1, \cdots, \tau. \qquad (4.72)$$

Again, typically, we expect $\mathcal{L}_t = \mathcal{H}_{\bar{\mathbf{x}}}$, so that $\mathcal{L}$ too would be unique for any given periodic trajectory as would the matrix representation $T$, such that

$$T(g)A^t = A^t T(g), \quad \forall g \in \mathcal{L}. \qquad (4.73)$$

It is, therefore, enough to know the symmetry properties of an arbitrary point of the periodic trajectory in order to establish the requirements on the control scheme similarly to the time-invariant case. If $\mathcal{L}_t$ is not unique, we can still use the commutation relation (4.73) for the subgroup $\mathcal{L}' = \mathcal{H}_{\bar{\mathbf{x}}}$ to obtain a lower bound on the minimal number of control parameters.

Finally, we note that although it is possible to obtain certain results for time-varying control matrices $B^t$, we assume, as is often the case in real systems, that $B^t$ is constant and drop the time index. As we will discover below, in the time-periodic case the restrictions imposed by symmetry on the structure of the matrix $B$ can typically be determined without the detailed knowledge of the Jacobian matrices, but based on the symmetry properties alone, similarly to the time-invariant case. Indeed, let us construct the representation $T$ of the group $\mathcal{L}'$ in the tangent space $\mathbb{R}^{n_x}$ and decompose it into the sum of irreducible representations. This again defines a set of invariant subspaces $L^{r\alpha}_{\mathcal{L}'}$ and a set of basis vectors $\{\mathbf{e}^{r\alpha}_i\}$, which we use to

construct the coordinate transformation matrix $P$ according to the definition (4.29).

Since the rank of the matrix (4.68) does not change under a coordinate transformation, the controllability condition (4.67) is equivalent to the condition

$$\mathrm{rank}(\bar{\mathcal{C}}_t) = n_x, \quad t = 1, \cdots, \tau \tag{4.74}$$

where

$$\bar{\mathcal{C}}_t = [\, \bar{B} \quad \bar{J}_1^t \bar{B} \quad \cdots \quad \bar{J}_{n_x-1}^t \bar{B} \,], \tag{4.75}$$

$\bar{B} = PB$ and $\bar{J}_k^t = PJ_k^t(P)^{-1}$. The products $J_k^t$ have the same symmetry properties as the Jacobian matrices $A^t$ for arbitrary $k$ and $t$, and, therefore, both the matrices $A^t$ and the products $J_k^t$ block-diagonalize in exactly the same way:

$$\bar{A}^t = PA^t(P)^{-1} = \begin{bmatrix} \bar{A}^{t,1} & & \\ & \ddots & \\ & & \bar{A}^{t,q} \end{bmatrix}, \tag{4.76}$$

and

$$\bar{J}_k^t = PJ_k^t(P)^{-1} = \begin{bmatrix} \bar{J}_k^{t,1} & & \\ & \ddots & \\ & & \bar{J}_k^{t,q} \end{bmatrix}. \tag{4.77}$$

Similarly to the time-invariant case, the blocks $\bar{A}^{t,r}$ and $\bar{J}_k^{t,r}$ are themselves block-diagonal

$$\bar{A}^{t,r} = \begin{bmatrix} \bar{\Lambda}^{t,r} & & \\ & \ddots & \\ & & \bar{\Lambda}^{t,r} \end{bmatrix}, \qquad \bar{J}^{t,r} = \begin{bmatrix} \bar{\Gamma}_k^{t,r} & & \\ & \ddots & \\ & & \bar{\Gamma}_k^{t,r} \end{bmatrix} \tag{4.78}$$

and consist of $d_r$ identical $p_r \times p_r$ blocks $\bar{\Lambda}^{t,r}$ and $\bar{\Gamma}_k^{t,r}$, respectively, whose matrix elements are defined by the scalar products

$$\begin{aligned} (\bar{\Lambda}^{t,r})_{\alpha\beta} &\equiv (\mathbf{e}_i^{r\alpha} \cdot A^t \mathbf{e}_i^{r\beta}), \\ (\bar{\Gamma}_k^{t,r})_{\alpha\beta} &\equiv (\mathbf{e}_i^{r\alpha} \cdot J_k^t \mathbf{e}_i^{r\beta}). \end{aligned} \tag{4.79}$$

Using the definition (4.66) one can check that for any $t$, $k$ and $r$ the matrix $\bar{\Gamma}_k^{t,r}$ can

be represented as the product

$$\bar{\Gamma}_k^{t,r} = \bar{\Lambda}^{t,r}\bar{\Lambda}^{t-1,r}\cdots\bar{\Lambda}^{t-k+1,r}. \tag{4.80}$$

Let us partition the transformed control matrix $\bar{B}$ into blocks $\bar{B}^r = P^r B$ and define the reduced controllability matrices

$$\bar{\mathcal{C}}_t^r = [\,\bar{B}^r \quad \bar{J}_1^{t,r}\bar{B}^r \quad \cdots \quad \bar{J}_{n_x-1}^{t,r}\bar{B}^r\,]. \tag{4.81}$$

Using relation (4.24) and the fact that the matrix $\bar{\mathcal{C}}_t^r$ has $d_r p_r$ rows one can write

$$\operatorname{rank}(\bar{\mathcal{C}}_t) = \operatorname{rank}\begin{bmatrix}\bar{\mathcal{C}}_t^1\\ \vdots \\ \bar{\mathcal{C}}_t^q\end{bmatrix} \leq \operatorname{rank}(\bar{\mathcal{C}}_t^1) + \cdots \operatorname{rank}(\bar{\mathcal{C}}_t^q) \leq d_1 p_1 \cdots d_q p_q = n_x \tag{4.82}$$

to obtain as a consequence of (4.74) the set of reduced controllability conditions

$$\operatorname{rank}(\bar{\mathcal{C}}_t^r) = d_r p_r, \quad r = 1, \cdots, q. \tag{4.83}$$

The blocks $\bar{J}_k^{t,r}\bar{B}^r$ of the matrix (4.81) can become linearly dependent for certain $\tau$, $d_r$ and $p_r$. Indeed, it is trivial to see that for a sequence of $n$ arbitrary $p \times p$ matrices $R_i$, it is always possible to find a set of coefficients $\mu_0, \mu_1, \cdots, \mu_n$ such that

$$\mu_0 I + \mu_1 R_1 + \cdots + \mu_n R_n = 0, \tag{4.84}$$

as long as $n \geq p^2$. Equally easy to establish is the fact that, if the matrices $R_i$ are not arbitrary, but satisfy the condition

$$R_i = W_1 W_2 \cdots W_i, \tag{4.85}$$

where $W_i$ is a sequence of arbitrary $p \times p$ matrices, such that $W_{i+\tau} = W_i$, equation (4.84) can always be satisfied for $n \geq \min(p^2, p\tau)$. The $p_r \times p_r$ matrices $\bar{\Gamma}_1^{t,r}, \cdots, \bar{\Gamma}_{n_x-1}^{t,r}$ form precisely the sequence satisfying the condition (4.85). Besides, if the condition (4.84) is satisfied for $R_i = \bar{\Gamma}_i^{t,r}$, it is satisfied for the sequence $R_i = \bar{J}_i^{t,r}$ as well. As a

result,

$$\mathrm{rank}(\bar{\mathcal{C}}_t^r) = \mathrm{rank}\,[\,\bar{B}^r \quad \bar{J}_1^{t,r}\bar{B}^r \quad \cdots \quad \bar{J}_{n-1}^{t,r}\bar{B}^r\,] \tag{4.86}$$

for $n = \min(p_r^2, p_r\tau)$ and arbitrary $\bar{B}^r$. Therefore, in order for the conditions (4.83), and hence (4.67), to be satisfied, one should have

$$\mathrm{rank}(P^r B) \geq \mathrm{ceil}\left(\max\left(\frac{d_r}{p_r}, \frac{d_r}{\tau}\right)\right), \quad r = 1, \cdots, q, \tag{4.87}$$

where $\mathrm{ceil}(x)$ denotes the smallest integer number $n$ such that $n \geq x$. The necessary conditions on the control matrix $B$, defined by (4.87) are the generalization of the time-invariant result (4.57). Instead of (4.56) one respectively obtains the restriction on the minimal number of independent control parameters required to satisfy the controllability condition (4.67) for a periodic target trajectory:

$$\bar{n}_u \geq \mathrm{ceil}\left(\max_{r=1,\cdots,q} \max\left(\frac{d_r}{p_r}, \frac{d_r}{\tau}\right)\right). \tag{4.88}$$

It is interesting to note that a periodic trajectory can be made controllable using the number of control parameters $n_u$ that could be smaller than the number required for a steady state with the same symmetry.

Three special cases deserve separate consideration. First of all, suppose that the Jacobian matrices $A^t$ commute with each other, so they can be simultaneously diagonalized. In this case the condition (4.84) can be satisfied by an appropriate choice of coefficients $\mu_1, \cdots, \mu_n$ for $n \geq p_r$, so the necessary conditions (4.88) and (4.87) will reduce to (4.56) and (4.57), respectively, and $\bar{n}_u$ will no longer depend on the period $\tau$ of the target trajectory.

Next, suppose there are no accidental degeneracies between the eigenvalues of the Jacobians $A^t$ and their products $J_k^t$, and no irreducible representation of $\mathcal{L}'$ appears in the decomposition (4.23) more than once (so that Jacobian matrices can again be simultaneously diagonalized). Now, however, identically to the time-invariant case one obtains the necessary and sufficient conditions (4.58) and (4.59) instead of the necessary conditions (4.56) and (4.57).

Finally, although we used the fact that the trajectory is periodic to derive the above results, this requirement could be lifted, provided the symmetry of all points

on the target trajectory is the same, and, therefore, the condition (4.73) is satisfied. A nonperiodic trajectory could then be treated as a periodic one, with period $\tau = \infty$, and the condition (4.84) will be satisfied by an appropriate choice of coefficients $\mu_1, \cdots, \mu_n$ for $n \geq p_r^2$. As a result, instead of the restriction (4.88) one will obtain

$$\bar{n}_u \geq \text{ceil}\left(\max_{r=1,\cdots,q} \frac{d_r}{p_r}\right). \tag{4.89}$$

## 4.3 Continuous-Time Systems

Most of the results obtained in the previous sections can be directly and naturally generalized to continuous-time systems. This is a rather valuable asset of the developed theory, since continuous-time control is, in general, a much more flexible and powerful technique than discrete-time control. In the presence of a decent continuous-time mathematical model (3.2), continuous-time control can often achieve far superior results. It is, however, a much more complicated technique as well. For simplicity we only discuss the control of time-invariant target states. Linearizing the evolution equation (3.2) around the steady target state $\bar{\mathbf{s}}$, one obtains

$$\Delta\dot{\mathbf{s}}(t) = A\Delta\mathbf{s}(t) + B\Delta\mathbf{u}(t), \tag{4.90}$$

where similarly to the discrete-time case we define the Jacobian

$$A = \mathbf{D_s}\mathbf{\Phi}(\bar{\mathbf{s}}, \bar{\mathbf{u}}) \tag{4.91}$$

and the control matrix

$$B = \mathbf{D_u}\mathbf{\Phi}(\bar{\mathbf{s}}, \bar{\mathbf{u}}). \tag{4.92}$$

The symmetries of the nonlinear evolution equation (3.2), the target state $\bar{\mathbf{s}}$, and the linearization (4.90) are determined identically to the discrete-time case using the relations (4.13), (4.14), and (4.16), yielding the symmetry groups $\mathcal{G}$, $\mathcal{H}_{\bar{\mathbf{s}}}$, and $\mathcal{L}$, respectively. The definitions of the notions of stabilizability and controllability in the continuous-time case are completely analogous to the ones given in section 4.1.1 for the discrete-time case.

The dynamical system described by equation (4.90) or the pair $(A, B)$ is said to be controllable if, for any initial state $\Delta\mathbf{s}(t_i) = \Delta\mathbf{s}_i$, times $t_f - t_i > 0$ and final state $\Delta\mathbf{s}_f$, there exists a (piecewise continuous) control perturbation $\Delta\mathbf{u}(t)$ such that the solution of equation (4.90) satisfies $\Delta\mathbf{s}(t_f) = \Delta\mathbf{s}_f$. Otherwise the system or the pair $(A, B)$ is called uncontrollable.

Similarly, the dynamical system or the pair $(A, B)$ is said to be stabilizable, if there exists a state feedback $\Delta\mathbf{u}(t) = -K\Delta\mathbf{s}(t)$ making the system stable, such that all eigenvalues of the matrix $A' = A - BK$ have a negative real part, $\mathrm{Re}(\lambda'_k) < 0$, $\forall k$. Otherwise the system or the pair $(A, B)$ is called unstabilizable.

The controllability of the pair $(A, B)$ again ensures that all eigenvalues of $A'$ can be chosen appropriately, so that any controllable continuous-time system is stabilizable as well. The controllability of a continuous-time system is also established using the same criterion (4.8) used to test for the controllability in the discrete-time case. As a result, the conditions imposed on the control matrix $B$ by the controllability condition in the presence of symmetry are exactly the same as those obtained for discrete-time systems.

### 4.3.1 Particle in a Symmetric Potential

The motion of a particle in a symmetric potential, such as a point charge in electric field, serves as an example of the relation between the groups $\mathcal{G}$ and $\mathcal{L}$. This and many other interesting physical systems, e.g., inverted pendulum, or a satellite in orbit, are described by the second order ordinary differential equation

$$m\ddot{\mathbf{r}} = -\nabla V(\mathbf{r}), \tag{4.93}$$

which can be trivially reduced to a system of first order differential equations of the form (3.2) introducing additional coordinate $\mathbf{v} = \dot{\mathbf{r}}$. Suppose the potential $V(\mathbf{r})$ possesses the cubic symmetry (described by the group O which is a subgroup of SO(3)), but is not spherically symmetric, for instance:

$$V(\mathbf{r}) = V_0 \cosh(kx)\cosh(ky)\cosh(kz). \tag{4.94}$$

The group $\mathcal{G} = \mathrm{O}$ defines the structural symmetry of the evolution equation (4.93). Linearizing it about the steady equilibrium point $\bar{\mathbf{r}} = 0$ we obtain

$$\partial_t \begin{bmatrix} \mathbf{r} \\ \mathbf{v} \end{bmatrix} = \begin{bmatrix} 0 & I \\ \omega^2 I & 0 \end{bmatrix} \begin{bmatrix} \mathbf{r} \\ \mathbf{v} \end{bmatrix}, \tag{4.95}$$

where $\omega^2 = -V_0 k^2/m$, while 0 and $I$ are $3 \times 3$ zero and unit blocks, respectively. If $V_0 < 0$ the equilibrium is unstable, and control should be applied to keep the system close to the equilibrium state.

Equation (4.95) is spherically symmetric, with $\mathcal{L}' = \mathrm{SO}(3)$ and, therefore, $\mathcal{G} \subset \mathcal{L}$, i.e., the symmetry of the linearized equation is higher than the symmetry of the original nonlinear evolution equation. (In fact, the full symmetry group of equation (4.95) is $\mathcal{L} = \mathrm{GL}(3)$, but we choose to use its subgroup $\mathcal{L}' = \mathrm{SO}(3)$, since it is physically more relevant, completely resolves the structure of the Jacobian matrix and, as such, correctly represents the effect of symmetry on the control setup.)

Next we notice that the representation $T$ of the group $\mathcal{L}'$ in the six-dimensional tangent space $\{\mathbf{r}, \mathbf{v}\}$ can be decomposed into a sum of two equivalent three-dimensional irreducible representations of SO(3) (vector representations, which coincide with the respective irreducible representation of GL(3)):

$$T = 2T^1, \qquad d_1 = 3. \tag{4.96}$$

This indicates that in order to control the unstable steady state $\bar{\mathbf{r}} = \bar{\mathbf{v}} = 0$ one needs at least three independent control parameters, $\bar{n}_u = 3$.

Arguably the simplest way to control such a system is to re-adjust the potential (applying external fields, shifting support point, etc.) based on the instantaneous values of the position $\mathbf{r}$ and velocity $\mathbf{v}$ of the particle. This corresponds to picking the control matrix in the following form:

$$B = \begin{bmatrix} 0 & 0 & 0 \\ \mathbf{b}_1 & \mathbf{b}_2 & \mathbf{b}_3 \end{bmatrix}, \tag{4.97}$$

where $\mathbf{b}_1$, $\mathbf{b}_2$, $\mathbf{b}_3$ could be chosen as any three linearly independent vectors in $\mathbb{R}^3$.

## 4.4 Symmetry Violation

In reality symmetries of physical systems displaying dynamical instabilities are almost never exact. Indeed, the cylinders in a Taylor-Couette experiment are never perfectly circular, the temperature inside a chemical reactor is never absolutely uniform, neither are the rotor blades of a turbocompressor exactly identical. The above analysis, on the other hand, has been conducted in the assumption of exact symmetry. Therefore, it is essential to understand how the obtained results change, if the symmetry is not exact or, in other words, what the effect of a weak symmetry violation is. Such an analysis is also crucial in the vicinity of points in the parameter space where symmetry increasing bifurcations or accidental degeneracies occur.

For simplicity let us again consider the time-invariant case. The Jacobian $A$ of a weakly perturbed symmetric system takes the form

$$A = A_0 + \epsilon A_1, \tag{4.98}$$

where $\epsilon$ denotes the magnitude of the perturbation and the unperturbed Jacobian $A_0$ is exactly symmetric with respect to all transformations $g$ of the group $\mathcal{L}$. For the group representation $T$ we thus have

$$T(g)A_0 - A_0T(g) = 0, \quad \forall g \in \mathcal{L}. \tag{4.99}$$

In general, the perturbation $\epsilon A_1$ will not be symmetric with respect to any element of the group $\mathcal{L}$, except the identity transformation $e$:

$$T(g)A_1 - A_1T(g) \neq 0, \quad \forall g \in \mathcal{L} \setminus \{e\}. \tag{4.100}$$

Therefore, since

$$T(g)A - AT(g) = \epsilon(T(g)A_1 - A_1T(g)), \tag{4.101}$$

the perturbation (4.98) completely destroys the symmetry of the linearized evolution equation (4.1) for any $\epsilon \neq 0$. As a result, the perturbed system can be made controllable using a single control parameter, irrespectively of the properties of the original symmetry group $\mathcal{L}$. For instance, calculating the controllability matrix of the

perturbed system with $n_u = 1$ and $B = \mathbf{b}$ one obtains

$$\mathcal{C} = \mathcal{C}_0 + \epsilon\mathcal{C}_1 + o(\epsilon^2), \tag{4.102}$$

where we defined

$$\begin{aligned} \mathcal{C}_0 &= [\,\mathbf{b} \quad A_0\mathbf{b} \quad \cdots \quad (A_0)^{n_x-1}\mathbf{b}\,], \\ \mathcal{C}_1 &= [\,0 \quad A_1\mathbf{b} \quad \cdots \quad ((A_0)^{n_x-2}A_1 + \cdots + A_1(A_0)^{n_x-2})\mathbf{b}\,]. \end{aligned} \tag{4.103}$$

$\mathcal{C}_0$ is clearly the controllability matrix of the unperturbed system with full symmetry, which does not have a full rank, if the decomposition (4.23) contains at least one irreducible representation $T^r$ with the dimensionality $d_r > 1$. Indeed, in the absence of accidental degeneracies that would mean

$$n_0 \equiv \mathrm{rank}(\mathcal{C}_0) \leq \sum_{r=1}^{q} p_r < n_x. \tag{4.104}$$

The controllability matrix $\mathcal{C}$ of the perturbed system, on the other hand, has full rank for any $\epsilon \neq 0$ because the symmetry is completely destroyed by the perturbation. Therefore, the perturbed *linear* system becomes controllable even though the unperturbed system is not, for *arbitrarily small* perturbations.

The controllability ensures that for any initial and final states of the linear system (4.1) the control can be found mapping the initial state to the final state in $n_x$ iterations. Using (4.4) one obtains explicitly

$$\Delta\mathbf{U}^t \equiv \begin{bmatrix} \Delta u^{t+n_x-1} \\ \vdots \\ \Delta u^t \end{bmatrix} = (\mathcal{C})^{-1}(\Delta\mathbf{x}^{t+n_x} - (A)^{n_x}\Delta\mathbf{x}^t). \tag{4.105}$$

Formally, if the system is controllable, the controllability matrix is invertible, and the solution (4.105) is well defined for any $\Delta\mathbf{x}^t$ and $\Delta\mathbf{x}^{t+n_x}$. However, when the matrix $\mathcal{C}$ is close to being singular its inverse is not well defined. It is convenient to use the singular value decomposition of the controllability matrix

$$\mathcal{C} = Q\Sigma R^\dagger, \tag{4.106}$$

where $Q = [\,\mathbf{q}_1 \quad \mathbf{q}_2 \quad \cdots \quad \mathbf{q}_{n_x}\,]$ and $R = [\,\mathbf{r}_1 \quad \mathbf{r}_2 \quad \cdots \quad \mathbf{r}_{n_x}\,]$ are some orthogonal $n_x \times n_x$ matrices, and

$$\Sigma = \begin{bmatrix} \sigma_1(\epsilon) & & \\ & \ddots & \\ & & \sigma_{n_x}(\epsilon) \end{bmatrix}. \tag{4.107}$$

The singular values are ordered such that $\sigma_1(\epsilon) \geq \sigma_2(\epsilon) \geq \cdots \geq \sigma_{n_x}(\epsilon)$ for $\forall\epsilon$. Additionally, equation (4.104) requires

$$\lim_{\epsilon \to 0} \sigma_i(\epsilon) = 0, \quad i = n_0 + 1, \cdots, n_x. \tag{4.108}$$

In terms of the matrices $Q$, $\Sigma$, and $R$ we can write the inverse of $\mathcal{C}$ as

$$(\mathcal{C})^{-1} = R(\Sigma)^{-1}Q^{\dagger} = \sum_{i=1}^{n_x} \sigma_i^{-1}(\epsilon)\mathbf{r}_i\mathbf{q}_i^{\dagger} \tag{4.109}$$

and, therefore, for small $\epsilon$ equation (4.105) gives

$$\Delta\mathbf{U}^t \approx \sum_{i=n_0+1}^{n_x} \frac{(\mathbf{q}_i \cdot \Delta\mathbf{x}^{t+n_x}) - (\mathbf{q}_i \cdot (A)^{n_x}\Delta\mathbf{x}^t)}{\sigma_i(\epsilon)}\mathbf{r}_i. \tag{4.110}$$

As a consequence, we obtain

$$\lim_{\epsilon \to 0} |\Delta\mathbf{U}^t| = \infty. \tag{4.111}$$

This relation means that at least one control perturbation of the feedback sequence $\Delta u^t, \cdots, \Delta u^{t+n_x-1}$ diverges as the symmetry breaking perturbation $\epsilon A_1$ of the Jacobian vanishes. Since no specific relation between the initial and the final state of the system was implied, the obtained result is general, and does not depend on the control method used to calculate the feedback.

In fact, a more general statement holds. Suppose the symmetry is violated only partially, such that the perturbed Jacobian (4.98) remains exactly symmetric with respect to a subgroup $\mathcal{L}'$ of the full symmetry group $\mathcal{L}$. Denote $\bar{n}_u$ and $\bar{n}'_u$ the minimal number of control parameters required (assuming exact symmetry) by the groups $\mathcal{L}$ and $\mathcal{L}'$, respectively. Then it can be shown that, similarly to the single-parameter case, at least one control perturbation of the feedback sequence $\Delta\mathbf{u}^t, \cdots, \Delta\mathbf{u}^{t+n_x-1}$ diverges as the symmetry breaking perturbation $\epsilon A_1$ of the Jacobian vanishes when-

ever $\bar{n}'_u \leq n_u < \bar{n}_u$. The same result is obtained if the independent with respect to the group $\mathcal{L}'$ control parameters become dependent with respect to the group $\mathcal{L}$, as indicated by the violation of the general independence condition (4.50). The time-periodic generalization is also straightforward. We will call this situation *parametric deficiency*.

In other words, although it might be possible to control a *linear* system with approximate symmetry using a number of control parameters which is smaller than that required in the assumption of exact symmetry, the stabilization requires feedback of very large magnitude. Such systems are called *weakly controllable* in the language of control theory. However, the linear system is only an abstraction. The linear approximation (3.11) of the evolution equation (3.9) is only valid for small perturbations $\Delta\mathbf{u}^t$ of the control parameters and small deviations $\Delta\mathbf{x}^t$ from the target trajectory. Besides, additional restrictions on the magnitude of the feedback are usually imposed by practical limitations, size and energy constraints, etc., at the implementation stage. One can, therefore, conclude that, since the feedback scales linearly with the deviation from the target trajectory, a nonlinear system with parametric deficiency can be stabilized using linear control only in an asymptotically contracting neighborhood of the target trajectory.

Finally, consider the vicinity of the point $\bar{\mathbf{u}}_0$ in the parameter space $\mathbb{R}^{n_u}$ at which an accidental degeneracy occurs, such that the dynamical symmetry is described by the group $\mathcal{L}'$ for $\bar{\mathbf{u}} \neq \bar{\mathbf{u}}_0$ and is increased to $\mathcal{L}$ (of which $\mathcal{L}'$ is a subgroup) for $\bar{\mathbf{u}} = \bar{\mathbf{u}}_0$. In this case $\mathcal{L}$ can be considered approximate symmetry in the vicinity of $\bar{\mathbf{u}}_0$, and the distance to that point determines how strongly (or weakly) the symmetry $\mathcal{L}$ is violated. Suppose the control scheme is such that there is a parametric deficiency. Then the system will remain controllable for $\bar{\mathbf{u}} \neq \bar{\mathbf{u}}_0$. However, the strength of feedback required to control the system will diverge as $\bar{\mathbf{u}}$ approaches $\bar{\mathbf{u}}_0$, at which point the system will become uncontrollable.

## 4.5 System Identification

In the conclusion of this chapter we return to the problem of phase space reconstruction discussed in chapter 3. In the present section we concentrate on the Takens' embedding theorem [34] which justifies the validity of the delay coordinate embedding technique. The theorem states that *generically* the embedding map $\mathbf{P} : \mathbf{s}(t) \to \mathbf{z}(t)$ generated by the vector (3.4) of sufficiently large dimensionality $n_z$ provides a global one-to-one representation of the chaotic attractor. And while this genericity assumption is satisfied for a typical system without symmetries, it is usually violated if symmetries are present. In other words, most symmetric systems are *nongeneric* in the sense of Takens. As a result of this nongenericity the state of the system becomes impossible to reconstruct using a single scalar output, no matter how large the dimensionality $n_z$ of the embedding space is, locally in the vicinity of highly symmetric periodic trajectories. The attractor of the system remains folded at certain points and along certain curves in the phase space, which prevents the global reconstruction as well. Using the language of control theory we will say that such systems are *unobservable* locally as well as globally.

The question of symmetry-caused nongenericity in the framework of phase space reconstruction of a general symmetric system was first considered by King and Stewart [49], who determined that the reason for the failure of the embedding theorem is the violation of one of Takens' generic assumptions that the flow defined by equation (3.2) has simple eigenvalues for low-period periodic trajectories. As we have seen above, symmetric systems typically (but not always) have degenerate eigenvalues (due to the fact that most nontrivial irreducible representations are multi-dimensional) and, as a consequence, are nongeneric. King and Stewart went on to formulate and prove a generalization of the Takens' embedding theorem, which required the output to be a *vector*, not a *scalar*, function of the actual state of the system $\mathbf{s}(t)$:

$$\mathbf{y}(t) = \mathbf{G}(\mathbf{s}(t)), \tag{4.112}$$

mapping the phase space $\mathcal{Q}$ of the original system onto an $n_y$-dimensional Euclidean

space. The state of the system can then be represented by a delay coordinate vector

$$\mathbf{z}(t) = \begin{bmatrix} \mathbf{y}(t+T_1) \\ \mathbf{y}(t+T_2) \\ \vdots \\ \mathbf{y}(t+T_{n_e}) \end{bmatrix}, \tag{4.113}$$

where now the dimensionality of the embedding space is $n_z = n_y n_e$. The question we have to answer is what conditions should the function $\mathbf{G}$ satisfy in order to allow a local (or global) one-to-one embedding. Since the exact form of the evolution equations is rarely known, in order to find the answer one can only exploit the symmetry properties of the system, which are often easy to establish based on the underlying symmetries of the physical space. Fortunately, the symmetry provides most of the necessary information.

Since we are interested in the issue of phase space reconstruction only as far as it applies to the problem of linear control, we will assume a local character for the observability property, unless explicitly stated otherwise. According to the analysis conducted in [49], local embedding in the vicinity of the periodic trajectory $\bar{\mathbf{s}}(t)$ requires $\mathbb{R}^{n_y}$ to contain at least one copy of every invariant subspace $L^{r\alpha}_{\mathcal{L}'}$ generated by the (unitary) irreducible representation $T^r$ of the respective isotropy symmetry group $\mathcal{L}' = \mathcal{H}_{\bar{\mathbf{s}}}$. This would lead one to assume that the minimal dimension $n_y$ of the output signal should be determined by the dimension of the largest irreducible representation $T^r$.

This assumption can be trivially verified using the formalism developed above for the control problem in the presence of symmetry. Indeed, let us again consider a time-invariant target state $\bar{\mathbf{s}}$. Linearizing the output (4.112) in the vicinity of this target state and denoting the displacement $\Delta\mathbf{y}(t) = \mathbf{G}(\mathbf{s}(t)) - \mathbf{G}(\bar{\mathbf{s}})$ one obtains:

$$\Delta\mathbf{y}(t) = C\Delta\mathbf{s}(t), \tag{4.114}$$

where the constant matrix $C$ is defined thus:

$$C = \mathbf{D}_{\mathbf{s}}\mathbf{G}(\bar{\mathbf{s}}). \tag{4.115}$$

The dynamical system defined by equations (4.90) and (4.114) or the pair $(A, C)$ is said to be *observable* if, for any times $t_f - t_i > 0$, the initial state $\Delta\mathbf{s}(t_i) = \Delta\mathbf{s}_i$ can be determined from the measurement of control perturbation $\Delta\mathbf{u}(t)$ and output $\Delta\mathbf{y}(t)$ in the interval $t \in [t_i, t_f]$. Otherwise, the system or the pair $(A, C)$ is said to be unobservable.

It can be shown that the notion of observability is dual to the notion of controllability. The crucial benefit of this duality is the fact that the observability condition for the pair $(A, C)$ is equivalent [50] to the controllability condition for the pair $(A^\dagger, C^\dagger)$. Since the commutation relation (4.19) directly implies that

$$T(g)^\dagger A^\dagger = A^\dagger T(g)^\dagger, \quad \forall g \in \mathcal{L}', \tag{4.116}$$

the symmetry properties of the matrices $A$ and $A^\dagger$ are essentially identical (as are the structures of their spectra, Jordan normal forms, etc.). As a result, all restriction imposed on the control matrix $B$ by the controllability condition in the presence of symmetry should be satisfied for the matrix $C^\dagger$ as well.

For instance, in case there are no accidental degeneracies and the representation $T$ contains at most one copy of each irreducible representation of the group $\mathcal{L}'$, one can claim that in order to reconstruct the dynamics in the vicinity of the time-invariant symmetric target state $\bar{\mathbf{s}}$ the number $n_y$ of measured scalar output signals $y_i(t)$ should be the same as the minimal number $\bar{n}_u$ of independent control parameters, i.e., $\bar{n}_y = \bar{n}_u$. Furthermore, the outputs have to be independent, so that $d_r$ of the projections $\hat{P}^r\mathbf{c}_i$, $i = 1, \cdots, n_y$ are linearly independent for every $r$, where $\hat{P}^r$ is the projection operator defined by (4.60) and (4.61), and $\mathbf{c}_i^\dagger$ is the $i$th row of the matrix $C$, which imposes a number of restrictions on the allowed form of the function $G$. In addition, similarly to the generic case, $n_e \geq n_s^h$ measurements of each output signal have to be performed to construct a one-to-one representation (4.113) of the system state, which increases the dimensionality of the embedding space to $n_z = \bar{n}_y n_s^h$. Local observability can be similarly defined for discrete-time systems (which is done in section 5.4.1). Careful consideration shows that symmetry produces similar constraints independent of the particular description.

In addition to the notion of controllability of individual eigenvectors it is often also convenient to define the notion of their observability. We will say that the eigenvector $\mathbf{e}$ of the Jacobian $A$ is observable, if there exists $i$, $1 \leq i \leq n_y$, such that $(\mathbf{e} \cdot \mathbf{c}_i) \neq 0$. Respectively, an eigenvector that is orthogonal to every row of the matrix $C$ is called unobservable. Clearly, the observability of the linearized system is equivalent to the observability of each and every eigenvector of the Jacobian matrix.

In the conclusion of this section we make a few comments regarding the problem of global phase space reconstruction. Often it is important to know how the symmetry of the continuous-time experimental system transpires in the structure of the discrete-time map (3.9) obtained as a result of the time delay embedding produced by a general output signal (4.112). King and Stewart [49] recognized that it is as important to preserve the symmetry of the attractor as it is to preserve its topology during the reconstruction. According to (4.112), using an arbitrary vector output $\mathbf{y}(t)$ to generate the delay coordinate representation of the system state corresponds to picking a function $\mathbf{G}$ which, in general, distorts the symmetry. In order to preserve the symmetry of the original attractor the function $\mathbf{G}$ has to be $\mathcal{G}$-equivariant

$$\mathbf{G}(g(\mathbf{s})) = g(\mathbf{G}(\mathbf{s})), \quad \forall g \in \mathcal{G}, \ \forall \mathbf{s} \in \mathcal{Q}, \tag{4.117}$$

where $\mathcal{G}$ is the structural symmetry group of the system (3.2) which will, in general, act differently in the phase space $\mathcal{Q}$ and Euclidean space $\mathbb{R}^{n_y}$. In addition, the dimensionality $n_y$ of the Euclidean space has to be chosen high enough to avoid local folding (obviously, $n_y$ should be no smaller than the number $\bar{n}_y$ evaluated for the steady or periodic trajectory with the highest isotropy symmetry). Finally, a global one-to-one embedding can be achieved by choosing $n_e \geq 2n_s^h + 1$ to preserve the topology of the attractor. The map (3.9) constructed using this embedding will preserve all dynamical symmetries of the original system. However, the structural symmetry of the differential equation (3.2) and the map (3.9) will, in general, be different.

# Chapter 5 Feedback Control

Once we have found the minimal number of control parameters $\bar{n}_u$ and determined that the linear response of the system to perturbation of these parameters, given by the control matrix $B$, satisfies the requirements imposed by the controllability condition, we can turn to the final part of the control problem, where our objective is to find a feedback that would actually stabilize the target state. The controllability condition determines whether such feedback exists, but it does not provide us with a method to find it. As it turns out, the choice of feedback is not unique and depends on the information available about the system and the assumptions made.

We restrict the scope of this chapter to discrete-time linear feedback control techniques, which is explained primarily by the fact that the most convenient and precise description of reconstructed chaotic dynamics in actual experimental systems is provided in terms of discrete-time mappings of the form (3.9) and their linearizations (3.11). These mappings are *deterministic*, and as such describe idealized systems in the absence of noise. In experiment a certain amount of noise is always present, so real systems are more adequately described by a stochastic generalization of the map (3.9):

$$\mathbf{x}^{t+1} = \mathbf{F}(\mathbf{x}^t, \mathbf{w}^t, \mathbf{u}^t), \tag{5.1}$$

where $\mathbf{w}^t$ is an $n_w$-dimensional uncertainty vector representing the effect of noise. Still, the majority of algorithms aimed at controlling chaotic dynamics assume that the effect of noise is negligible, $\mathbf{w}^t = \mathbf{0}$, in the derivation of the feedback law. The resulting closed-loop systems usually can tolerate a certain amount of noise without being destabilized. However, one can take a more active approach and design the feedback aimed at suppressing noise, rather than ignoring it, which yields far superior results.

During the past fifty years or so control theory has generated a number of extremely powerful and general linear feedback control techniques, some of which were later

applied to the problem of chaos control and, occasionally, given new names. Nonlinear dynamics, in addition, contributed quite a number of feedback control techniques specialized to chaos control problems (see, for example, the review by Lindner and Ditto [53]). Most of the techniques currently used to control chaos are rather simple and intuitive, but the vast majority use single control parameter. Those that do employ multi-parameter control [11; 46] required by symmetric systems are poorly suited to deal with stochastic dynamical systems and cannot be easily generalized to handle the *output feedback* control problem, which arises when complete information about the state of the controlled system is not available.

Extended OGY control and dead-beat control, the two discrete-time techniques predominantly used to control chaotic systems, use single control parameter, but admit multi-parameter generalizations. Although derived with the assumption of deterministic dynamics, these two techniques can be adapted for use in the stochastic regime by making certain modifications necessary to reduce the effect of noise. Nevertheless, they still cannot match the performance of optimal multi-parameter control techniques, such as linear-quadratic (or $H_2$) control and worst case (or $H_\infty$) control, derived in the assumption of stochastic dynamics. Perhaps surprisingly, the optimal control techniques produce better results in the deterministic case as well, which makes them preferable for controlling extended chaotic systems.

## 5.1 OGY Approach

The original OGY method was developed by Ott, Grebogi and Yorke (hence the name OGY) [54] for a very restricted class of problems. However, due to its easy geometrical interpretation, the method attracted considerable attention of the physics audience, and was subsequently developed [17; 10] into a powerful control technique. This technique successfully overcame many of the limitations of the original method to become the tool predominantly used by physicists to control systems displaying chaotic behavior. A number of low-dimensional experimental systems, such as a magnetoelastic ribbon [55], a parametrically driven pendulum [56], a diode resonator [57], nonlinear lasers [58], and heart [4] and brain tissue [5] were successfully controlled

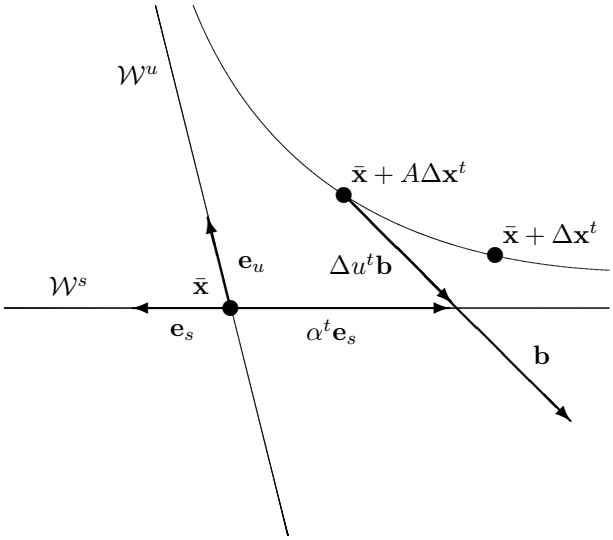


Figure 5.1: OGY control of the unstable fixed point: the control perturbation $\Delta u^t$ is chosen such that the state vector $\mathbf{x}^t$ is mapped onto the stable manifold $\mathcal{W}^s$ of the fixed point $\bar{\mathbf{x}}$.

using the OGY approach. Despite certain limitations, which we will discuss below, this method is still in active use.

### 5.1.1 Original OGY Method

The idea of the method is to make the maximal use of the hyperbolic structure of the map (3.9) in the vicinity of the fixed point $\bar{\mathbf{x}}$, which is to be stabilized. The key idea is to adjust the control parameter $u$ such that the state of the system is mapped onto the stable manifold of the fixed point at time $t_0$. In the absence of noise, this is enough to guarantee that eventually the state of the system $\mathbf{x}^t$ will approach the fixed point

$$\lim_{t\to\infty} \mathbf{x}^t = \bar{\mathbf{x}} \tag{5.2}$$

even without further control, i.e., for $u^t = \bar{u},\ t \geq t_0$.

Consider a deterministic two-dimensional dynamical system, described by the map (3.9) with a fixed point $\bar{\mathbf{x}}$, and suppose that the Jacobian $A = \mathbf{D}_{\mathbf{x}}\mathbf{F}(\bar{\mathbf{x}}, \bar{u})$ at this point has one stable direction and one unstable direction defined by the eigenvectors $\mathbf{e}_s$ and $\mathbf{e}_u$, respectively. These directions determine the local orientations of the stable and unstable manifolds $\mathcal{W}^s$ and $\mathcal{W}^u$ (see figure 5.1). For such a system it is, in general, possible to perturb the single available parameter $u^t$ in such a way that an arbitrary

state $\mathbf{x}^t$ of the system is mapped onto the stable manifold, $\mathbf{x}^{t+1} = \mathbf{F}(\mathbf{x}^t, \bar{u}+\Delta u^t) \in \mathcal{W}^s$, at the next iteration. Since this condition cannot be resolved with respect to $\Delta u^t$ in the general nonlinear case, its linearization about $\mathbf{x} = \bar{\mathbf{x}}$ and $u = \bar{u}$ is used to obtain an approximate solution. Substituting the vector $\mathbf{b} = B = \partial_u \mathbf{F}(\bar{\mathbf{x}}, \bar{u})$ into the linearized evolution equation (4.1), one obtains

$$\alpha^t \mathbf{e}_s = \Delta\mathbf{x}^{t+1} = A\Delta\mathbf{x}^t + \mathbf{b}\Delta u^t, \tag{5.3}$$

where $\alpha^t$ is a constant to be determined. If we define the matrix

$$\mathcal{S} = [\,\mathbf{e}_s \quad \mathbf{b}\,], \tag{5.4}$$

which coincides with the stabilizability matrix (4.11) for the matrices $A$ and $B$ corresponding to the fixed point solution $\bar{\mathbf{x}}$, the linear equation (5.3) can be trivially solved to yield

$$\begin{bmatrix} -\alpha^t \\ \Delta u^t \end{bmatrix} = -(\mathcal{S})^{-1} A\Delta\mathbf{x}^t, \tag{5.5}$$

provided the matrix $\mathcal{S}$ is nonsingular, i.e., the vector $\mathbf{b}$ is not parallel to the stable manifold $\mathcal{W}^s$. This defines the linear feedback solution in the form (4.2):

$$\Delta u^t = -K\Delta\mathbf{x}^t, \tag{5.6}$$

which stabilizes the fixed point $\bar{\mathbf{x}}$ of the map (3.9). According to (5.5), the feedback gain matrix is given by

$$K = [\,0 \quad 1\,]\,(\mathcal{S})^{-1} A. \tag{5.7}$$

If, however, the vector $\mathbf{b}$ is parallel to the stable manifold, $\mathbf{b} = \beta\mathbf{e}^s$, it becomes an eigenvector of the Jacobian $A$. As a consequence, the corresponding controllability matrix becomes rank-deficient,

$$\mathrm{rank}(\mathcal{C}) = \mathrm{rank}\,[\,\mathbf{b} \quad \lambda_s\mathbf{b}\,] = 1 < n_x = 2, \tag{5.8}$$

and both the stabilizability and the controllability condition are violated. We thus conclude that as long as the two-dimensional hyperbolic system is stabilizable, it

can be controlled by perturbing the single available parameter using linear feedback, calculated according to the OGY method.

Nonlinearities and noise, which are always present in real experimental systems described by the map (5.1) rather than (3.9) continuously drive the trajectory away from the linear approximation of the stable manifold. As a consequence, setting $\Delta u^t = 0$ for all times $t$ after we first managed to bring the system to the stable manifold, will not achieve the desired stabilization of the fixed point. We, therefore, have to apply feedback defined by (5.6) and (5.7) repeatedly at every iteration in an attempt to correct for the destabilizing effect of the nonlinearities and noise. Note that, according to (5.6), the feedback $\Delta u^t$ vanishes when the system approaches the fixed point. Respectively, the magnitude of perturbations required to maintain control in the stochastic case decreases with decreasing noise, but never goes to zero as long as nonzero noise is present.

### 5.1.2 Time-Periodic States

Romeiras *et al.* [17] noted that the original OGY method, which was outlined in the previous section, can be easily generalized to deal with time-periodic states and systems with higher dimensionality and, most important, with an arbitrary number of unstable directions, $n_x^u \geq 1$. Indeed, the time-varying nature of the target state is not an obstacle, since any period-$\tau$ trajectory $\bar{\mathbf{x}}^1, \bar{\mathbf{x}}^2, \cdots, \bar{\mathbf{x}}^\tau$ of the map (3.9) can be thought of as a collection of fixed points of the superposition $\mathbf{F}^\tau$ of $\tau$ maps $\mathbf{F}$. Furthermore, an arbitrary point of the stable manifold, independent of the manifold's dimensionality, is attracted to the fixed point. As a result, the idea of the method can be preserved completely: the perturbations $\Delta u^t$ should be applied in such a way as to eventually bring the state of the system onto the stable manifold.

As far as the calculation of the feedback is concerned, however, a number of technical comments has to be made. First of all, since the target state $\bar{\mathbf{x}}^t$ is not time-invariant anymore, all the matrices in the linearization (3.11) become time-dependent, and we have to restore the time index, bearing in mind that the matrices are periodic in this index with period $\tau$, e.g., $A^{t+\tau} = A^t$. Second, the eigenvectors of instantaneous Jacobians $A^t$ no longer define the stable and unstable manifolds. Instead, we use the

stable and unstable manifolds of the fixed points $\bar{\mathbf{x}}^t$ of the superposition of maps $\mathbf{F}^\tau$, whose local orientation in the time-periodic case is determined by the eigenvectors of the matrices $J_\tau^{t+\tau-1}$ defined by (4.66). Since the products $J_\tau^t$ and $J_\tau^{t'}$ only differ by a cyclic permutation for $t \neq t'$, their spectra are the same. The eigenvectors, however, change with time. As a consequence, the orientations of the manifolds become time-dependent, although the dimensions of both the stable and the unstable manifold, which we denoted respectively $n_x^s$ and $n_x^u$, remain constant and satisfy the relation $n_x^u + n_x^s = n_x$ (we assume there is no accidental degeneracy between eigenvalues of matrices $J_\tau^t$).

Third, if $n_x^u > 1$, it becomes impossible to map an arbitrary state vector $\mathbf{x}^t$ onto the stable manifold applying a single control perturbation. It can be easily seen that $n_x^u$ consecutive control perturbations are required. Indeed, the control matrices defined by (3.13) become vectors in the single-parameter case, $B^t = \mathbf{b}^t$, and starting at time $t$ one would have at time $t + n$:

$$\Delta\mathbf{x}^{t+n} = J_n^{t+n-1}\Delta\mathbf{x}^t + \sum_{k=0}^{n-1} J_{n-1-k}^{t+n-1}\mathbf{b}^{t+k}\Delta u^{t+k}. \tag{5.9}$$

The algorithm requires that $\mathbf{x}^{t+n}$ lies on the stable manifold $\mathcal{W}^s$ of the point $\bar{\mathbf{x}}^{t+n}$, which in the linear approximation can be written as

$$\Delta\mathbf{x}^{t+n} = \alpha_1^{t+n}\mathbf{e}_1^{t+n} + \cdots + \alpha_{n_x^s}^{t+n}\mathbf{e}_{n_x^s}^{t+n}, \tag{5.10}$$

where $\mathbf{e}_k^t$ denote the $n_x^s$ linearly independent stable eigenvectors of the matrix $J_\tau^{t+\tau-1}$, and $\alpha_1^t, \cdots, \alpha_{n_x^s}^t$ are the constants to be determined. Equation (5.9) uniquely defines the perturbation of the control parameter for the time steps $t$ through $t + n - 1$ only for $n + n_x^s = n_x$ and, therefore, we should set $n = n_x^u$.

If we define a sequence of matrices

$$\mathcal{S}_t = \left[\, \mathbf{e}_1^{t+1} \quad \cdots \quad \mathbf{e}_{n_x^s}^{t+1} \quad \mathbf{b}^t \quad \cdots \quad J_{n_x^u-1}^t\mathbf{b}^{t-n_x^u+1} \,\right], \tag{5.11}$$

the solution for control perturbations $\Delta u^t$ through $\Delta u^{t+n_x^u-1}$ can be obtained in the

form similar to (5.5):

$$\begin{bmatrix} -\alpha_1^{t+n_x^u} \\ \vdots \\ -\alpha_{n_x^s}^{t+n_u} \\ \Delta u^{t+n_x^u-1} \\ \vdots \\ \Delta u^t \end{bmatrix} = -(\mathcal{S}_{t+n_x^u-1})^{-1} J_{n_x^u}^{t+n_x^u-1} \Delta \mathbf{x}^t, \tag{5.12}$$

again provided the matrices $\mathcal{S}_t$ are nonsingular or, equivalently,

$$\operatorname{rank}(\mathcal{S}_t) = n_x, \quad t = 1, \cdots, \tau. \tag{5.13}$$

The sequence (5.11) is nothing more than a time-dependent generalization of the stabilizability matrix (4.11), while the condition (5.13) replaces the stabilizability condition (4.10) for periodic target trajectories.

Similarly to the previous section, in case of real experimental systems described by equation (5.1) we choose to apply the feedback at every step to correct for the deviations from the stable manifold caused by nonlinearity and noise. Indeed, starting at time $t$ from the state $\mathbf{x}^t$ and applying the sequence of control perturbations $\Delta u^t$ through $\Delta u^{t+n_x^u-1}$ calculated using (5.12), we arrive at another state $\mathbf{x}^{t+n_x^u}$, which generally will not lie exactly on the stable manifold. Therefore, we will have to repeat the procedure by applying another sequence of $n_x^u$ control perturbations calculated based on the state $\mathbf{x}^{t+n_x^u}$ and so on.

However, if there are many unstable directions (which is usually the case in spatiotemporally chaotic extended systems), the sequence of precalculated control perturbations becomes very long and the above procedure does not allow the control algorithm to react to noise promptly enough. One of the possible solutions is to calculate only the first step $\Delta u^t$ of the control sequence and then reset the algorithm. We then repeat the process, evaluating $\Delta u^{t+1}$ based on the new state $\mathbf{x}^{t+1}$ using the formula (5.12) with $t \to t+1$, etc. Doing so again results in linear proportional feedback

$$\Delta u^t = -K^t \Delta \mathbf{x}^t, \tag{5.14}$$

but now the gain matrix becomes time-dependent

$$K^t = [\,0 \quad \cdots \quad 0 \quad 1\,](\mathcal{S}_{t+n_x^u-1})^{-1} J_{n_x^u}^{t+n_x^u-1}. \tag{5.15}$$

In the absence of noise and nonlinearities (5.12) and (5.14) give the same feedback. For real experimental systems the latter approach is preferable, because usually it can tolerate higher levels of noise and stronger nonlinearities.

### 5.1.3 Multi-Parameter Control

In the conventional single-control-parameter form the OGY technique is not applicable to most chaotic systems with nontrivial symmetries, which require a larger number of control parameters, $n_u > 1$. However, this approach is flexible enough to allow a multi-parameter generalization. Below we propose a simple way to achieve such a generalization using a number of straightforward modifications of the algorithm described in the previous section. First of all, we note that increasing the number of control parameters allows a greater degree of control, so the target condition (5.10) can be reached in a number of steps fewer than the number $n_x^u$ of unstable directions. In the multi-parameter case the control matrix $B^t$ consists of a number of columns equal to the number of control parameters. Using the notation (4.5) for the columns of $B^t$, we obtain instead of equation (5.9):

$$\begin{aligned} \Delta\mathbf{x}^{t+n} &= J_n^{t+n-1}\Delta\mathbf{x}^t + \sum_{k=0}^{n-1} J_{n-1-k}^{t+n-1} B^{t+k} \Delta\mathbf{u}^{t+k} \\ &= J_n^{t+n-1}\Delta\mathbf{x}^t + \sum_{k=0}^{n-1}\sum_{m=1}^{n_u} J_{n-1-k}^{t+n-1} \mathbf{b}_m^{t+k} \Delta u_m^{t+k}, \end{aligned} \tag{5.16}$$

which together with condition (5.10) forms a system of $n_x$ linear equations in $n_u n + n_x^s$ unknowns. Therefore, in general, a sequence of $n_t$ control perturbations, where

$$n_t \geq \frac{n_x^u}{n_u} \tag{5.17}$$

is required to satisfy the target condition (5.10).

For a typical high-dimensional system we expect $n_u \ll n_x^u \ll n_x^s$. If $n_x^u$ is a

multiple of $n_u$, then we can take $n = n_t = n_x^u/n_u$ and proceed similarly to the single-parameter case. If $n_x^u$ is not a multiple of $n_u$, on the other hand, the system becomes underdetermined and additional conditions have to be imposed to obtain a unique solution. Let us define $n_t$ as the smallest integer satisfying relation (5.17), i.e., $n_t = \text{ceil}(n_x^u/n_u)$. The $n_t n_u - n_x^u$ missing conditions can be supplied in a number of ways. For instance, one can impose additional conditions by requesting that after $n_t$ iterations the state of the system is mapped onto the subset of the stable manifold defined by the $n_x - n_t n_u$ stable eigenvectors with smallest respective eigenvalues. Assuming the stable eigenvalues are labelled in the order of increasing magnitude, $|\lambda_1^s| \leq |\lambda_2^s| \leq \cdots \leq |\lambda_{n_x^s}^s|$, these additional conditions can be written as

$$\alpha_i^{t+n_t} = 0, \quad i = n_x - n_t n_u + 1, \cdots, n_x^s. \tag{5.18}$$

Condition (5.18) effectively collapses the state along the most dangerous directions inside the stable manifold, which become especially susceptible to noise when the magnitude of the respective eigenvalues becomes close to one. There are other ways to choose $n_t n_u - n_x^u$ additional conditions, e.g., by projecting $\Delta\mathbf{x}^{t+n_t}$ orthogonally to the intersection manifold defined by equation (5.10), as suggested by Warncke *et al.* [11]. However, the advantages of the latter choice are unclear, while the implicit assumption that $n_u > n_x^u$ is hardly ever satisfied in an experimental setting.

Conditions (5.10) and (5.18) determine both the projection on the stable manifold $\mathcal{W}^s$ and the control perturbations $\Delta\mathbf{u}^t$ through $\Delta\mathbf{u}^{t+n_t-1}$ based on the knowledge of the state of the system at time $t$:

$$\begin{bmatrix} -\alpha_1^{t+n_t} \\ \vdots \\ -\alpha_{n_x-n_t n_u}^{t+n_t} \\ \Delta\mathbf{u}^{t+n_t-1} \\ \vdots \\ \Delta\mathbf{u}^t \end{bmatrix} = -(\tilde{\mathcal{S}}_{t+n_t-1})^{-1} J_{n_t}^{t+n_t-1} \Delta\mathbf{x}^t, \tag{5.19}$$

where the matrices $\tilde{\mathcal{S}}_t$ are given by

$$\tilde{\mathcal{S}}_t = [\, \mathbf{e}_1^{t+1} \quad \cdots \quad \mathbf{e}_{n_x - n_t n_u}^{t+1} \quad B^t \quad \cdots \quad J_{n_t-1}^t B^{t-n_t+1} \,]\,. \tag{5.20}$$

Finally, using the first control perturbation of the sequence determined by (5.19) similarly to the single-parameter case we obtain the linear proportional feedback

$$\Delta \mathbf{u}^t = -K^t \Delta \mathbf{x}^t \tag{5.21}$$

with the time-periodic gain

$$K^t = [\, 0_{n_u \times n_x - n_u} \quad I_{n_u \times n_u} \,](\tilde{\mathcal{S}}_{t+n_t-1})^{-1} J_{n_t}^{t+n_t-1}. \tag{5.22}$$

In order for the solution (5.19) to be defined, the matrices $\tilde{\mathcal{S}}_t$ should be nonsingular for every $t = 1, \cdots, \tau$. This requires the satisfaction of the time-dependent generalization of the stabilizability condition (5.13) for the sequence of stabilizability matrices

$$\mathcal{S}_t = [\, \mathbf{e}_1^{t+1} \quad \cdots \quad \mathbf{e}_{n_x^s}^{t+1} \quad B^t \quad \cdots \quad J_{n_x^u-1}^t B^{t-n_x^u+1} \,]\,. \tag{5.23}$$

Indeed, one can easily check that, since the matrix $\tilde{\mathcal{S}}_t$ can be obtained from the matrix $\mathcal{S}_t$ by removing a number of columns, $\mathrm{rank}(\tilde{\mathcal{S}}_t) \leq \mathrm{rank}(\mathcal{S}_t)$. However, stabilizability is only a necessary, not sufficient, condition and, therefore, not all stabilizable systems can be controlled using the multi-parameter generalization of the OGY technique. In the single-parameter case $\tilde{\mathcal{S}}_t = \mathcal{S}_t$ and stabilizability becomes the sufficient condition as well.

## 5.2 Dead-Beat Control

Equally compelling from the geometrical point of view, the dead-beat control technique discussed in the framework of chaos control by a number of authors [12; 18; 46] in fact has several advantages over the conventional OGY approach, although it imposes slightly more stringent conditions on the system. Instead of controlling the system indirectly by steering it towards the stable manifold, one can try to steer the

system directly towards the target trajectory $\bar{\mathbf{x}}^t$. From the mathematical point of view, this is equivalent to replacing the target condition (5.10) with

$$\Delta\mathbf{x}^{t+n} = 0. \tag{5.24}$$

Keeping in mind that symmetric systems require several control parameters, we assume from the outset that $n_u > 1$. A multi-parameter version of the dead-beat control has been, in fact, discussed in the chaos control literature [46]. However, the proposed algorithm, obtained as a special case of the pole placement technique, is unnecessarily complicated and completely lacks the intuitive connection with the geometrical interpretation suggested above.

Instead we propose a different and more illustrative approach. Similarly to the OGY algorithm, substituting (5.24) into (5.16) yields a system of $n_x$ linear equations in $nn_u$ unknowns. The target condition (5.24) can be reached in a number of iterations $n \geq n_t$, where

$$n_t = \mathrm{ceil}(n_x/n_u). \tag{5.25}$$

Let us take $n = n_t$. In order to obtain a unique solution for the perturbation $\Delta\mathbf{u}^t$, if $n_x$ is not a multiple of $n_u$, one has to specify $n_t n_u - n_x$ additional conditions. Since the perturbation vectors $\Delta\mathbf{u}^t$ through $\Delta\mathbf{u}^{t+n_t-1}$ are the only unknowns in the problem, the additional conditions have to be imposed on their components. For instance, this can be achieved by requiring that the system is mapped onto the target trajectory without perturbing the last $n_t n_u - n_x$ components of the parameter vector on the last step of the control sequence. Introducing the shorthand notation $n_c = n_x - (n_t - 1)n_u$ this can be written as

$$\Delta u_m^{t+n_t-1} = 0, \quad m = n_c + 1, \cdots, n_u. \tag{5.26}$$

The solution for the sequence of control perturbations $\Delta\mathbf{u}^t, \cdots, \Delta\mathbf{u}^{t+n_t-1}$ driving the system from an arbitrary state $\mathbf{x}^t$ directly to the point $\bar{\mathbf{x}}^{t+n_t}$ of the the target

trajectory is then defined by (5.26) and the equation

$$\begin{bmatrix} \Delta u_1^{t+n_t-1} \\ \vdots \\ \Delta u_{n_c}^{t+n_t-1} \\ \Delta \mathbf{u}^{t+n_t-2} \\ \vdots \\ \Delta \mathbf{u}^{t} \end{bmatrix} = -(\tilde{\mathcal{C}}_{t+n_t-1})^{-1} J_{n_t}^{t+n_t-1} \Delta \mathbf{x}^t, \tag{5.27}$$

where the matrices $\tilde{\mathcal{C}}_t$ are given by

$$\tilde{\mathcal{C}}_t = [\, \mathbf{b}_1^t \quad \cdots \quad \mathbf{b}_{n_c}^t \quad J_1^t B^{t-1} \quad \cdots \quad J_{n_t-1}^t B^{t-n_t+1} \,]. \tag{5.28}$$

Again, discarding all but the first control perturbations of the sequence determined by (5.27) we obtain the linear proportional feedback (5.21) with the time-periodic gain

$$K^t = [\, 0_{n_u \times n_x - n_u} \quad I_{n_u \times n_u} \,](\tilde{\mathcal{C}}_{t+n_t-1})^{-1} J_{n_t}^{t+n_t-1}. \tag{5.29}$$

As expected, in the single-parameter time-invariant case equation (5.29) coincides with the respective pole placement result. Indeed, we have $n_u = 1$, so that $n_t = n_x$ and $\tilde{\mathcal{C}}_t = \mathcal{C}$, where $\mathcal{C}$ is the controllability matrix defined by (4.9). Setting all eigenvalues in Ackermann's formula [46]

$$K = [\, 0 \quad \cdots \quad 0 \quad 1 \,](\mathcal{C})^{-1}(A - \lambda_1' I) \cdots (A - \lambda_{n_x}' I) \tag{5.30}$$

to zero, $\lambda_1' = \cdots = \lambda_{n_x}' = 0$, one obtains the same feedback gain matrix $K$ as the one given by (5.29). The Jacobian $A' = A - BK$ of the respective closed-loop system is not only stable, but nilpotent, $(A')^{n_t} = 0$. Closed-loop systems of this type are called *dead-beat* in control theory.

The solution (5.27) is defined only when the matrices $\tilde{\mathcal{C}}_t$ are nonsingular, which is equivalent to

$$\operatorname{rank}(\tilde{\mathcal{C}}_t) = n_x, \quad t = 1, \cdots, \tau. \tag{5.31}$$

Furthermore, the matrix $\tilde{\mathcal{C}}_t$ can be obtained from the controllability matrix $\mathcal{C}_t$ by

removing a number of columns, so $\text{rank}(\tilde{\mathcal{C}}_t) \leq \text{rank}(\mathcal{C}_t)$ and, therefore, in the multi-parameter case the controllability of the system is required for, but does not guarantee, the existence of the solution (5.27). In the single-parameter case controllability becomes the sufficient condition as well.

Comparing the extended OGY approach with the dead-beat control method we see more similarities than differences, including the fact that the OGY approach reduces to dead-beat control when there is no stable manifold. However, there are a number of distinctions, which could make one method preferable to the other in certain conditions. Dead-beat control is simpler: it does not require the knowledge of the eigenvalues and eigenvectors of the Jacobians and their products, evaluation of which could be a rather complicated and numerically costly procedure, especially for high-dimensional systems. The OGY method performs poorly when there are stable eigenvalues with magnitude close to one. Since the largest stable eigenvalue determines the rate at which the state approaches the target trajectory, such a system will typically be very sensitive to noise. An illustration of this effect is presented in figure 6.4, where the sensitivity of different control techniques to noise is compared for a sample high-dimensional system. The peaks in the noise amplification produced by the OGY-type feedback correspond to the values of parameter $\epsilon$ at which eigenvalues of the Jacobian cross the unit circle $|\lambda| = 1$. The same figure, though, shows that the OGY control performs better than the dead-beat control for most other values of parameter, especially for small $\epsilon$, where the sample system has an intrinsic degeneracy.

## 5.3 Linear-Quadratic Control

Next, we turn to the linear-quadratic control technique which has become one of the cornerstones of modern optimal control theory [59]. Surprisingly, this method never found its way into chaos control theory, despite its many advantages. The idea and methodology of linear-quadratic control is rooted in the theory of stochastic processes familiar to physicists and mathematicians alike. Unlike the OGY approach and the dead-beat control technique, linear-quadratic control alone provides a framework for the systematic and consistent treatment of both the steady and time-periodic control

problem with or without noise, using full or partial information about the system state. Another significant benefit of this technique is the possibility to tune the feedback to obtain the best performance for a specific system.

### 5.3.1 Time-Invariant States

In the preceding sections we did not make a distinction between the deviations from the linearized dynamics described by equation (3.11) caused by nonlinearities and external noise. The noise in an experimental system can be reduced; however, the nonlinearities are intrinsic and always have to be considered when the validity of linear feedback control is considered. For simplicity let us assume that the target state $\bar{\mathbf{x}}$ is time-invariant and that the noise is absent. Any stabilizing linear feedback of the form (4.2) will eventually (and usually rather rapidly) bring the system arbitrarily close to the target state $\bar{\mathbf{x}}$, provided the system is in the neighborhood $\mathcal{N}(\bar{\mathbf{x}})$ of the target state when the control is turned on. The neighborhood $\mathcal{N}(\bar{\mathbf{x}})$ can be defined as the basin of attraction of the steady state $\bar{\mathbf{x}}$ of the nonlinear closed-loop system

$$\mathbf{x}^{t+1} = \mathbf{F}(\mathbf{x}^t, \bar{\mathbf{u}} - K[\mathbf{x}^t - \bar{\mathbf{x}}]). \tag{5.32}$$

The major difference between linear control algorithms in the deterministic case is, therefore, in the size and shape of this basin of attraction.

We assume that the dynamics of the system is chaotic, i.e., the system evolves on a chaotic attractor $\mathcal{A}$, and the evolution is ergodic, so that the system visits every neighborhood of any steady or periodic state embedded in the attractor as time goes on. Therefore, a natural (and often the only possible) way to enforce linear control for the target state $\bar{\mathbf{x}} \in \bar{\mathcal{A}}$ is to wait, with the control turned off, until the systems gets in the neighborhood $\mathcal{N}(\bar{\mathbf{x}})$ of the target state and then turn the control on. However, it is difficult to check if the condition $\mathbf{x} \in \mathcal{N}(\bar{\mathbf{x}})$ is satisfied, since the shape of the basin of attraction is usually very irregular.

In practice one instead checks for $\mathbf{x} \in \mathcal{P}(\bar{\mathbf{x}})$, where $\mathcal{P}(\bar{\mathbf{x}}) \subset \mathcal{N}(\bar{\mathbf{x}})$ is a regularly shaped neighborhood of $\bar{\mathbf{x}}$, which best approximates $\mathcal{N}(\bar{\mathbf{x}})$. The linear size $\delta x$ of $\mathcal{P}(\bar{\mathbf{x}})$ is extremely important, especially for high-dimensional systems like the ones we study

here, because it determines the probability for the system to visit this neighborhood, which scales as $(\delta x)^{n_x^p}$, where $n_x^p$ is the local pointwise dimension of the attractor, and thus defines the average time $t_c \propto (\delta x)^{-n_x^p}$ one has to wait to turn the control on (also called the *capture* time). Therefore, both the size and the shape of the neighborhood $\mathcal{N}(\bar{\mathbf{x}})$ are important, if the linear control algorithm is to be practically effective.

The size of $\mathcal{N}(\bar{\mathbf{x}})$ crucially depends on the assumptions made during the derivation of the linear control law. In particular, the linear approximation (4.1) is valid only when both the deviation $\Delta\mathbf{x}^t$ from the target state and the perturbation $\Delta\mathbf{u}^t$ of the control parameters are sufficiently small, so that the combined state-plus-parameter vector belongs to a neighborhood $\mathcal{M}(\bar{\mathbf{x}}, \bar{\mathbf{u}}) \subset \mathbb{R}^{n_x} \times \mathbb{R}^{n_u}$ of the point $(\bar{\mathbf{x}}, \bar{\mathbf{u}})$ inside of which nonlinear corrections are negligible. Choosing the feedback gain $K$ produces the constraint (4.2) projecting the set $\mathcal{M}(\bar{\mathbf{x}}, \bar{\mathbf{u}})$ onto the tangent space $\mathbb{R}^{n_x}$, which yields a first-order approximation

$$\mathcal{N}^{(1)}(\bar{\mathbf{x}}) = \{\forall \mathbf{x} \mid (\mathbf{x}, \bar{\mathbf{u}} - K[\mathbf{x} - \bar{\mathbf{x}}]) \in \mathcal{M}(\bar{\mathbf{x}}, \bar{\mathbf{u}})\} \tag{5.33}$$

of the basin of attraction $\mathcal{N}(\bar{\mathbf{x}})$ (one has to ensure that equation (4.1) is valid for all consecutive steps as well, i.e., $\bar{\mathbf{x}} + (A - BK)^t(\mathbf{x} - \bar{\mathbf{x}}) \in \mathcal{N}^{(1)}(\bar{\mathbf{x}})$, $t = 1, 2, \cdots$). As a result, the feedback gain $K$ usually has to be chosen such that the control perturbation $\Delta\mathbf{u}^t$ is minimized in order to maximize the size of $\mathcal{N}^{(1)}(\bar{\mathbf{x}})$. Such feedback can be found as an optimal solution which minimizes the functional

$$V(\Delta\mathbf{x}^0) = \sum_{t=0}^{\infty} \left[H_s(\Delta\mathbf{x}^t) + H_c(\Delta\mathbf{u}^t)\right], \tag{5.34}$$

with the constraint (4.1) for every initial deviation $\Delta\mathbf{x}^0$. We introduced the following notations here:

$$\begin{aligned} H_s(\Delta\mathbf{x}) &= \Delta\mathbf{x}^\dagger Q \Delta\mathbf{x}, \\ H_c(\Delta\mathbf{u}) &= \Delta\mathbf{u}^\dagger R \Delta\mathbf{u}, \end{aligned} \tag{5.35}$$

where $Q$ and $R$ are the feedback parameters, which could be chosen as arbitrary positive semidefinite symmetric matrices in order to tune the control scheme by "weight-

ing" different components of the state and control vectors.

Although the dynamics of the system is, in general, non-Hamiltonian, it is interesting to note the following analogy with mechanical description of Hamiltonian systems: $H_s(\Delta\mathbf{x})$ and $H_c(\Delta\mathbf{u})$ can be interpreted as the Hamiltonian function of the linearized system and the energy of its interaction with the controller, so that the functional $V(\Delta\mathbf{x})$ represents the discrete-time action.

Using variational calculus it can be shown [59] that the minimal value of the action (5.34) is reached for $\Delta\mathbf{u}^t = -K\Delta\mathbf{x}^t$ and is quadratic in the initial deviation, $V(\Delta\mathbf{x}) = \Delta\mathbf{x}^\dagger P\Delta\mathbf{x}$, where $P$ is a solution of the discrete-time algebraic Riccati equation

$$P = Q + A^\dagger PA - A^\dagger PB(R + B^\dagger PB)^{-1}B^\dagger PA, \tag{5.36}$$

which essentially is the discrete-time version of the respective Hamilton-Jacobi equation, and the feedback gain $K$ is given by:

$$K = (R + B^\dagger PB)^{-1}B^\dagger PA. \tag{5.37}$$

It can be also shown [59] that, if $R$ is positive definite, $Q = D^\dagger D$ and the pairs $(A, B)$ and $(A^\dagger, D^\dagger)$ are controllable, there exists a unique positive definite solution $P$ to equation (5.36), and the closed-loop system (4.3) with feedback gain (5.37) is stable. Formally, the derivation of the Riccati equation is only valid for $R \neq 0$. However, since the limit

$$P = \lim_{R\to 0} P(R) \tag{5.38}$$

is usually well defined, the Riccati equation can be used to find the optimal feedback for $R = 0$ as well. Although it is generally impossible to find the solution of the Riccati equation analytically, extensive software exists for solving nonlinear matrix equations of this type numerically. The easiest way to find the solution $P$ numerically is by direct iteration of equation (5.36).

### 5.3.2 Control of Stochastic Systems

When the external noise is not negligible, $\mathbf{w}^t \neq \mathbf{0}$, the control problem has to be considerably reformulated. First of all, feedback still has to be chosen such that the closed-loop system is stable. However, the system will never converge exactly to the target state, since noise will continuously drive it away. Therefore, now the objective of control is to keep the system as close as possible to the target state for arbitrary magnitude of noise. Second, the system becomes stochastic and has to be described probabilistically instead of deterministically, using the stochastic generalization (5.1) of the map (3.9). In particular, the linearization (4.1) has to be replaced with

$$\Delta\mathbf{x}^{t+1} = A\Delta\mathbf{x}^t + B\Delta\mathbf{u}^t + E\mathbf{w}^t, \tag{5.39}$$

where we defined the new matrix $E = \mathbf{D_w F}(\bar{\mathbf{x}}, \mathbf{0}, \bar{\mathbf{u}})$, while the Jacobian and the control matrix are determined as stochastic generalizations of equations (3.12) and (3.13), $A = \mathbf{D_x F}(\bar{\mathbf{x}}, \mathbf{0}, \bar{\mathbf{u}})$ and $B = \mathbf{D_u F}(\bar{\mathbf{x}}, \mathbf{0}, \bar{\mathbf{u}})$.

Similarly to the deterministic case, the linearization (5.39) has to be valid in order for linear control to succeed. Consequently, the range of permissible deviations $\Delta\mathbf{x}^t$ from the target trajectory is again maximized by minimizing the control perturbation $\Delta\mathbf{u}^t$, which brings us back to the functional (5.34). A few changes should be made, however, in keeping with the probabilistic description of the problem. To make the value of the functional (5.34) independent of noise, we average it over all possible noise signals $\mathbf{w}^0, \mathbf{w}^1, \cdots$. In addition, we replace the infinite sum with the infinite time average to ensure convergence:

$$V = \left\langle \lim_{T\to\infty} \frac{1}{T} \sum_{t=0}^{T} \left[ H_s(\Delta\mathbf{x}^t) + H_c(\Delta\mathbf{u}^t) \right] \mid \Delta\mathbf{x}^0 = \Delta\mathbf{x}_i \right\rangle. \tag{5.40}$$

Suppose the noise is described by a stationary zero-mean random process $\mathbf{w}^t$, which is $\delta$-correlated in time, such that[1]

$$\langle \mathbf{w}_t \mathbf{w}_{t'}^\dagger \rangle = \Xi\, \delta_{t,t'}, \tag{5.41}$$

[1] We choose to lower the time index where appropriate for notational convenience.

where the matrix $\Xi$ describes the spatial correlations of the process. Then the minimum of the functional (5.40) is again reached for $\Delta\mathbf{u}^t = -K\Delta\mathbf{x}^t$, but now it is quadratic in noise, $V = \mathrm{Tr}(PE\Xi E^\dagger)$, and is independent of the initial displacement $\Delta\mathbf{x}_i$ [59]. The matrix $P$ is again calculated as the solution of the Riccati equation (5.36), and the feedback gain $K$ is given by the same expression (5.37) as in the noise-free case. In other words, for the kind of noise considered here the feedback gain calculated in the assumption of completely deterministic dynamics is, in fact, optimal in the stochastic case as well.

In the presence of nonvanishing noise and with the control turned on, the system will fluctuate about the target state. The statistical measure of the amplitude of this fluctuation is given by the state correlation matrix $\Upsilon = \langle\Delta\mathbf{x}_t\Delta\mathbf{x}_t^\dagger\rangle$, which can be easily found analytically, provided the process noise is not correlated with the system state, $\langle\Delta\mathbf{x}_t\mathbf{w}_t^\dagger\rangle = 0$. Indeed, the stochastic closed-loop system with feedback gain $K$ is described by the dynamical equation

$$\Delta\mathbf{x}^{t+1} = (A - BK)\Delta\mathbf{x}^t + E\mathbf{w}^t. \tag{5.42}$$

Multiplying equation (5.42) by its transpose and taking the average yields

$$\Upsilon = (A - BK)\Upsilon(A - BK)^\dagger + E\Xi E^\dagger, \tag{5.43}$$

and, since the matrix $A - BK$ is stable, the solution in the form of the convergent series is obtained:

$$\Upsilon = \sum_{n=0}^{\infty}(A - BK)^n E\Xi E^\dagger (A - BK)^{n\dagger}. \tag{5.44}$$

We note that $\Upsilon$ is a linear function of $\Xi$, so that the average deviation from the target state is linearly proportional to the strength of noise. As a result, the ratio of the two is an invariant quantity dependent only on the choice of feedback gain $K$. It is called the *noise amplification* factor and is defined thus:

$$\nu \equiv \left[\frac{\langle|\Delta\mathbf{x}^t|^2\rangle}{\langle|\mathbf{w}^t|^2\rangle}\right]^{1/2} = \left[\frac{\mathrm{Tr}(\Upsilon)}{\mathrm{Tr}(\Xi)}\right]^{1/2}. \tag{5.45}$$

Clearly, the smaller $\nu$ is, the better the control setup can suppress noise. Examination

of the definition (5.40) with $Q = I$ and $R = 0$ shows that $V = \mathrm{Tr}(P_0 E \Xi E^\dagger) = \mathrm{Tr}(\Upsilon_0)$. Consequently, the minimal value of the noise amplification factor

$$\nu_0 = \left[ \frac{\mathrm{Tr}(P_0 E \Xi E^\dagger)}{\mathrm{Tr}(\Xi)} \right]^{1/2} \tag{5.46}$$

is achieved for the optimal feedback gain $K = K_0$ calculated using equations (5.36) and (5.37) with $Q = I$ and $R = 0$.

### 5.3.3 Time-Periodic States

So far our discussion of the linear-quadratic control method was limited to time-invariant target states. If the target state is periodic with period $\tau > 1$, the analysis does not change conceptually. However, minimal number of technical modifications of the algorithm have to be made in order to solve the time-periodic control problem using the formalism outlined in previous sections. Let us denote the target state $\bar{\mathbf{x}}^t$, where due to the periodicity $\bar{\mathbf{x}}^{t+\tau} = \bar{\mathbf{x}}^t$. Linearizing the stochastic evolution equation (5.1) about $\bar{\mathbf{x}}^t$ yields

$$\Delta \mathbf{x}^{t+1} = A^t \Delta \mathbf{x}^t + B^t \Delta \mathbf{u}^t + E^t \mathbf{w}^t, \tag{5.47}$$

where the Jacobian $A^t = \mathbf{D}_\mathbf{x}\mathbf{F}(\bar{\mathbf{x}}^t, \mathbf{0}, \bar{\mathbf{u}})$, the control matrix $B^t = \mathbf{D}_\mathbf{u}\mathbf{F}(\bar{\mathbf{x}}^t, \mathbf{0}, \bar{\mathbf{u}})$, and the matrix $E^t = \mathbf{D}_\mathbf{w}\mathbf{F}(\bar{\mathbf{x}}^t, \mathbf{0}, \bar{\mathbf{u}})$ all become time-varying and periodic in the index $t$.

Similarly to the noisy time-invariant case, the objective of control is to minimize the deviation from the target trajectory, simultaneously minimizing the magnitude of control perturbations. The optimal feedback that achieves this objective can again be found by minimizing the functional (5.40) with the weights $Q$ and $R$ which can, in principle, be chosen time-periodic, thus acquiring the time index as well. The minimum of the functional is again reached for $\Delta \mathbf{u}^t = -K^t \Delta \mathbf{x}^t$, where the feedback gain now also becomes time-periodic:

$$K_t = (R_t + B_t^\dagger P_{t+1} B_t)^{-1} B_t^\dagger P_{t+1} A_t. \tag{5.48}$$

The matrix $P^t$ denotes the time-periodic solution of the system of $\tau$ coupled Riccati

equations (collectively called the discrete periodic Riccati equation)

$$P_t = Q_t + A_t^\dagger P_{t+1} A_t - A_t^\dagger P_{t+1} B_t (R_t + B_t^\dagger P_{t+1} B_t)^{-1} B_t^\dagger P_{t+1} A_t, \tag{5.49}$$

which can be formally reduced to a single Riccati equation of larger dimensionality using the following ansatz.

Let us introduce the $\tau n_x \times \tau n_x$ cyclic-shift matrix

$$Z = \begin{bmatrix} 0 & \cdots & 0 & I \\ I & \cdots & 0 & 0 \\ \vdots & \ddots & \vdots & \vdots \\ 0 & \cdots & I & 0 \end{bmatrix}, \tag{5.50}$$

consisting of $n_x \times n_x$ zero and unit blocks (we set $Z = I$ if $\tau = 1$), and form block-diagonal time-invariant matrices $A$, $B$, $E$, $Q$ and $R$ from the sequences of time-periodic matrices $A^t$, $B^t$, $E^t$, $Q^t$ and $R^t$, respectively, according to the rule

$$A = \begin{bmatrix} A^1 & & \\ & \ddots & \\ & & A^\tau \end{bmatrix}. \tag{5.51}$$

Then the solution of the system of equations (5.49) is obtained by finding the block-diagonal solution

$$P = \begin{bmatrix} P^1 & & \\ & \ddots & \\ & & P^\tau \end{bmatrix}. \tag{5.52}$$

of the Riccati equation

$$P = Q + A^\dagger Z^\dagger P Z A - A^\dagger Z^\dagger P Z B (R + B^\dagger Z^\dagger P Z B)^{-1} B^\dagger Z^\dagger P Z A. \tag{5.53}$$

Thus, from the control point of view, the time-periodic linear system (5.47) is formally equivalent to the time-invariant linear system

$$\Delta \mathbf{X}^{t+1} = Z A \Delta \mathbf{X}^t + Z B \Delta \mathbf{U}^t + Z E \mathbf{W}^t. \tag{5.54}$$

A more technical discussion of various numerical techniques used to solve the discrete

periodic Riccati equations of the form (5.49) can be found in [60].

## 5.4 Output Feedback Control

Spatiotemporally chaotic dynamics of weakly correlated extended systems are usually extremely complicated due to a large number of excited degrees of freedom. In other words, the Hausdorff dimension $n_s^h$ of the respective chaotic attractor is very high. As a result, local dynamics in the vicinity of a typical target trajectory $\bar{\mathbf{x}}^t$ embedded in the attractor will also involve a large number of degrees of freedom. On the other hand, it can be argued that the precision in the evaluation of the linear model (3.11) obtained as a result of the local phase space reconstruction is much more important than the precision in the evaluation of the state of the system during control. As a consequence, one might be forced to use an extended set of $n_y^r \gg \bar{n}_y$ independent observables during the identification stage,

$$\mathbf{y}_r(t) = \begin{bmatrix} \mathbf{y}(t) \\ \mathbf{y}_a(t) \end{bmatrix}, \tag{5.55}$$

where $\mathbf{y}(t)$ is the set of $n_y$ observables used for both system identification and control, and the vector $\mathbf{y}_a(t)$ represents the $n_y^r - n_y$ additional observables used only for system identification. (In case of spatially extended systems it might correspond to monitoring the system at additional spatial locations.) This is especially helpful if there is considerable amount of noise, in which case the noise reduction techniques mentioned in section 3.4 can be employed to use additional data to improve the accuracy of the linear model.

If $n_y < n_y^r$, we cannot construct the state $\mathbf{x}^k$ of the system from the measurements of the output $\mathbf{y}(t)$ no matter how many successive measurements $\mathbf{y}(t_k), \mathbf{y}(t_k + T_D), \cdots$ are made. Furthermore, since the state of the system is not available, we cannot use the control techniques described above to calculate the feedback $\Delta\mathbf{u}^k$, because they all assume that the state is known. Fortunately, there is a way out. First of all, assuming that the same delay times are used during both system identification and control, we conclude that the measured output is just a linear function of the actual state $\mathbf{x}^k$.

One can, therefore, try to dynamically construct an estimate $\hat{\mathbf{x}}^k$ of the actual state of the system using the output and find the feedback based on this estimate. That turns out quite doable, provided the model equations describing the local dynamics are available. This approach is usually called *output feedback control*.

Similar situation occurs when the model equations for the system under consideration are known *a priori*, but direct determination of the system state is inconvenient, impractical, or just impossible — the situation often encountered in real experimental systems. In order to compensate for the lack of knowledge about the state of the system, in addition to the control structure that employs feedback (controller), we will need to introduce another structure, usually called the *filter*, that would monitor, collect and process the available information about the system with the purpose of reconstructing its actual state with the best accuracy possible. Since the errors introduced by the filter become amplified by control, it is equally as important to have an optimal filter as it is to have optimal control. Optimal filtering techniques derived for the dynamic state reconstruction problem [59] have much in common with optimal control techniques. As a consequence, similar results often apply.

### 5.4.1 Dynamic State Reconstruction

We are interested in reconstructing the system state only in the vicinity of the target state $\bar{\mathbf{x}}^t$, where the dynamics of the system is described with adequate precision by the linearized evolution equation (5.47). Assume that a (vector) output $\mathbf{y}^t$ of the system can be measured. In general, the measurements are imperfect, with the deviation from the perfect values described by the measurement errors, represented by an $n_v$-dimensional vector $\mathbf{v}^t$:

$$\mathbf{y}^t = \mathbf{G}(\mathbf{x}^t, \mathbf{v}^t). \tag{5.56}$$

For simplicity let us also assume that the target state is time-invariant. Linearizing the output (5.56) in the vicinity of the target state and introducing the notation $\Delta\mathbf{y}^t = \mathbf{G}(\mathbf{x}^t, \mathbf{v}^t) - \mathbf{G}(\bar{\mathbf{x}}, \mathbf{0})$, one obtains:

$$\Delta\mathbf{y}^t = C\Delta\mathbf{x}^t + D\mathbf{v}^t, \tag{5.57}$$

where $C = \mathbf{D_x G}(\bar{\mathbf{x}}, \mathbf{0})$ and $D = \mathbf{D_v G}(\bar{\mathbf{x}}, \mathbf{0})$.

In general, the problem of dynamical state reconstruction can be cast in a number of different ways. Here we pursue the one which is most easily treated in the framework of optimal control. Our goal is to use the available information about the system, i.e., the time series of control and output signals, to construct a vector $\Delta\hat{\mathbf{x}}^t$, which we call the *state estimate*, that would approximate the actual state $\Delta\mathbf{x}^t$. First of all, similarly to the dynamics of the actual state, the dynamics of the state estimate at time $t$ should depend deterministically on the present value of the state estimate $\Delta\hat{\mathbf{x}}^t$, the control perturbation $\Delta\mathbf{u}^t$ and the output $\Delta\mathbf{y}^t$. Consistent with our linear approximation we obtain the general dynamical equation of the form

$$\Delta\hat{\mathbf{x}}^{t+1} = \hat{A}\Delta\hat{\mathbf{x}}^t + \hat{B}\Delta\mathbf{u}^t + \hat{K}\Delta\mathbf{y}^t, \tag{5.58}$$

where $\hat{A}$, $\hat{B}$ and $\hat{K}$ are some as yet undefined matrices. Next, notice that in the absence of noise and measurement errors, if the state estimate and the actual state coincide at time $t_0$, they should coincide at all later times $t > t_0$ as well, and, therefore, equation (5.58) should coincide with equation (4.1) upon substituting (5.57) with $\mathbf{v}^t = \mathbf{0}$ for arbitrary $\Delta\mathbf{u}^t$ and $\Delta\hat{\mathbf{x}}^t = \Delta\mathbf{x}^t$:

$$\Delta\mathbf{x}^{t+1} = (\hat{A} + \hat{K}C)\Delta\mathbf{x}^t + \hat{B}\Delta\mathbf{u}^t. \tag{5.59}$$

This requires $\hat{A} = A - \hat{K}C$ and $\hat{B} = B$, so that (5.58) yields the dynamical equation

$$\Delta\hat{\mathbf{x}}^{t+1} = A\Delta\hat{\mathbf{x}}^t + B\Delta\mathbf{u}^t + \hat{K}(\Delta\mathbf{y}^t - C\Delta\hat{\mathbf{x}}^t), \tag{5.60}$$

where $\hat{K}$ is called the *filter gain* matrix. Finally, we need $\Delta\hat{\mathbf{x}}^t$ to be a good estimate of the actual state, i.e., the difference $\Delta\tilde{\mathbf{x}}^t = \Delta\mathbf{x}^t - \Delta\hat{\mathbf{x}}^t$ between the actual state and its estimate should be small even when finite noise or measurement errors are present. Subtracting (5.60) from (5.39) and substituting (5.57) we obtain

$$\Delta\tilde{\mathbf{x}}^{t+1} = (A - \hat{K}C)\Delta\tilde{\mathbf{x}}^t + \tilde{\mathbf{w}}^t, \tag{5.61}$$

where $\tilde{\mathbf{w}}^t = E\mathbf{w}^t - \hat{K}D\mathbf{v}^t$ denotes the sum of all stochastic terms on the right-hand

side of equation (5.61). This equation has the same form as equation (5.42) for the stochastic closed-loop system and, as a consequence, the matrix $A' = A - \hat{K}C$ has to be *stable*.

A number of comments should be made regarding the state reconstruction problem in the absence of noise and measurement errors. First of all, if the matrix $A'$ is stable, the estimate $\bar{\mathbf{x}} + \Delta\hat{\mathbf{x}}^t$ asymptotically (in a finite number of steps, if $A'$ is nilpotent) converges to the actual state $\mathbf{x}^t$. Strictly speaking, if the matrix $A'$ is stable, but not nilpotent, the estimate will never exactly coincide with the actual state. However, since the convergence is exponential, arbitrarily good approximation is obtained after a logarithmically small number of steps.

Second, the state reconstruction problem is effectively equivalent to the chaotic synchronization problem [61; 62]. Indeed, the original system (5.1) can be thought of as the drive system, the filter (5.60) as the response system, and the output (5.56) as the driving signal. Clearly the two systems will become synchronized in the vicinity of the target state (see, e.g., the discussion in [62]), with the response system following the evolution of the drive system.

Third, unlike the system identification problem considered in chapter 3, in the dynamic state reconstruction problem the dynamical equations are assumed to be known and are used to reconstruct the state of the system. However, similarly to the state identification problem, the output (5.56) has to satisfy a number of conditions in order for the state reconstruction problem to have a solution. Following the discussion in section 4.5 we define the discrete-time version of the *observability* condition for the matrix pair $(A, C)$ which ensures that the state of the system can be reconstructed given the measurement of the output. The dynamical system defined by equations (4.1) and (5.57) or the pair $(A, C)$ is said to be observable if, for any times $t_f - t_i \geq n_x$, the initial state $\Delta\mathbf{x}^{t_i} = \Delta\mathbf{x}_i$ can be determined from the measurement of control perturbation $\Delta\mathbf{u}^t$ and output $\Delta\mathbf{y}^t$ in the interval $t \in [t_i, t_f]$.

Similarly to the continuous-time case, the observability condition is formally equivalent and dual to the controllability condition for the matrix pair $(A^\dagger, C^\dagger)$ and, as a result, the restrictions imposed on the output signal (5.57) are identical to those derived in section 4.5. We, therefore, conclude that the observability condition has

the same fundamental role in the problem of dynamical state reconstruction as the controllability condition has in the control problem.

### 5.4.2 Linear-Quadratic Filter

If nonzero noise and/or measurement errors are present, the estimate does not converge to the actual state, but fluctuates about it, being constantly driven away by noise. The precision with which the actual state is approximated depends not only on the strength of noise, but also on the choice of the filter gain $\hat{K}$. Assuming the measurement errors are random, unbiased, $\delta$-correlated in time,

$$\langle \mathbf{v}_t \mathbf{v}_{t'}^\dagger \rangle = \Theta \, \delta_{t,t'}, \tag{5.62}$$

and uncorrelated with the process noise, $\langle \mathbf{w}_t \mathbf{v}_{t'}^\dagger \rangle = 0$, we conclude that $\tilde{\mathbf{w}}^t$ is a stationary zero-mean random process with correlation

$$\langle \tilde{\mathbf{w}}_t \tilde{\mathbf{w}}_{t'}^\dagger \rangle = (\hat{K} \hat{R} \hat{K}^\dagger + \hat{Q}) \, \delta_{t,t'}, \tag{5.63}$$

where we introduced the shorthand notations $\hat{R} = D\Theta D^\dagger$ and $\hat{Q} = E\Xi E^\dagger$. As a consequence, the optimal filter gain can be found using the linear-quadratic formalism described in the previous sections. Specifically, we determine the optimal filter gain by requiring the estimation error of the form

$$\hat{V}(\mathbf{d}) = \lim_{t \to \infty} \left\langle \Delta \tilde{\mathbf{x}}_t^\dagger \mathbf{d} \mathbf{d}^\dagger \Delta \tilde{\mathbf{x}}_t \right\rangle \tag{5.64}$$

to be minimal for every vector $\mathbf{d}$ selected (e.g., $\mathbf{d} = (1, 0, \cdots, 0)$, which corresponds to minimizing the mean-squared error in the first component of the state vector).

It turns out [59] that the stochastic time-invariant optimal state estimation problem defined by equations (5.60) and (5.64) is formally equivalent (and dual) to the deterministic time-invariant optimal control problem defined by equations (4.1) and (5.34), with the following correspondence between parameters: $A \leftrightarrow A^\dagger$, $B \leftrightarrow C^\dagger$, $Q \leftrightarrow \hat{Q}$, $R \leftrightarrow \hat{R}$, $\Delta \mathbf{x}^0 \leftrightarrow \mathbf{d}$, $P \leftrightarrow S$ and $K \leftrightarrow \hat{K}^\dagger$. As a result, the minimal value of

the estimation error, $\hat{V}(\mathbf{d}) = \mathrm{Tr}(S\mathbf{d}\mathbf{d}^\dagger)$, is reached for

$$\hat{K} = ASC^\dagger(\hat{R} + CSC^\dagger)^{-1}, \tag{5.65}$$

where $S$ is the solution of yet another discrete-time Riccati equation

$$S = \hat{Q} + ASA^\dagger - ASC^\dagger(\hat{R} + CSC^\dagger)^{-1}CSA^\dagger. \tag{5.66}$$

As we have seen in section 5.3.1, in order to guarantee the existence of a positive definite solution $S$ to equation (5.66), the pair of matrices $(A^\dagger, C^\dagger)$ should be controllable or, equivalently, the pair of matrices $(A, C)$ should be observable.

The generalization to periodic target states can be accomplished using the procedure discussed in section 5.3.3. Assuming the period of the target state is $\tau$, we construct the constant matrices $A$, $C$, $\hat{Q}$ and $\hat{R}$ from the respective time-periodic matrices according to the rule (5.51). The optimal filter gain $\hat{K}^t$ becomes time-periodic as well and is determined by

$$\hat{K}_t = A_t S_{t-1} C_t^\dagger (\hat{R}_t + C_t S_{t-1} C_t^\dagger)^{-1}, \tag{5.67}$$

where $S^{t+\tau} = S^t$, and $S^1$ through $S^\tau$ are the blocks found on the diagonal of the block-diagonal solution $S$ of the Riccati equation

$$S = \hat{Q} + AZSZ^\dagger A^\dagger - AZSZ^\dagger C^\dagger (\hat{R} + CZSZ^\dagger C^\dagger)^{-1} CZSZ^\dagger A^\dagger. \tag{5.68}$$

Putting all the pieces together, one finally concludes that the time-periodic output feedback control problem with additive noise

$$\begin{aligned} \Delta\mathbf{x}^{t+1} &= A^t \Delta\mathbf{x}^t + B^t \Delta\mathbf{u}^t + E^t \mathbf{w}^t, \\ \Delta\mathbf{y}^t &= C^t \Delta\mathbf{x}^t + D^t \mathbf{v}^t, \end{aligned} \tag{5.69}$$

requires the feedback $\Delta\mathbf{u}^t$, calculated according to the equations

$$\begin{aligned} \Delta\hat{\mathbf{x}}^{t+1} &= (A^t - B^t K^t - \hat{K}^t C^t)\Delta\hat{\mathbf{x}}^t + \hat{K}^t \Delta\mathbf{y}^t, \\ \Delta\mathbf{u}^t &= -K^t \Delta\hat{\mathbf{x}}^t. \end{aligned} \tag{5.70}$$

This construction is called the *Kalman-Bucy* filter in control theory. Furthermore, using the fact that $\Delta\hat{\mathbf{x}}^t$ and $\Delta\tilde{\mathbf{x}}^t$ are uncorrelated, it can be shown [59] that the feedback gain $K^t$ and filter gain $\hat{K}^t$ in equation (5.70) which are optimal with respect to (minimize) the performance measure

$$V = \lim_{t\to\infty} \left\langle H_s^t(\Delta\mathbf{x}^t) + H_c^t(\Delta\mathbf{u}^t) \right\rangle \tag{5.71}$$

are given by (5.48) and (5.67) ($H_s^t(\Delta\mathbf{x}^t)$ and $H_c^t(\Delta\mathbf{u}^t)$ are defined by (5.35) with time-varying matrices $Q^t$ and $R^t$).

Finally, we should note that in the case of output feedback control one cannot measure the distance to the target trajectory directly, because the actual state of the system is not available. However, if the system is sufficiently close to the point $\bar{\mathbf{x}}^{t_0}$ at time $t$, the difference $\mathbf{y}^t - \mathbf{G}(\bar{\mathbf{x}}^{t_0}, \mathbf{0})$ should be small. Verifying this condition at a succession of times usually ensures that the system indeed closely follows the trajectory $\bar{\mathbf{x}}^{t_0}, \bar{\mathbf{x}}^{t_0+1}, \cdots$. The state estimate $\Delta\hat{\mathbf{x}}^t$ can be reset to zero when the system is far from the target state and filtering should be turned on simultaneously with feedback when the system approaches one of the points $\bar{\mathbf{x}}^{t_0}$, $t_0 = 1, \cdots, \tau$ of the target trajectory.

### 5.4.3 Worst Case Control

So far we assumed that the noise and measurement errors are zero-mean, random and uncorrelated with the state of the system and with each other. However, this assumption is also an idealization. For instance, deviations stemming from neglecting nonlinear terms in the evolution equation (3.9) or from modeling errors (imprecise evaluation of internal parameters of the system) will, in general, be both biased and correlated with the state of the system. As a result, the linear-quadratic analysis will be, strictly speaking, invalid. Since we usually know the properties of neither the noise $\mathbf{w}^t$ nor the measurement errors $\mathbf{v}^t$ present in the system, it is often advantageous to take a different approach to the control problem.

First of all, there is no reason to distinguish between noise and measurement errors, since both are unknown and act as a destabilizing factor in the control problem. We,

therefore, combine them in a single vector

$$\hat{\mathbf{w}}^t = \begin{bmatrix} \mathbf{w}^t \\ \mathbf{v}^t \end{bmatrix}. \tag{5.72}$$

If we also define the matrices

$$\begin{aligned} \hat{E}^t &= [\, E^t \quad 0_{n_x \times n_v} \,], \\ \hat{D}^t &= [\, 0_{n_y \times n_w} \quad D^t \,], \end{aligned} \tag{5.73}$$

the dynamical equations (5.69) can then be rewritten in the equivalent form

$$\begin{aligned} \Delta\mathbf{x}^{t+1} &= A^t \Delta\mathbf{x}^t + B^t \Delta\mathbf{u}^t + \hat{E}^t \hat{\mathbf{w}}^t, \\ \Delta\mathbf{y}^t &= C^t \Delta\mathbf{x}^t + \hat{D}^t \hat{\mathbf{w}}^t. \end{aligned} \tag{5.74}$$

The objective of the algorithm presented below is to find an output feedback law similar to (5.70) that would achieve the stabilization of the target trajectory $\bar{\mathbf{x}}^t$ for the worst case sequence of perturbations $\hat{\mathbf{w}}^0, \hat{\mathbf{w}}^1, \cdots$ from the class of *all* perturbations bounded in the appropriate vector norm (which automatically guarantees stabilization in the presence of an arbitrary sequence of bounded perturbations). In the mathematical terms the goal of the worst case control (also called $H_\infty$ control in control theory) can be stated as the minimization of the induced power norm of the transfer operator $\mathbf{T}: \hat{\mathbf{w}} \to \Delta\mathbf{z}$ defined as

$$\gamma \equiv \|\mathbf{T}\|_P = \max_{\|\hat{\mathbf{w}}\|_P < \infty} \frac{\|\Delta\mathbf{z}\|_P}{\|\hat{\mathbf{w}}\|_P}, \tag{5.75}$$

where the $n_z$-dimensional performance vector

$$\Delta\mathbf{z}^t = F^t \Delta\mathbf{x}^t + G^t \Delta\mathbf{u}^t \tag{5.76}$$

gives the weighted measure of the deviation from the target state, and the power norm is defined as

$$\|\mathbf{z}\|_P \equiv \left[ \lim_{T\to\infty} \frac{1}{T} \sum_{t=0}^{T} |\mathbf{z}^t|^2 \right]^{1/2}. \tag{5.77}$$

The weight matrices $F^t$ and $G^t$ are seen to be direct analogs of the weight matrices

$Q^t$ and $R^t$ used in the linear-quadratic approach. Indeed, choosing $G^t$ and $F^t$ such that $G_t^\dagger F_t = 0$, $F_t^\dagger F_t = Q^t$ and $G_t^\dagger G_t = R^t$, one obtains

$$\|\Delta \mathbf{z}\|_P^2 = \lim_{T\to\infty} \frac{1}{T} \sum_{t=0}^{T} \left[ H_s^t(\Delta \mathbf{x}^t) + H_c^t(\Delta \mathbf{u}^t) \right]. \tag{5.78}$$

The solution to the time-periodic output feedback control problem defined by equations (5.74), (5.75) and (5.76) can be obtained using the generalization of the results of $H_\infty$ control theory [51] for linear time-invariant systems. In particular, Dullerud and Lall showed [63] that, if a stabilizing linear feedback exists, it could be written as

$$\begin{aligned} \Delta \hat{\mathbf{x}}^{t+1} &= \hat{A}^t \Delta \hat{\mathbf{x}}^t + \hat{B}^t \Delta \mathbf{y}^t \\ \Delta \mathbf{u}^t &= \hat{C}^t \Delta \hat{\mathbf{x}}^t + \hat{D}^t \Delta \mathbf{y}^t, \end{aligned} \tag{5.79}$$

where $\hat{A}^t$, $\hat{B}^t$, $\hat{C}^t$, and $\hat{D}^t$ are matrices with the same periodicity $\tau$ as the target orbit $\bar{\mathbf{x}}^t$, and $\hat{\mathbf{x}}^t$ is the $n_{\hat{x}}$-dimensional internal state of the controller. This setup can be considered a direct generalization of the Kalman-Bucy filter (5.70).

Let us construct constant block-diagonal matrices $A$, $B$, $C$, $\hat{D}$, $\hat{E}$, $F$, and $G$ according to the rule (5.51). Using these matrices it can be shown [63] that a stabilizing feedback of the form (5.79) with $n_{\hat{x}} \geq n_x$ for the system (5.74) exists and the closed-loop performance inequality $\gamma < 1$ is satisfied, if and only if there exist positive definite block-diagonal matrices $P$ and $S$, satisfying linear matrix inequalities

$$\begin{bmatrix} P & I \\ I & S \end{bmatrix} \geq 0 \tag{5.80}$$

and

$$\begin{bmatrix} N_S^\dagger & 0 \\ 0 & I \end{bmatrix} \begin{bmatrix} A^\dagger Z^\dagger S Z A - S & A^\dagger Z^\dagger S Z \hat{E} & F^\dagger \\ \hat{E}^\dagger Z^\dagger S Z A & \hat{E}^\dagger Z^\dagger S Z \hat{E} - I & 0 \\ F & 0 & -I \end{bmatrix} \begin{bmatrix} N_S & 0 \\ 0 & I \end{bmatrix} < 0,$$

$$\begin{bmatrix} N_P^\dagger & 0 \\ 0 & I \end{bmatrix} \begin{bmatrix} A P A^\dagger - Z^\dagger P Z & A P F^\dagger & \hat{E} \\ F P A^\dagger & F^\dagger P F - I & 0 \\ \hat{E}^\dagger & 0 & -I \end{bmatrix} \begin{bmatrix} N_P & 0 \\ 0 & I \end{bmatrix} < 0, \tag{5.81}$$

where the unitary matrices $N_P$ and $N_S$ satisfy

$$\begin{aligned} \operatorname{Im} N_P &= \ker \begin{bmatrix} B^\dagger & G^\dagger \end{bmatrix} \\ \operatorname{Im} N_S &= \ker \begin{bmatrix} C & \hat{D} \end{bmatrix}. \end{aligned} \tag{5.82}$$

The feedback law corresponding to thus found matrices $P$ and $S$, in general, will not be optimal. The optimal feedback can be found by executing the following algorithm. Let us rescale the weight matrices $F^t$ and $G^t$ by the factor of $1/\gamma_0$, such that the above condition tests for $\gamma < \gamma_0$ instead of $\gamma < 1$. If the corresponding matrices $P$ and $S$ can be found, we decrease $\gamma_0$ and repeat the process until the test fails. Standard software exists to do this. If there is *any* linear stabilizing controller, we can, therefore, find it using this algorithm. Strictly speaking, this algorithm will yield a feedback that will not be optimal, but will be very close to the optimal feedback, which is adequate for all practical purposes. Once the block-diagonal matrices

$$P = \begin{bmatrix} P^1 & & \\ & \ddots & \\ & & P^\tau \end{bmatrix} \quad \text{and} \quad S = \begin{bmatrix} S^1 & & \\ & \ddots & \\ & & S^\tau \end{bmatrix} \tag{5.83}$$

corresponding to the smallest $\gamma_0$ are determined, the matrices in (5.79) can be found using the following procedure. First, construct nonsingular matrices $M^t$ and $N^t$, such that

$$M_t N_t^\dagger = I - P_t S_t \tag{5.84}$$

and determine $X^t$ as the solution of the matrix equation

$$\begin{bmatrix} S_t & I \\ N_t^\dagger & 0 \end{bmatrix} = X_t \begin{bmatrix} I & P_t \\ 0 & M_t^\dagger \end{bmatrix}. \tag{5.85}$$

Next, define the matrix

$$Y^t = \begin{bmatrix} -X_{t+1}^{-1} & \tilde{A}_t & \tilde{E}_t & 0 \\ \tilde{A}_t^\dagger & -X_t & 0 & \tilde{F}_t^\dagger \\ \tilde{E}_t^\dagger & 0 & -I & 0 \\ 0 & \tilde{F}_t & 0 & -I \end{bmatrix}, \tag{5.86}$$

where we introduced the shorthand notations for the blocks

$$\tilde{A}^t = \begin{bmatrix} A^t & 0 \\ 0 & 0 \end{bmatrix}, \qquad \tilde{E}^t = \begin{bmatrix} \hat{E}^t \\ 0 \end{bmatrix}, \qquad \tilde{F}^t = [\, F^t \quad 0 \,], \tag{5.87}$$

and the matrices

$$\begin{aligned} W^t &= [\, W_1^t \quad W_2^t \quad W_3^t \quad W_4^t \,], \\ U^t &= [\, U_1^t \quad U_2^t \quad U_3^t \quad U_4^t \,], \end{aligned} \tag{5.88}$$

where we denoted

$$W_1^t = \begin{bmatrix} 0 & I \\ B_t^\dagger & 0 \end{bmatrix}, \qquad W_2^t = \begin{bmatrix} 0 & 0 \\ 0 & 0 \end{bmatrix}, \qquad W_3^t = \begin{bmatrix} 0 \\ 0 \end{bmatrix}, \qquad W_4^t = \begin{bmatrix} 0 \\ G_t^\dagger \end{bmatrix} \tag{5.89}$$

and

$$U_1^t = \begin{bmatrix} 0 & 0 \\ 0 & 0 \end{bmatrix}, \qquad U_2^t = \begin{bmatrix} 0 & I \\ C^t & 0 \end{bmatrix}, \qquad U_3^t = \begin{bmatrix} 0 \\ \hat{D}^t \end{bmatrix}, \qquad U_4^t = \begin{bmatrix} 0 \\ 0 \end{bmatrix}. \tag{5.90}$$

Finally, the matrices $\hat{A}^t$, $\hat{B}^t$, $\hat{C}^t$ and $\hat{D}^t$ can be extracted from the solution

$$V^t = \begin{bmatrix} \hat{A}^t & \hat{B}^t \\ \hat{C}^t & \hat{D}^t \end{bmatrix} \tag{5.91}$$

of the linear matrix inequality

$$Y_t + U_t^\dagger V_t^\dagger W_t + W_t^\dagger V_t U_t < 0. \tag{5.92}$$

Despite the complicated algebra, linear matrix inequalities such as (5.80) and (5.92) can be conveniently solved using the tools of convex optimization theory, which have one very important feature — namely guaranteed convergence. This feature is especially valuable if the evolution operators of the linearized system (5.74) are highly degenerate, which routinely happens in weakly coupled extended chaotic systems (we will see an example of this in chapter 6). On the negative side, solving linear matrix inequalities is usually more time consuming compared to nonlinear matrix equations like the Riccati equation (5.36).

## 5.5 Degeneracies and Blowups

In the conclusion of the chapter we return to the state feedback control problem, which allows one to compare the performance of the four techniques we discussed above: OGY control, dead-beat control, linear-quadratic control and worst case control. Since the latter two techniques are optimized for *stochastic* applications, they clearly provide far superior performance in this case. Instead we consider the deterministic case, where the benefits of the optimal control techniques are not immediately apparent. Alas, even in this case OGY control and dead-beat control do not perform on par with the optimal control techniques.

Although both OGY control and dead-beat control work adequately well in most circumstances, they have a common deficiency, which limits their applicability to extended systems, which are the focus of the present study. As we noted above, the assumption under which the solutions (5.12) and (5.27) are defined is violated when the matrices $\tilde{\mathcal{S}}_t$ and $\tilde{\mathcal{C}}_t$, respectively, become singular for some $t$. It is easy to see that this routinely happens in a seemingly innocent situation when the Jacobian $A^t$ becomes close to a multiple of a unit matrix at a certain point on the target trajectory:

$$A^{t_0} = \alpha(I + \epsilon H), \tag{5.93}$$

where $\alpha = O(1)$ is a constant, $\epsilon \ll 1$ is a constant, and $H$ is an arbitrary matrix with the unit norm. This situation can be a result of accidental degeneracy, but may also be a consequence of the weak symmetry violation in a highly symmetric system (see, e.g., the discussion in section 4.4 and later in section 6.2.2).

For simplicity, consider the single-parameter case and assume that the control matrix is constant, $B = \mathbf{b} = const$. It is rather easy to see that the magnitude of the control perturbation calculated using both OGY approach and dead-beat control diverges during the iteration $t = t_0 - 1$, $|\Delta u^{t_0-1}| \to \infty$ as the Jacobian $A^{t_0}$ approaches a multiple of a unit matrix, $\epsilon \to 0$. Indeed, let us calculate the feedback gain at time $t = t_0 - 1$. For instance, for the dead-beat control method $n_t = n_x$ and (5.29) gives

$$K^{t_0-1} = [\,0 \quad \cdots \quad 0 \quad 1\,](\tilde{\mathcal{C}}_{t_0+n_x-2})^{-1} J_{n_x}^{t_0+n_x-2}, \tag{5.94}$$

where the matrix $\tilde{\mathcal{C}}_{t_0+n_x-2}$ coincides with the controllability matrix (4.68) evaluated for $t = t_0 + n_x - 2$:

$$\begin{aligned}\tilde{\mathcal{C}}_{t_0+n_x-2} &= [\,\mathbf{b} \quad \cdots \quad J_{n_x-2}^{t_0+n_x-2}\mathbf{b} \quad J_{n_x-1}^{t_0+n_x-2}\mathbf{b}\,] \\ &= [\,\mathbf{b} \quad \cdots \quad J_{n_x-2}^{t_0+n_x-2}\mathbf{b} \quad J_{n_x-2}^{t_0+n_x-2}A^{t_0}\mathbf{b}\,] \\ &= [\,\mathbf{b} \quad \cdots \quad J_{n_x-2}^{t_0+n_x-2}\mathbf{b} \quad \alpha J_{n_x-2}^{t_0+n_x-2}\mathbf{b} + \epsilon\alpha J_{n_x-2}^{t_0+n_x-2}H\mathbf{b}\,], \end{aligned} \tag{5.95}$$

with the two last columns which become degenerate as $\epsilon$ vanishes. In order to evaluate the gain matrix $K^{t_0-1}$ one needs to calculate the inverse of $\tilde{\mathcal{C}}_{t_0+n_x-2}$ which is most easily accomplished using the singular value decomposition $\tilde{\mathcal{C}}_{t_0+n_x-2} = Q\Sigma R^\dagger$ (compare this to the the discussion in section 4.4). Let us define the matrix $S$ such that

$$\begin{aligned} S &= \Sigma R^\dagger = Q^\dagger \tilde{\mathcal{C}}_{t_0+n_x-2} \\ &= [\,Q^\dagger\mathbf{b} \quad \cdots \quad Q^\dagger J_{n_x-2}^{t_0+n_x-2}\mathbf{b} \quad \alpha Q^\dagger J_{n_x-2}^{t_0+n_x-2}\mathbf{b} + \epsilon\alpha Q^\dagger J_{n_x-2}^{t_0+n_x-2}H\mathbf{b}\,], \end{aligned} \tag{5.96}$$

whose two last columns also become degenerate for vanishing $\epsilon$ and arbitrary $Q$. We can use this fact to obtain the relation between the elements of the two last rows of the matrix $R$:

$$\sigma_i(\epsilon)R_{n_x i} = S_{in_x} = \alpha S_{in_x-1} + O(\epsilon) = \alpha\sigma_i(\epsilon)R_{n_x-1i} + O(\epsilon), \tag{5.97}$$

where $\sigma_i(\epsilon) = \Sigma_{ii}$ denote the singular values. Similarly to section 4.4 we conclude that the smallest singular value scales linearly with $\epsilon$, $\sigma_{n_x}(\epsilon) = O(\epsilon)$, while the rest of the singular values do not, $\sigma_i(\epsilon) = O(1)$, $i = 1, \cdots, n_x - 1$. Discarding the terms of order $\epsilon$ we, therefore, obtain $R_{n_x i} = \alpha R_{n_x-1i}$ for all $i = 1, \cdots, n_x - 1$. The relation for $R_{n_x n_x}$ and $R_{n_x-1 n_x}$ can be obtained using the fact that $R$ is an orthogonal matrix, so that

$$\sum_{i=1}^{n_x} R_{n_x i}^2 = 1, \qquad \sum_{i=1}^{n_x} R_{n_x-1i}^2 = 1, \qquad \sum_{i=1}^{n_x} R_{n_x i}R_{n_x-1i} = 0. \tag{5.98}$$

After trivial manipulations we obtain $R_{n_x-1 n_x} = -\alpha R_{n_x n_x}$ and, consequently,

$$R_{n_x n_x} = [\alpha^2 + 1]^{-1/2} = O(1). \tag{5.99}$$

According to equation (5.96), the degeneracy only affects the structure of the matrices $R$ and $\Sigma$, but not $Q$, so all elements of $Q$ are generically of order one and, in particular, $Q_{kn_x} = O(1)$, $k = 1, \cdots, n_x$. Finally, writing down the elements of the feedback gain matrix (5.94) we obtain

$$\begin{aligned} K_j^{t_0-1} &= \sum_{k=1}^{n_x} (R(\Sigma)^{-1} Q^\dagger)_{n_x k} (J_{n_x}^{t_0+n_x-2})_{kj} \\ &= \sum_{i=1}^{n_x} R_{n_x i} \sigma_i^{-1} \sum_{k=1}^{n_x} Q_{ki} (J_{n_x}^{t_0+n_x-2})_{kj} \\ &\approx [\alpha^2+1]^{-1/2} \sigma_{n_x}^{-1} \sum_{k=1}^{n_x} Q_{kn_x} (J_{n_x}^{t_0+n_x-2})_{kj}. \end{aligned} \tag{5.100}$$

As a result, the feedback

$$\Delta u^{t_0-1} = -\sum_{j=1}^{n_x} K_j^{t_0-1} \Delta x_j^{t_0-1} = O(\epsilon^{-1}) |\Delta \mathbf{x}^{t_0-1}| \tag{5.101}$$

diverges for (almost) every $\Delta \mathbf{x}^{t_0-1} \neq \mathbf{0}$ as $\epsilon$ vanishes, leading to the divergence of the noise amplification factor (5.45).

The same statement holds for the OGY type control. According to (5.15), the evaluation of the feedback gain $K^{t_0-1}$ requires taking the inverse of the stabilizability matrix (5.12) with $t = t_0 + n_x^u - 2$:

$$\tilde{\mathcal{S}}_{t_0+n_x^u-2} = [\, \mathbf{e}_1^{t_0+n_u^x-1} \quad \cdots \quad J_{n_x^u-2}^{t_0+n_x^u-2} \mathbf{b} \quad \alpha J_{n_x^u-2}^{t_0+n_x^u-2} \mathbf{b} + \epsilon \alpha J_{n_x^u-2}^{t_0+n_x^u-2} H \mathbf{b} \,], \tag{5.102}$$

whose two last columns become degenerate for vanishing $\epsilon$, similarly to the case of dead-beat control (compare with (5.95)). Therefore, the same analysis and conclusions apply.

Similar statements can be made in the more general multi-parameter case. In other words, the blowup of the control perturbation is not an artifact of the single-parameter realization of the above techniques, but rather a generic feature that transpires in certain conditions, specifically, when the Jacobian becomes highly degenerate at a certain point on the target trajectory. This kind of blowup appears even more surprising if $|\alpha| < 1$, when the matrix $A^{t_0}$ is *stable* and, intuitively, *no* control is needed.

It can be argued that the situation considered above is highly relevant for many systems, specifically systems with symmetries. For instance, many spatially extended chaotic systems with low degree of spatial correlation can be thought of as a number of identical spatially distributed and weakly coupled subsystems. The diagonal elements of the Jacobian matrix (5.93) would then describe local dynamics of each subsystem, while the off-diagonal elements would correspond to weak interactions between subsystems and will, therefore, be small. An example of such an extended system will be studied in detail in chapter 6.

Here we consider another example, a system of two identical chaotic systems with mistuned parameters, each modeled by a one-dimensional chaotic map. Since the choice of the map is not important, we take the most often used one, the logistic map. Furthermore, we assume that the systems are weakly and unidirectionally coupled (bidirectional coupling can be chosen as well), so that the combined dynamics is described by the following two-dimensional map:

$$\begin{aligned} x_1^{t+1} &= a_1 x_1^t (1 - x_1^t) + \Delta u^t \\ x_2^{t+1} &= a_2 x_2^t (1 - x_2^t) + \epsilon (x_1^t - x_2^t) - \Delta u^t, \end{aligned} \tag{5.103}$$

where $\Delta u^t$ denotes the feedback we use to control the system. The parameters are, respectively, $a_1 = 3.8$, $a_2 = 4.0$, and $\epsilon = 0.01$. As a target state we choose a period-six trajectory $\bar{\mathbf{x}}^t$, which makes the Jacobian

$$A^t = \begin{bmatrix} a_1(1 - 2\bar{x}_1^t) & 0 \\ \epsilon & a_2(1 - 2\bar{x}_2^t) - \epsilon \end{bmatrix} \tag{5.104}$$

almost degenerate at time $t = t_0 = 1$, when $\alpha = a_1(1 - 2\bar{x}_1^1) = a_2(1 - 2\bar{x}_2^1) + O(\epsilon)$, such that

$$A^1 = \alpha \begin{bmatrix} 1 & 0 \\ O(\epsilon) & 1 + O(\epsilon) \end{bmatrix}. \tag{5.105}$$

The feedback is chosen such that the control matrix is constant

$$B = \mathbf{b} = \begin{bmatrix} 1 \\ -1 \end{bmatrix}, \tag{5.106}$$

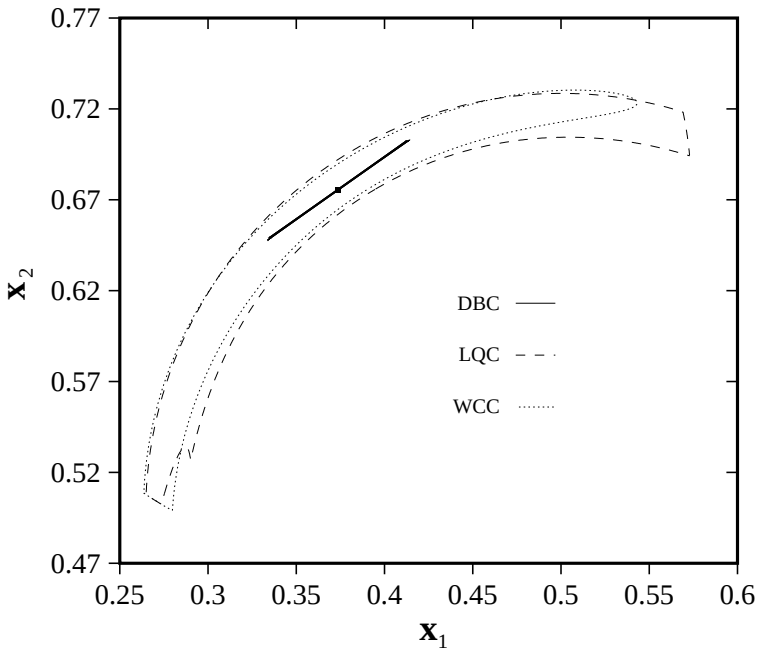


Figure 5.2: Basin of attraction of the closed-loop system at the point $\bar{\mathbf{x}}^6$ of the period-six target trajectory. The boundary is found numerically for feedback corresponding to dead-beat control (solid line), linear-quadratic control (dashed line), and worst case control (dotted line).

so that the results of the above analysis directly apply. In order to illustrate the blowup effect and compare the performance of different feedback control techniques, we numerically calculate the basin of attraction of the resulting nonlinear closed-loop system obtained upon substituting the respective feedback law into the map (5.103) at time $t = (t_0 - 1) \bmod 6 = 6$. (For the worst case control, we set $C^t = I$ in (5.74), so that the output $\Delta\mathbf{y}^t$ coincides with the state $\Delta\mathbf{x}^t$.) The results are presented in figure 5.5.

One can clearly see that the basin of attraction $\mathcal{N}_{DBC}(\bar{\mathbf{x}}^6)$ corresponding to the dead-beat control technique is extremely narrow, due to the blowup effect described above. The direction along which the basin of attraction is aligned can be extracted from (5.100) by solving the equation

$$K_1^6 \Delta x_1 + K_2^6 \Delta x_2 = 0, \tag{5.107}$$

which determines where the diverging contributions to the feedback (5.101) from different degrees of freedom cancel out. On the contrary, the basins of attraction

corresponding to the linear-quadratic control and worst case control are rather large. To get a quantitative description of the size of the basin of attraction in each case, we calculated the smallest distance $\delta x$ from the point $\bar{\mathbf{x}}^6$ of the target trajectory to the boundary of the basin of attraction. The numerical values, $\delta x_{DBC} \approx 2.7 \times 10^{-4}$, $\delta x_{LQC} \approx 1.0 \times 10^{-2}$, and $\delta x_{WCC} \approx 8.8 \times 10^{-3}$ speak strongly in favor of the optimal control techniques. As we determined in section 5.3.1, the size of the domain of attraction is critical for the success of linear feedback control, especially if the system is high-dimensional, which makes either of the optimal control techniques a superior choice for controlling spatiotemporally chaotic dynamics.

A few comments should be made. First of all, neither the linear-quadratic control nor the worst case control were tuned to obtain the largest possible basin of attraction (which can be accomplished using the methods of robust control [51]). So the results obtained primarily emphasize how narrow the basin of attraction corresponding to the dead-beat control is compared to the other two methods. Second, in the present thesis we limit ourselves to considering the problem of linear control. However, by using *nonlinear* control [64] it is often possible to make target trajectory the global attractor, especially for simple systems like the one considered here.

# Chapter 6 Extended Chaotic Systems

## 6.1 The Model

Now that we have constructed the formalism that can handle symmetric deterministic as well as stochastic systems, the problem of controlling a general extended chaotic system seems rather straightforward. First we need a mathematical model, or a set of dynamical equations describing the evolution of a given experimental system. Assuming no theoretical model of the system is available, the dynamics will have to be reconstructed using the time series measurement of a set of observables consistent with the symmetry, as discussed in chapter 3 and section 4.5. The reconstruction has a hidden benefit. Extended systems are often infinite-dimensional. The methods of control theory, though, are only applicable to finite-dimensional systems. Therefore, some sort of dimensional reduction, such as a Galerkin truncation [38], has to be performed anyway (discussion of other model reduction techniques is available in many control theory texts, e.g., [51]). However, since the chaotic attractor of finite extended systems is typically finite-dimensional, the reconstructed dynamics will automatically be finite-dimensional.

Consistent reconstruction will yield a model, which should preserve the symmetries of the system. However, most of the information regarding the local properties of the original system will be lost. As we will see below, the locality of interactions in the system is important both for the analysis of the control problem and for the interpretation of the obtained results. As a consequence, the loss of the local structure would prevent us from gaining a valuable system-independent insight. Therefore, instead of considering the reconstructed mathematical model of some specific experimental system we select a model system which, on the one hand, has the dynamics and the spatiotemporal structure characteristic of extended spatiotemporally chaotic systems in general and, on the other hand, is simple enough to analyze and compute. In particular, we require the model system to be symmetric. In order to facilitate the

analysis we also require the model to be finite-dimensional, which puts the system on a spatial lattice. Furthermore, since the analysis of continuous- and discrete-time systems is very similar, we choose to discretize time as well. It can be argued that the results obtained after this reduction should still be applicable to extended systems in general, continuous or discrete in space as well as time.

We do not regard our model as an exact description of the dynamics of any particular system, but rather as an approximation that captures the behavior of the dominant modes of the actual system. The state $\mathbf{x}^t$ of our finite-dimensional approximation cannot fully represent the state of the infinite-dimensional system either. Therefore, the dynamics of the state vector $\mathbf{x}^t$ should be affected (however weakly) by the unmodeled dynamics of unaccounted degrees of freedom as well as the unknown interaction with the environment. Consequently, the evolution equation should include both deterministic and stochastic components. The effect of the latter is usually rather small and can be treated as random noise $\mathbf{w}^t$ (often called the *process* noise). As a result, the evolution equation should be of the form (5.1) rather than the form (3.9) assumed in chapters 3 and 4.

Since interactions in extended physical systems often have a rather short range, if we associate one degree of freedom $x_i^t$ with each site $i$ of the spatial lattice, we can neglect the dependence of the dynamics of a variable $x_i^t$ on the variables $x_j^t$ associated with all lattice sites $j$, except the few nearest neighbors of the site $i$. (We do not consider systems with long range interactions here to avoid unnecessarily complicating the discussion, although they can be treated equally successfully using the formalism outlined below.) For simplicity the lattice can be chosen as one-dimensional (this is often justified for large aspect ratio systems in higher dimensions), and then our reduced model is naturally represented by a stochastic generalization of the deterministic coupled map lattice (CML) with nearest neighbor diffusive coupling [65]:

$$x_i^{t+1} = \epsilon f(x_{i-1}^t, a) + (1-2\epsilon) f(x_i^t, a) + \epsilon f(x_{i+1}^t, a) + \Psi_i(\mathbf{x}^t, \mathbf{w}^t), \tag{6.1}$$

where index $i = 1, 2, \cdots, n_x$ labels the lattice sites, and the last term (we assume $\Psi_i(\mathbf{x}, \mathbf{0}) = 0$ for every $i$) represents the net effect of stochastic perturbations at site $i$.

Imposing the periodic boundary condition, $x^t_{i+n_x} = x^t_i$, emulates the translational (or rotational for, e.g., a Taylor Couette system) invariance. We also assume that both $a$ and $\epsilon$ are the same throughout the lattice.

The local map $f(x, a)$ can be chosen as an arbitrary (nonlinear) function with parameter $a$, which typically represents the process of generation of chaotic fluctuations by the local dynamics of the system, while diffusive coupling typically plays the opposite role of dissipating local fluctuations. Therefore, the parameters $a$ and $\epsilon$ specify the degree of instability and the strength of dissipation in the system, respectively. For the purpose of control, however, details of the local map are not important. The only aspect of the control problem affected by any particular choice is the set of existing unstable periodic trajectories.

Our ultimate goal is to construct a linear control scheme able to stabilize any steady or time-periodic state of the CML (6.1) of arbitrary length $n_x$ in the presence of nonzero noise and assuming that complete information about the state of the system is unavailable and has to be extracted from the noisy time series measurement of a limited number of scalar observables. Furthermore, we would like the control scheme to provide optimal performance with or without noise and be practically realizable. In particular, we would like the number of independent control parameters to be much less than the number of degrees of freedom. The major ingredients of such a control scheme are expected to be system-independent and, hence, applicable to extended spatiotemporally chaotic systems in general.

## 6.2 Control Parameters

### 6.2.1 Symmetry of the Lattice

Before we proceed with the analysis of the general problem of controlling arbitrary time-periodic target states of our noisy model (6.1) based on partial measurements of the state, we study the simplest case of linear steady state control in the absence of noise and assuming the full knowledge of the state of the system. The solution for the general case is then obtained as a sequence of rather straightforward generalizations. The first problem that we face here is that there is no natural choice of control

parameters in the problem. Besides, as we will see shortly, not every control parameter is suitable.

The analysis of the controllability condition conducted in chapter 4 shows that, if the system is symmetric, certain symmetry-imposed restrictions on the choice of control parameters should be satisfied in order to achieve control. In fact, our model is by construction highly symmetric. The symmetry is that of the spatial lattice: the evolution equation (6.1) is invariant with respect to translations by an integer number of lattice sites (periodic boundary condition makes the group finite) and reflections about any site (or midplane between any adjacent sites), which map the lattice back onto itself without destroying the adjacency relationship. The corresponding point group $\mathrm{C}_{n_x v}$ (we assume $n_x$ – even) has a total of $n_x/2 + 3$ nonequivalent irreducible representations. The first four are one-dimensional, $d_1 = d_2 = d_3 = d_4 = 1$, while the rest $n_x/2 - 1$ are two-dimensional, $d_r = 2$, $r \geq 5$. In comparison, breaking the reflection symmetry reduces the group to $\mathrm{C}_{n_x}$, which only has one-dimensional irreducible representations.

The dynamical symmetry group can be trivially obtained using the observation that the Jacobian matrix in the linearized evolution equation (5.47) of the CML (6.1) can always be represented as a product of two matrices, $A^t = MN^t$, where

$$M_{ij} = (1 - 2\epsilon)\delta_{i,j} + \epsilon(\delta_{i,j-1} + \delta_{i,j+1}) \tag{6.2}$$

describes diffusive coupling, and

$$N^t_{ij} = \partial_x f(\bar{x}^t_i, a)\delta_{i,j} \tag{6.3}$$

defines the strength of local instability, with $\delta_{i,j\pm1}$ extended to comply with periodic boundary condition. This partition of the Jacobian explicitly shows how the symmetry group $\mathcal{L}$ depends on the symmetry properties of the nonlinear evolution equation (6.1) and those of the controlled state $\bar{\mathbf{x}}^t$. The matrix $M$ has all the symmetries imposed by the chosen inter-site couplings of the nonlinear model:

$$T(g)M = MT(g), \quad \forall g \in \mathcal{G}, \tag{6.4}$$

while the matrix $N^t$ has all the symmetries of the target state $\bar{\mathbf{x}}^t$:

$$T(g)N^t = N^t T(g), \quad \forall g \in \mathcal{H}_{\bar{\mathbf{x}}}, \tag{6.5}$$

where similarly to chapter 4, $T$ denotes the matrix representation of $\mathcal{L}$, and $\mathcal{H}_{\bar{\mathbf{x}}}$ is defined as a subgroup of $\mathcal{G}$. Since the Jacobian $A^t$ commutes with all matrices that commute with both $M$ and $N^t$, we conclude that generically $\mathcal{L} = \mathcal{H}_{\bar{\mathbf{x}}} \subseteq \mathcal{G}$, in agreement with the general result (4.72).

Since the analysis conducted in chapter 4 is valid for every subgroup $\mathcal{L}'$ of the dynamical symmetry group, we take $\mathcal{L}' = \mathcal{L}$. Constructing the $n_x$-dimensional representation $T$ of $\mathcal{L}$ and decomposing it into the sum of the irreducible representations of $\mathrm{C}_{n_x v}$ we easily determine the restrictions imposed by the symmetry on the minimal number of control parameters $n_u$ and the structure of the control matrix $B$. For instance, a zigzag state gives $\mathcal{L} = \mathrm{C}_{nv}$ with $n = n_x/2$ and, according to (4.58), $\bar{n}_u = 2$; a non-reflection-invariant state with spatial period $s$ corresponds to $\mathcal{L} = \mathrm{C}_n$ with $n = n_x/s$ and $\bar{n}_u = 1$, etc.

Let us consider the uniform target state, which has the highest symmetry possible, $\mathcal{L} = \mathrm{C}_{n_x v}$, in more detail. The decomposition (4.23) gives

$$T = T^1 \oplus T^4 \oplus T^5 \oplus \cdots \oplus T^{n_x/2+3}, \tag{6.6}$$

and the corresponding basis of normal modes which transform according to these irreducible representations is given by the eigenvectors of the operators of translation and reflection, i.e., Fourier modes $\mathbf{g}^i$:

$$(\mathbf{g}^i)_j = \cos(jk_i + \phi_i). \tag{6.7}$$

Here $\phi_i$ are arbitrary phase shifts, and $k_i$ are the wavevectors defined thus: $k_1 = 0$, $k_i = k_{i+1} = \pi i/n_x$ for $i = 2, 4, 6, \cdots$, and, for $n_x$ – even, $k_{n_x} = \pi$. Fourier modes with the same wavevectors $k$ define invariant subspaces $L^k \subset \mathbb{R}^{n_x}$. The subspaces $L^k$ with $0 < k < \pi$ correspond to the representations $T^r$ with $r \geq 5$, $L^0$ corresponds to $T^1$, and $L^\pi$ to $T^4$. Since the two-dimensional irreducible representations are present in the decomposition (6.6), $\bar{n}_u = 2$. Therefore, in order to control an unstable uniform

steady state of the coupled map lattice we need at least two control parameters. This is the reflection of symmetric coupling in the model (6.1). Note that, since every two-dimensional irreducible representation occurs in the decomposition (6.6) once, $p_5 = \cdots = p_{n_x/2+3} = 1$, according to the results of section 4.2, the minimal number of control parameters remains the same for a spatially uniform target trajectory of arbitrary time period $\tau$.

On the other hand, since for any length $n_x$ of the lattice the group $\mathcal{G} = \mathrm{C}_{n_x v}$ only has one- and two-dimensional irreducible representations and $\mathcal{L}$ is a subgroup of $\mathcal{G}$, it is sufficient to have just two control parameters to make the dynamics of the coupled map lattice controllable in the vicinity of a target state with arbitrary symmetry properties and temporal period. Choosing the minimal number of control parameters, $n_u = 2$, we can determine the conditions making them independent with respect to a particular target state: the linear response of the CML to perturbation of the two parameters, given by the columns of the control matrix $B = [\,\mathbf{b}_1 \quad \mathbf{b}_2\,]$, has to satisfy conditions (4.22) and (4.62).

Failure to satisfy the necessary condition (4.22) rules out the possibility of using global parameters, such as the coupling $\epsilon$ or parameter $a$ of the local map $f(x, a)$ for control of symmetric steady states. Taking $\mathbf{u} = (a, \epsilon)$, so that

$$\mathbf{b}_1 = \partial_a \mathbf{F}(\bar{\mathbf{x}}, \mathbf{0}, \bar{\mathbf{u}}) = M \begin{bmatrix} \partial_a f(\bar{x}_1, \bar{a}) \\ \vdots \\ \partial_a f(\bar{x}_{n_x}, \bar{a}) \end{bmatrix}, \tag{6.8}$$

and

$$\mathbf{b}_2 = \partial_\epsilon \mathbf{F}(\bar{\mathbf{x}}, \mathbf{0}, \bar{\mathbf{u}}) = (\bar{\epsilon})^{-1}(M - I) \begin{bmatrix} f(\bar{x}_1, \bar{a}) \\ \vdots \\ f(\bar{x}_{n_x}, \bar{a}) \end{bmatrix}, \tag{6.9}$$

we observe that condition (4.22) is only satisfied, if the group $\mathcal{L}$ is trivial, $\mathcal{L} = \{e\}$. This result holds for both steady and time-periodic symmetric target states.

### 6.2.2 Locality and Pinning Control

The two major results of the previous section are especially important. First of all, irrespectively of the length of the lattice $n_x$, it is impossible to control *every* steady

or periodic state of the CML (6.1) using a single control parameter. However, an arbitrary target state can be controlled using two (or more) independent control parameters. The minimal number of control parameters depends on the symmetry properties of the target state, and the higher the symmetry is, the stricter requirements are imposed on the control scheme. Since we are looking to construct a general control scheme independent of the details of the particular target state, we assume that at least two control parameters should be available.

Second, it is impossible to control symmetric target states using global system parameters, such as $a$ and $\epsilon$. As a consequence, feedback has to be applied *locally*. On the other hand, practical considerations would suggest that it is much easier to use a number of actuators to perturb the system locally at distinct spatial locations, e.g., applying local fields, local pressure gradients, injecting chemical reactants, etc. This type of feedback represents interaction with the controller considered to be a part of the environment, and cannot be adequately described using only the internal system parameters like those characterizing the rate of growth of local chaotic fluctuations and the strength of spatial dissipation. Instead, it is most naturally described by generalizing the term $\Psi_i(\mathbf{x}^t, \mathbf{w}^t)$ in equation (6.1) to include the interaction with the controller, so that

$$x_i^{t+1} = \epsilon f(x_{i-1}^t, a) + (1-2\epsilon) f(x_i^t, a) + \epsilon f(x_{i+1}^t, a) + \Psi_i(\mathbf{x}^t, \mathbf{w}^t, \mathbf{u}^t), \tag{6.10}$$

where now vector $\mathbf{u}^t$ describes the strength of interaction with the controller. The equilibrium value $\bar{\mathbf{u}}$ can be selected arbitrarily, so we will assume $\bar{\mathbf{u}} = \mathbf{0}$ below. Without noise and control the last term in (6.10) vanishes, so one should have $\mathbf{\Psi}(\mathbf{x}, \mathbf{0}, \mathbf{0}) = \mathbf{0}$. Consequently, the linearization about the target state $\bar{\mathbf{x}}^t$ again yields (5.47), but now with $B^t = \mathbf{D_u}\mathbf{\Psi}(\bar{\mathbf{x}}, \mathbf{0}, \mathbf{0})$ and $E^t = \mathbf{D_w}\mathbf{\Psi}(\bar{\mathbf{x}}, \mathbf{0}, \mathbf{0})$.

For simplicity we further assume that the interaction between the system and the controller is limited to only a few lattice sites $i_m$, which we call pinnings following Hu and Qu [15]:

$$\frac{\partial \Psi_i(\mathbf{x}, \mathbf{w}, \mathbf{0})}{\partial u_j} = 0 \tag{6.11}$$

for all $j$ and $i \neq i_m$, $m = 1, 2, \cdots, n_u$. Then, without loss of generality, the control

matrix $B$ can be chosen as a matrix with dimensions $n_x \times n_u$:

$$B_{ij} = \sum_{m=1}^{n_u} \delta_{j,m}\delta_{i,i_m}, \tag{6.12}$$

such that $\Delta u_m^t$ describes the strength of the control perturbation applied at the lattice site $i = i_m$ at time $t$. The number of pinnings (equal to the number of control parameters) can be, in principle, chosen arbitrarily in the range $\bar{n}_u \leq n_u \leq n_x$, where $\bar{n}_u = 2$ as we established above.

In fact, the same minimal number of pinnings is required to control one-dimensional spatially continuous extended system in the most frequently used geometry, a line segment with the periodic boundary condition, or an annulus. The respective symmetry group is $\mathrm{C}_{\infty v} = \mathrm{S}_2 \times \mathrm{SO}(2)$ (translation restricted by the periodic boundary condition plus reflection). The most surprising fact is that, in the absence of noise, the minimal density of pinnings is not bounded from below and is independent of the number of excited modes and, consequently, strength of spatial correlations in the system.

We model the effect of the process noise by applying uncorrelated random perturbations to each site of the lattice. Combined with the chosen arrangement of pinnings, this corresponds to picking the stochastic term in equation (6.10) as

$$\Psi_i(\mathbf{x}^t, \mathbf{w}^t, \mathbf{u}^t) = \sum_{m=1}^{n_u} \delta_{i,i_m} u_m^t + w_i^t, \tag{6.13}$$

and, consequently, setting $E^t = \mathbf{D}_{\mathbf{w}}\boldsymbol{\Psi}(\bar{\mathbf{x}}, \mathbf{0}, \mathbf{0}) = I$ in the linearization (5.47). Furthermore, we choose the individual perturbations $w_i^t$ as independent random variables uniformly distributed in the interval $[-\sigma_w, \sigma_w]$, so that the noise correlation matrix is given by $\Xi = (\sigma_w^2/3)I$. This latter choice is made to simplify the interpretation of the results and does not affect the control problem otherwise.

Localized control has its downside. In the weak coupling limit, $\epsilon \to 0$, the coupled map lattice with local feedback becomes a weakly controllable system. The symmetry of the lattice of uncoupled maps is described by the permutation group $\mathcal{G} = \mathrm{S}_{n_x}$, while the linearization about a uniform target state increases the symmetry to $\mathcal{L} = \mathrm{GL}(n_x)$: since the respective Jacobian is a multiple of the unit matrix, $A_{ij} = \partial_x f(\bar{x}, \bar{a})\delta_{i,j}$, the

linearized system is symmetric with respect to all (complex) nonsingular coordinate transformations. When coupling is restored, $\epsilon > 0$, the symmetry of both the nonlinear evolution equation (6.1) and its linearization (5.47) reduces to $\mathcal{G}' = \mathcal{L}' = \mathrm{C}_{n_x v}$.

The matrix representation $T$ of the group $\mathrm{GL}(n_x)$ in $\mathbb{R}^{n_x}$ is already irreducible. Consequently, $n_u = n_x$ independent control parameters are required to control the steady uniform state of the uncoupled lattice. This result is rather intuitive. Obviously, one can no longer control the system applying control perturbations at just two lattice sites, $i_1$ and $i_2$. Since the control perturbation does not propagate to adjacent sites of the lattice, feedback has to be applied directly at each site.

If the coupling is nonzero, but very small, the controllability property is restored for $n_u = 2$, but, according to section 4.4, feedback of very large magnitude is required to control the system due to parametric deficiency. Indeed, in order to affect the dynamics at site $i$ away from $i_1$ and $i_2$ the control has to propagate a certain distance decaying by roughly a factor of $\epsilon$ per iteration. As a result, the magnitude of the perturbation required to control an arbitrary site of the lattice diverges approximately as $\epsilon^{-n_x/2}$ for $\epsilon \to 0$, resulting in the loss of control [14]. This effect will be discussed in more detail in section 6.5.2.

## 6.3 Periodic Array of Pinnings

Symmetric target states are arguably the most practically interesting and important of all, so these will be the focus of the discussion that follows. It is no accident that by far the most common target state, a spatially uniform time-invariant state $\bar{x}_1 = \cdots = \bar{x}_{n_x} = \bar{x}$, is the state which has the highest symmetry and, as a consequence, requires the controller with the most complicated spatial structure. On the other hand, symmetry usually significantly simplifies the analysis of system dynamics, and the neighborhood of the steady uniform state benefits most from this simplification. All of this makes it the perfect target state to test the general results on. Since the steady uniform state is period one in both space and time, we will often use the shorthand notation S1T1 for it.

Naively it seems that the most natural choice is to place the pinnings in a periodic

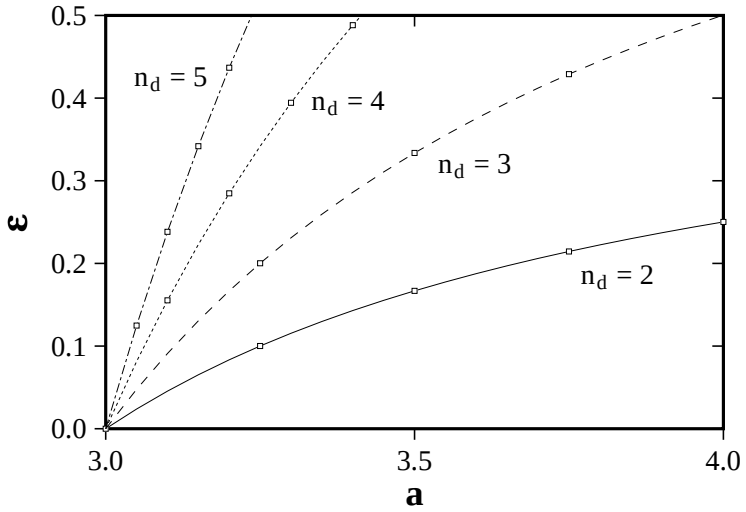


Figure 6.1: Periodic array of single pinning sites: minimal coupling $\epsilon$ as a function of parameter $a$. The dots represent the numerical results from figure 2 of [15], with $\epsilon$ rescaled by a factor of two to make it compatible with our definition.

array, such that the distance between all $n_u$ pinnings is constant, $i_{m+1} - i_m = n_d$, $\forall m$. However, it can be shown that with this setup the uniform target state could only be stabilized with a rather dense array of pinnings, and that the distance $n_d$ sensitively depends on the values of system parameters $a$ and $\epsilon$. Figure 6.3 shows the minimal coupling $\epsilon$ for which the stabilization was achieved in the absence of noise in the numerical experiment [15] as a function of parameter $a$ for several values of $n_d$. The logistic map

$$f(x, a) = ax(1 - x) \tag{6.14}$$

with the fixed point $\bar{x} = 1 - a^{-1}$ was taken as the local chaotic map. In particular, in the physically interesting interval of parameters $3.57 < a \leq 4.0$, where the independent logistic maps are chaotic, control fails unless $n_d \leq 3$ even for relatively strong coupling $\epsilon = 0.4$. It is interesting to note that the distance between periodically placed pinnings can be increased significantly, if the symmetry of the system is lower, such as when the parity symmetry is broken [28].

One can easily verify that the control matrix (6.12) calculated for a periodic array of pinning sites does not satisfy the controllability condition. It is trivial to check

that the eigenvectors of the Jacobian

$$A = \partial_x f(\bar{x}, a)M \tag{6.15}$$

are given by the Fourier modes (6.7). This is consistent with the results of the section 4.1.3: since the uniform state is invariant with respect to both translations and reflections of the lattice and no irreducible representations of the respective dynamical symmetry group $\mathcal{L} = \mathrm{C}_{n_x v}$ occur in the decomposition (6.6) more than once, the basis vectors of the invariant subspaces $L^k$ should coincide with the eigenvectors of the invariant Jacobian.

Let us again use the notation $\mathbf{b}_m$ for the $m$th column of the matrix $B$. According to the results of section 4.1.5, the controllability condition is only satisfied when the projections of the vectors $\mathbf{b}_m$, $m = 1, \cdots, n_u$ span every invariant subspace $L^k$. The pinnings are placed with period $n_d$, so

$$(\mathbf{g}^i \cdot \mathbf{b}_m) = \cos([i_1 + (m-1)n_d]k_i + \phi_i) = 0 \tag{6.16}$$

for every $m$, whenever $k_i = \pi/n_d, 2\pi/n_d, 3\pi/n_d, \cdots$ and $\phi_i = i_1 k_i + \pi/2$. As a consequence, only a one-dimensional subspace of $L^{k_i}$ will be spanned, while $\dim(L^k) = 2$, $0 < k < \pi$. Therefore, feedback through the periodic array of pinnings does not affect the normal modes (6.7) whose nodes happen to lie at the pinnings, i.e., modes with periods $2\pi/k_i$ equal to $2n_d$, $2n_d/2$, $2n_d/3$, etc., provided those are integer. In other words, such modes are uncontrollable. (By contrast, in the systems with the broken parity symmetry, such as the one considered in [28], invariant subspaces are all one-dimensional and the same arrangement of pinnings leaves no normal modes uncontrollable.)

The control succeeds only when *all* uncontrollable normal modes are stable, i.e., when the weaker stabilizability condition is satisfied. This, however, imposes excessive restrictions on the density $\rho \equiv n_u/n_x = 1/n_d$ of pinnings in the array. The condition for stabilizability can be obtained from the spectrum of eigenvalues of the Jacobian matrix (6.15):

$$\lambda_i = \alpha(1 - 2\epsilon(1 - \cos(k_i)), \tag{6.17}$$

where $\alpha = \partial_x f(\bar{x}, a) = 2 - a$. Specifically, we need

$$\left|(a-2)\left[1 - 2\epsilon\left(1 - \cos\left(\frac{\pi j}{n_d}\right)\right)\right]\right| < 1 \tag{6.18}$$

for all $j = 1, \cdots, n_x - 2$, such that $n_d/j$ is integer. Using this criterion one can obtain the relation between the minimal coupling, the distance between pinnings $n_d$, and the parameter $a$ of the local chaotic map for a stabilizable system. For instance, $j = 1$ yields

$$\epsilon = \frac{a-3}{2(a-2)\left(1 - \cos\left(\frac{\pi}{n_d}\right)\right)}. \tag{6.19}$$

The curves defined by equation (6.19) are plotted in figure 6.3 together with the numerical results of Hu and Qu [15] and are seen to be in excellent agreement. Alternatively, equation (6.19) can be used to find the minimal value of $\rho$ as a function of $a$ and $\epsilon$ for the target state S1T1. Similar restrictions on the minimal density of pinnings can be obtained for target states of arbitrary spatial and temporal periodicity (e.g., S2T1 and S1T2 [66]).

The analysis of section 6.2 suggests that one can get rid of all uncontrollable modes placing pinning sites differently. Arranging the pinnings, such that the controllability condition for the matrices (6.15) and (6.12) is satisfied, will enable us to control the system *anywhere* in the parameter space at the same time using a *smaller* number of pinnings, simplifying the control setup. What is equally important, similar results are applicable to spatially continuous systems as well. This means that one can obtain the restrictions on the mutual arrangement of pinnings for arbitrary extended systems using symmetry considerations alone.

## 6.4 Control at the Boundaries

Let us take the minimal number of pinnings, $n_u = 2$, and place them at the lattice sites $i_1$ and $i_2$. This results in the control matrix

$$B_{ij} = \delta_{j,1}\delta_{i,i_1} + \delta_{j,2}\delta_{i,i_2}, \tag{6.20}$$

which is independent of the target state. The restrictions imposed by the controllability condition on the mutual arrangement of the pinnings $i_1$ and $i_2$ are established trivially. For instance, in the case of the steady uniform target state the length of the lattice $n_x$ should not be a multiple of the distance between pinnings $|i_2 - i_1|$, otherwise the mode with the period $2|i_2 - i_1|$ becomes uncontrollable. One particular arrangement, however, deserves special attention: applying feedback through the pinnings placed at the "beginning" $i_1 = 1$ and the "end" $i_2 = n_x$ of the lattice is equivalent to controlling a spatially uniform system of finite length adjusting the boundary conditions.

The importance of this arrangement, however, is rather dubious unless there exists a whole class of periodic trajectories that can be controlled by adjusting the boundary conditions. In fact, using condition (4.62) one can show that taking the control matrix in the form (6.20) with $i_1 = 1$ and $i_2 = n_x$ ensures the controllability of *any* target state of the CML (6.10), irrespectively of the symmetry properties of that state. In the absence of noise this translates into being able to control arbitrary steady or time periodic states of the coupled map lattice with an arbitrary (but finite) length, switch between states, track target states as the system parameters change and so on, which ensures extreme flexibility of the control scheme. If noise is present, the maximal length of the lattice that can be controlled with two pinnings is limited by the nonlinearity. This will be discussed in detail in section 6.5.2.

Choosing the set of control parameters does not completely define the control scheme. As the next and final step, one should choose the feedback control method. In principle, we can use any of the methods described in the previous chapter. However, given the assumptions made, there is a clear preference. Since we are looking to eventually construct a general control scheme able to stabilize the model system to a prescribed target trajectory with desired properties in the presence of noise of finite amplitude *and* without requiring the complete knowledge of the system state, we have to select between the linear-quadratic control and the worst case control. Furthermore, since we chose the process noise as random and uncorrelated with the state of the system, the linear-quadratic control should achieve the optimal results, so we choose it over the more complicated worst case control.

Before we proceed with the calculation of feedback, we need to define the weight matrices. Unless there is a very compelling reason to distinguish between different points of a periodic target trajectory, it usually does not make much sense to make the weights time-dependent, so we assume that the weight matrices are constant irrespectively of whether the target state is periodic or not. Furthermore, since the model system (6.10) is translationally invariant, it is often natural to choose the weight matrices as multiples of a unit matrix:

$$\begin{aligned} Q &= qI, \quad q \geq 0, \\ R &= rI, \quad r \geq 0. \end{aligned} \tag{6.21}$$

Since the weight matrices are symmetric and the minimization problem is invariant with respect to rescaling the functional (5.40), $(n_x(n_x+1)+n_u(n_u+1))/2-1$ independent parameters are thus replaced with a single adjustable parameter, $q/r > 0$. The remaining adjustable parameter can be chosen to satisfy a selected criterion, be that the minimization of the noise amplification factor $\nu$ or the maximization of the largest magnitude of noise $\bar{\sigma}_w$ tolerated by the resulting control scheme.

Now that the control scheme is completely defined, we can turn to numerical experiments and the analysis of their results. Following Hu and Qu [15] we use the logistic map (6.14) to describe the local dynamics. Also, throughout the remainder of this section we control the coupled map lattice by applying feedback at the boundaries, which corresponds to setting

$$\Psi_i(\mathbf{x}^t, \mathbf{w}^t, \mathbf{u}^t) = \delta_{i,1} u_1^t + \delta_{i,n_x} u_2^t + w_i^t. \tag{6.22}$$

Numerical simulations show that the CML defined by equations (6.10) and (6.22) can be stabilized using the linear-quadratic control method in a wide range of parameters $a$ and $\epsilon$, as we expected. The results are demonstrated for an intermediate value of coupling, $\epsilon = 0.33$, and $a = 4.0$.

Consider the steady uniform target state (which we denoted as S1T1) with $\bar{x} = 1-a^{-1} = 0.75$. The local dynamics of the model system of length $n_x = 8$ in the vicinity of this state is characterized by three unstable and five stable normal modes. The

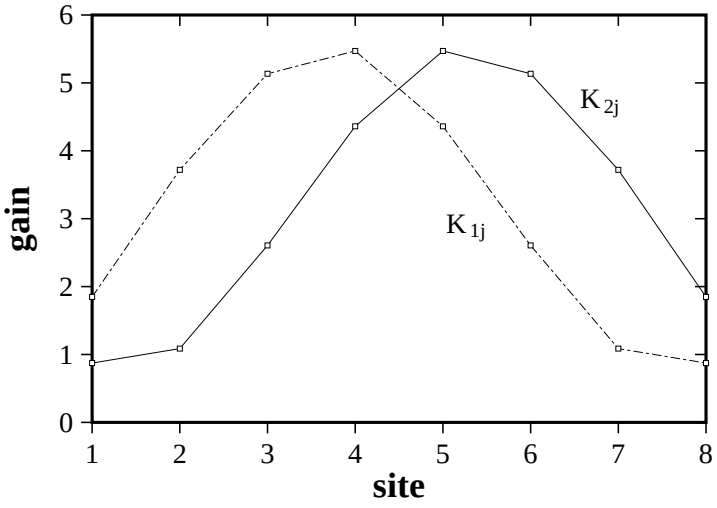


Figure 6.2: Optimal feedback gain for the steady state S1T1: feedback gains $K_{1j}$ and $K_{2j}$ for the two pinnings placed at the sides of the lattice ($i_1 = 1, i_2 = 8$) as functions of the lattice site $j$ for $a = 4.0$ and $\epsilon = 0.33$.

solution of equations (5.36) and (5.37) for the feedback gain matrix $K$ is presented graphically in figure 6.4 for the choice of the weight matrices $Q = I$ and $R = I$. Naturally, the contribution $K_{mj}\Delta x_j^t$ to the control perturbation $\Delta u_m^t$ from the site $j$ far away from the pinning site $i_m$ is larger: since the feedback is applied indirectly through coupling to the neighbors, the perturbation introduced at the pinnings decays with increasing distance from the pinning sites. As a result, feedback becomes very sensitive to the changes in the state of the sites in the middle of the lattice.

One might argue that the lattice with just eight sites is too short to be an adequate model for a typical extended dynamical system. However, the purpose of this section is to illustrate the application of different feedback control techniques introduced in the previous chapter to the problem of controlling the spatially extended system modeled by a coupled map lattice. Here we describe *how* the control techniques can be used under various conditions in the context of our particular model rather than explore their limits of applicability, which is done later in section 6.5, where a scalable generalization of the present control setup is introduced.

First, we stabilize the system in the absence of noise, setting $\sigma_w = 0$. Figure 6.4(a) shows the state of the system as the evolution takes it along a trajectory which passes through the neighborhood $\mathcal{N}(\bar{\mathbf{x}})$ of the uniform target state, and subsequently as

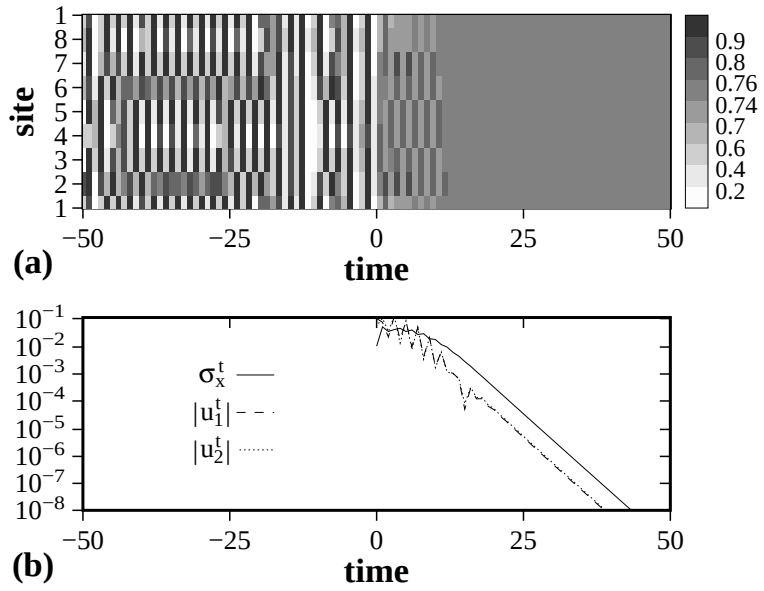


Figure 6.3: State feedback control of the steady state S1T1: (a) system state, (b) its deviation $\sigma_x^t$ from the target state and magnitude of control perturbations $u_1^t$ and $u_2^t$. Feedback is turned on at $t = 0$.

control, turned on at time $t = 0$, drives the system towards the target state. One can see that even though the dimensionality of the system is much larger than the number of control parameters, it only takes about ten time steps for the observable deviations from the uniform configuration to disappear. One can obtain a more quantitative description of the convergence speed by looking at the standard deviation

$$\sigma_x^t = \left[ \frac{1}{n_x} \sum_{i=1}^{n_x} |\Delta x_i^t|^2 \right]^{1/2} \tag{6.23}$$

from the target state as a function of time, presented in figure 6.4(b) along with the magnitude of control perturbations $\Delta u_1^t$ and $\Delta u_2^t$.

We repeat the procedure for the lattice of the same length and using the same feedback gain, but now introducing random noise of finite amplitude $\sigma_w = 10^{-5}$. The state of the system before and after the control is turned on is presented in figure 6.4(a). Large fluctuations about the target state disappear after about ten iterations, as in the noise-free case, although after that, instead of converging to the uniform target state at a constant rate, the system settles into smaller amplitude fluctuation driven by external noise, as evidenced by the standard deviation $\sigma_x^t$ presented in figure

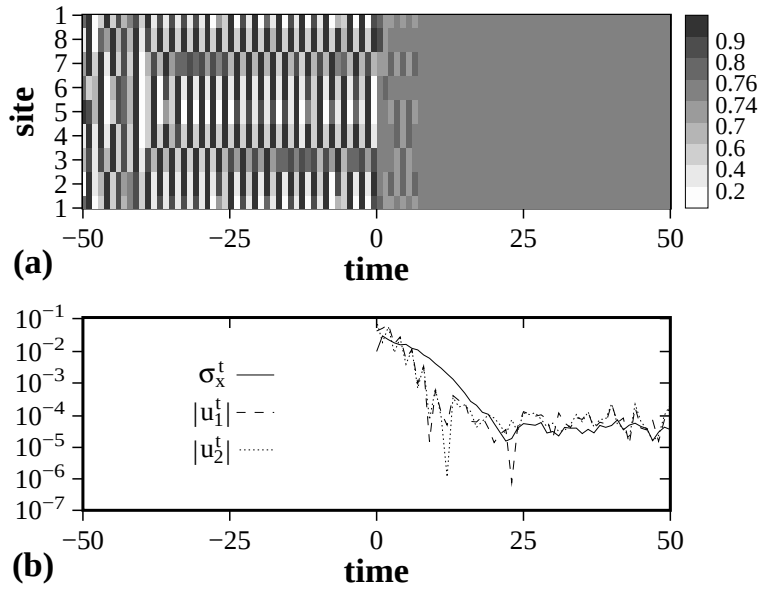


Figure 6.4: State feedback control of the steady state S1T1 with noise: (a) system state, (b) its deviation $\sigma_x^t$ from the target state and magnitude of control perturbations $u_1^t$ and $u_2^t$. The amplitude of noise is $\sigma_w = 10^{-5}$. Feedback is turned on at $t = 0$.

6.4(b) along with the magnitude of control perturbations.

Adding even the smallest amount of noise provides a very good indicator of how well a given method performs with respect to other control methods: the performance is characterized by how well the noise is suppressed. When the noise is small compared to the size $\delta x$ of the basin of attraction $\mathcal{N}(\bar{\mathbf{x}})$ of the target trajectory, such a characteristic is provided by the noise amplification factor $\nu$, which determines the average deviation of the closed-loop system from the target trajectory in the presence of noise of fixed amplitude. When the noise cannot be considered small, minimizing the maximal strength of noise $\bar{\sigma}_w$ that the control scheme can tolerate becomes a much more important criterion than minimizing the noise amplification factor. In general, $\bar{\sigma}_w$ depends not only on $\nu$, but also on $\delta x$ which, in turn, depends on the strength of feedback. For the CML (6.10), however, it was found numerically that setting $R = 0$ to obtain the smallest $\nu$ usually yields the largest $\bar{\sigma}_w$, thus satisfying both criteria.

We compare the noise amplification factor (5.45) for the linear-quadratic control method, the multi-parameter generalization of the OGY method, and the dead-beat control method using the lattice with $n_x = 16$ sites. As expected, the linear-quadratic

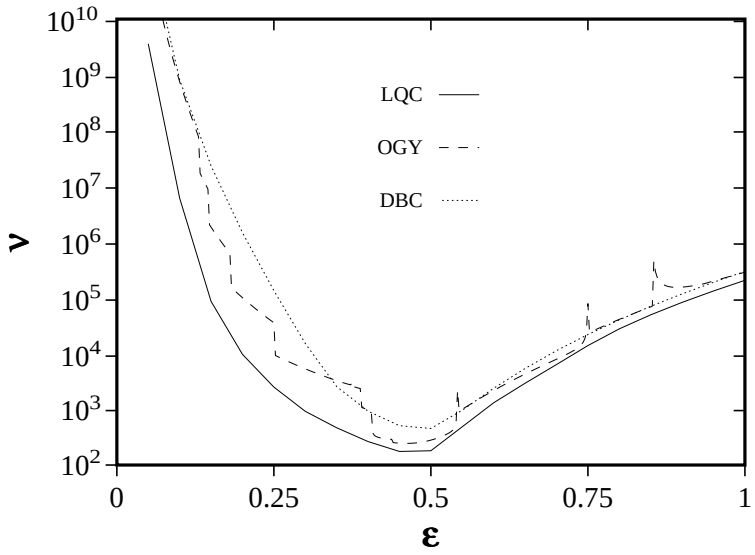


Figure 6.5: Noise amplification factor as a function of coupling calculated for the steady target state S1T1 using linear-quadratic control (solid line), OGY control (dashed lined), and dead-beat control (dotted line). We used $Q = I$ and $R = 0$.

control performs considerably better (see figure 6.4) than the other two methods, especially for small coupling when the degeneracy is most significant. The linear-quadratic control method is also capable of tolerating the noise of much larger amplitude. Using the lattice with $n_x = 8$ sites we found $\bar{\sigma}_w \approx 3 \times 10^{-3}$ for the linear-quadratic control versus $\bar{\sigma}_w \approx 10^{-7}$ for the other two methods — a difference of more than few orders of magnitude. Similar results were obtained for a number of target states besides S1T1, which shows superior robustness properties of the linear-quadratic control, justifying our choice of the control technique.

Time-periodic target states can be controlled equally successfully using the time-dependent generalization of the linear-quadratic control technique described in section 5.3.3. Let us again take the lattice with $n_x = 8$ sites and pick a period four nonuniform (S8T4) trajectory, which is invariant with respect to reflections about sites $i = 4$ and $i = 8$, as our target state. Since the temporal period of this target state is four, the feedback gain matrix obtained by solving equations (5.53) and (5.48) is also periodic with the same period. Numerical experiments again show that the control scheme obtained is rather robust and can withstand noise of considerable amplitude. As seen from figure 6.4, by applying feedback calculated with $Q = I$ and $R = 0$ we managed to stabilize the system despite the rather high level of noise, $\sigma_w = 8 \times 10^{-3}$.

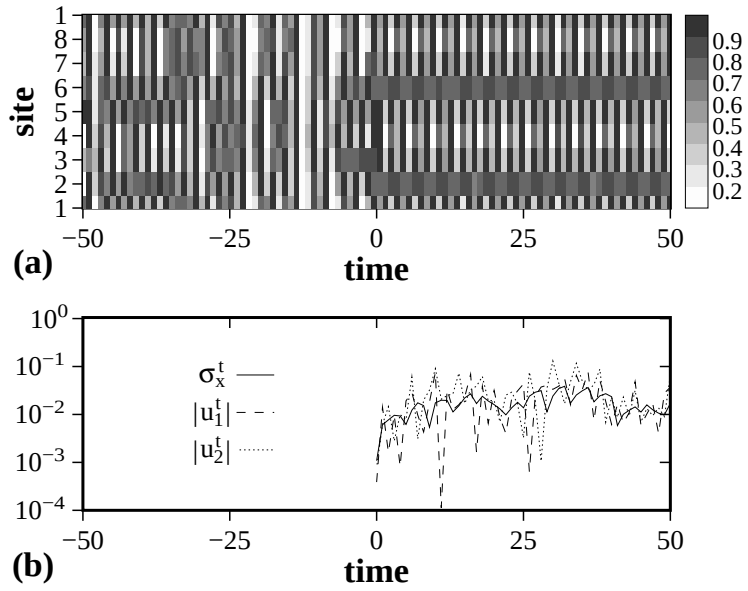


Figure 6.6: State feedback control of the periodic state S8T4 with noise: (a) system state, (b) its deviation $\sigma_x^t$ from the target state and magnitude of control perturbations $u_1^t$ and $u_2^t$. The amplitude of noise is $\sigma_w = 8 \times 10^{-3}$. Feedback is turned on at $t = 0$.

Although the feedback gain (5.48) is by construction optimal for both deterministic and stochastic systems, it can be further tuned by finding the weight matrices optimizing the performance criteria selected in either case. For instance, in the stochastic case it is usually more desirable to increase the tolerance of the control scheme to noise. Hence, for each target state we can set $Q = I$ and $R = rI$ and find the maximal noise strength $\bar{\sigma}_w$ for various $r$, thus determining the optimal weights. This process is illustrated using the target state S8T4. As one can see from figure 6.4, the value of $\bar{\sigma}_w$ varies over almost an order of magnitude, reaching the maximum of approximately $8 \times 10^{-3}$ for the smallest value of $r$ considered, which supports the general observation that in our model $\bar{\sigma}_w$ is maximized by minimizing the noise amplification factor $\nu$. Different target states, however, are sensitive to the choice of the relative magnitude of $Q$ and $R$ to a different degree, e.g., for the steady uniform target state S1T1 $\bar{\sigma}_w \approx 3 \times 10^{-3}$ is essentially independent of the choice of weight matrices.

Finally, we show how our model can be stabilized using output feedback control when the state of the system cannot be determined directly. As we discussed in section 5.4, the state can be dynamically reconstructed using a sequence of measurements of the output. During the observation one usually extracts information about an

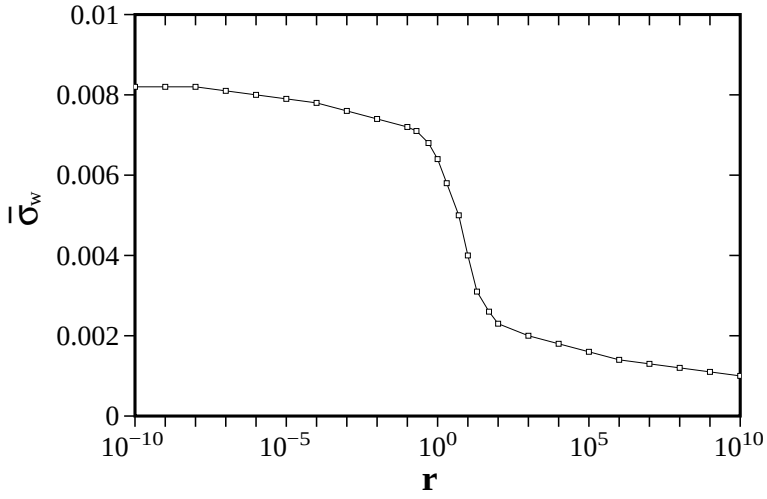


Figure 6.7: Maximal noise amplitude tolerated by state feedback control: $\bar{\sigma}_w$ is plotted for the periodic state S8T4 as a function of $r$, where $R = rI$. Matrix $Q = I$ is kept constant.

extended system locally at a number of distinct spatial locations. This comes as no surprise, since most sensors provide information of extremely local character. In the context of our particular model, this implies that the state of each sensor depends only on the state of the lattice in some small neighborhood of that sensor. Similarly to the number of control parameters $n_u$, the number of scalar output signals $n_y$ is bounded from below for highly symmetric target states by the observability condition. Placing sensors at the pinnings and assuming that the neighborhood only includes the pinning site itself, we conclude that $C = B^\dagger$, so that the observability condition is satisfied automatically and $n_y = n_u$. In particular, this arrangement of sensors ensures that there are no unobservable normal modes.

We illustrate the application of output feedback control again using the lattice of length $n_x = 8$. The feedback and filter gains were calculated using equations (5.53), (5.48) and (5.68), (5.70), respectively. We successfully stabilized a number of steady and time-periodic states of the model (6.10) in the presence of both the process noise and measurement errors (measurement errors were assumed to be random, independent and uniformly distributed in the interval $[-\sigma_v, \sigma_v]$, similar to the process noise). The difference $\Delta\tilde{\mathbf{x}}^t$ between the actual and the reconstructed state of the system is plotted in figure 6.4(a) for the target state S8T4 with moderate level of noise, while figure 6.4(b) shows the deviation $\sigma_x^t$ from the same target state and the estimation

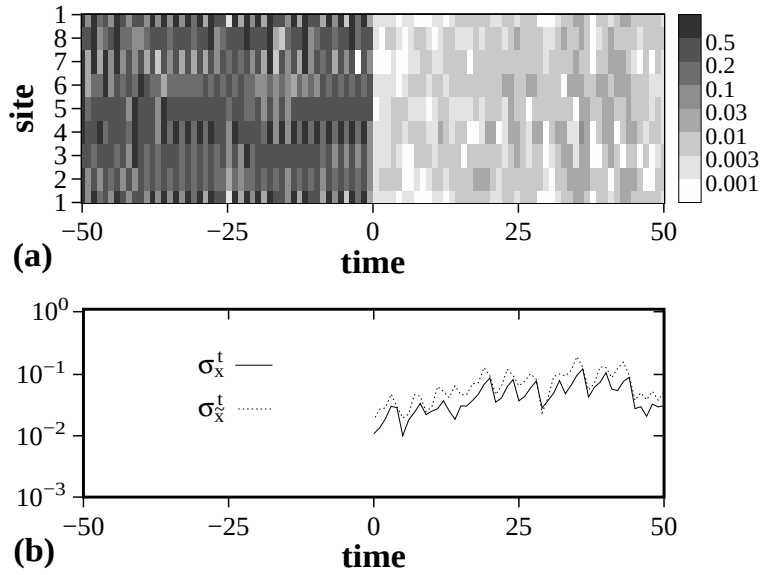


Figure 6.8: Output feedback control of the periodic state S8T4 with noise and imperfect measurements: (a) difference $\Delta\tilde{\mathbf{x}}^t$ between the actual and the estimated system state, (b) deviation $\sigma_x^t$ from the target state and the reconstruction error $\sigma_{\tilde{x}}^t$. The amplitudes of the process noise and measurement errors are $\sigma_w = 10^{-3}$ and $\sigma_v = 10^{-5}$. Feedback and filtering are turned on simultaneously at $t = 0$.

error

$$\sigma_{\tilde{x}}^t = \left[ \frac{1}{n_x} \sum_{i=1}^{n_x} |\Delta\tilde{x}_i^t|^2 \right]^{1/2} . \tag{6.24}$$

## 6.5 Density of Pinnings

### 6.5.1 Lattice Partitioning

To facilitate practical implementation, the control algorithm presented above should be easily extendable to systems of arbitrary size. However, even though it is theoretically possible to control the deterministic coupled map lattice of any length using just two pinning sites, practical limitations require the introduction of additional pinning sites as the length of the lattice grows. Since the total number of pinnings changes, when the lattice becomes large, it makes more sense to talk about the minimal density of pinnings, or the maximal number of lattice sites per pinning, that allows successful control under given conditions.

Furthermore, since coupling between lattice sites is local, the feedback $u_m^t$ only affects the dynamics of the sites $i$ which are sufficiently close to the pinning site $i_m$.

Conversely, we expect the feedback $u_m^t$ to be essentially independent of the state of the lattice sites $i$ far away from the pinning $i_m$. Using this observation allows one to simplify the construction of the control scheme substantially by explicitly defining the neighborhood of each pinning $i_m$ that contributes to, and is affected by, the feedback $u_m^t$. We thus naturally arrive at the idea of distributed control.

By arranging the pinnings regularly we ensure that the lattice is partitioned into a number of identical subdomains of length $n_d \ll n_x$, described by identical evolution equations. To simplify the analysis we assume that each subdomain contains the minimal number of pinning sites, i.e., two. Placing the pinnings at the boundaries of subdomains allows one to choose boundary conditions for each of the subdomains at will, so we assume that boundary conditions are periodic. This effectively decouples adjacent subdomains, which can now be treated independently (one should understand that this is only true for a one-dimensional lattice with one state variable per site, and the generalization to more complicated cases could be highly nontrivial). The general problem of controlling the lattice of arbitrary length $n_x$ is thus reduced to the simpler problem of controlling the lattice of fixed length $n_d$ with two pinning sites, which was studied in detail in the preceding sections.

Indeed, let the domain span the sites $i_1$ through $i_2 = i_1 + n_d - 1$ of the lattice. Then arbitrary boundary conditions

$$\begin{aligned} x_{i_1-1}^t &= \psi_1(x_{i_1}^t, \cdots, x_{i_2}^t), \\ x_{i_2+1}^t &= \psi_2(x_{i_1}^t, \cdots, x_{i_2}^t) \end{aligned} \tag{6.25}$$

can be imposed by adjusting the feedback as follows:

$$\begin{aligned} \Delta u_1^t &\rightarrow \Delta u_1^t + \epsilon f(\psi_1(x_{i_1}^t, \cdots, x_{i_2}^t)) - \epsilon f(x_{i_1-1}^t), \\ \Delta u_2^t &\rightarrow \Delta u_2^t + \epsilon f(\psi_2(x_{i_1}^t, \cdots, x_{i_2}^t)) - \epsilon f(x_{i_2+1}^t), \end{aligned} \tag{6.26}$$

which only requires the knowledge about the state of the system inside the subdomain and at two adjacent sites $i_1 - 1$ and $i_2 + 1$. If the exact form of the evolution equation (6.10) is not known, the linearization of the rule (6.26) can be used instead. The nonlinear version, however, has a significant additional benefit associated with it:

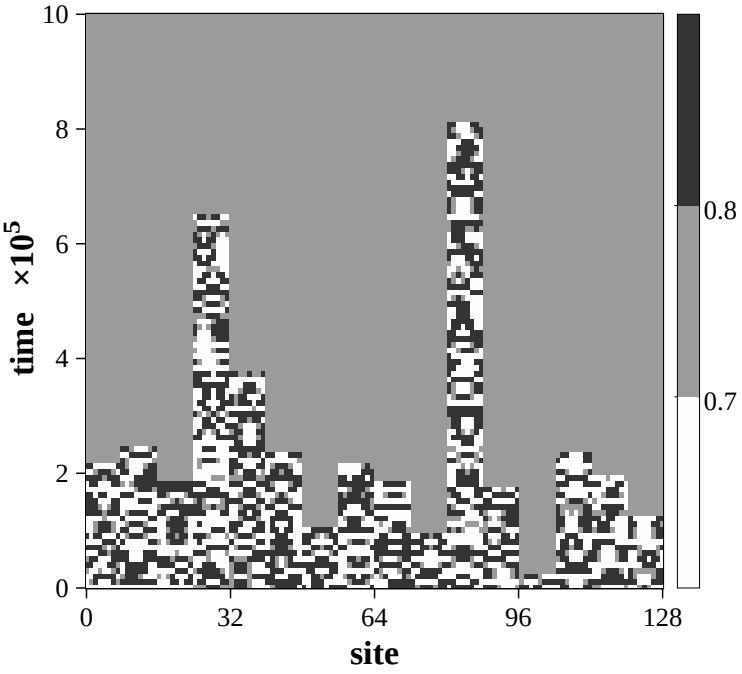


Figure 6.9: Stabilizing steady uniform state: a large lattice ($n_x = 128$) is controlled by an array of double pinning sites, placed at the boundaries of subdomains with length $n_d = 8$. The state of the system was plotted at each $10^4$th step.

nonlinear decoupling of adjacent subdomains dramatically decreases the capture time by decreasing the effective dimensionality of the system.

We demonstrate the effectiveness of nonlinear decoupling by stabilizing the target state S1T1 of the CML defined by equations (6.10), (6.13) and (6.14) with $a = 4.0$ and $\epsilon = 0.33$. The lattice with $n_x = 128$ sites was divided into subdomains of length $n_d = 8$, each controlled by two pinning sites placed at the boundaries. The results presented in figure 6.5.1 show the evolution of the system from the initial condition chosen to be a collection of random numbers in the interval $[0, 1]$. The average time to achieve control in each of the subdomains, $t_c$, is seen to be of order $10^5$ iterations even though the subdomains were chosen relatively small. In general, $t_c$ grows exponentially with the pointwise dimension of the attractor, $t_c \propto (\delta x)^{-n_x^p}$, and, since $n_x^p \propto n_d$ for large $n_d$, the time $t_c$ can become prohibitively large, imposing restrictions on the largest size of the subdomain.

The major factor limiting our ability to locally control arbitrarily large systems with local interactions, however, is noise. The strength of noise and the values of

system parameters determine the maximal length $\bar{n}_x$ of the lattice that can be controlled with two pinnings placed at the boundaries, which subsequently defines the minimal density of pinning sites $\rho = 2/\bar{n}_x$. It is interesting to note that, at least for the target state S1T1, the length $\bar{n}_x$ can be estimated analytically with a rather good precision using the conditions of controllability and observability, highlighting their fundamental role in the control problem.

### 6.5.2 State Feedback

First, assume that the state of the system can be determined directly at any time, so that state feedback control can be used. In the deterministic case the controllability condition determines whether there exists a control sequence $\Delta\mathbf{u}^{t_i}, \cdots, \Delta\mathbf{u}^{t_f-1}$, bringing an arbitrary initial state $\Delta\mathbf{x}^{t_i}$ to an arbitrary final state $\Delta\mathbf{x}^{t_f}$, where $t_f = t_i + n_x$. In the presence of noise and without assuming any functional relationship between the state and the feedback we can write

$$\Delta\mathbf{x}^{t_i+n_x} = (A)^{n_x}\Delta\mathbf{x}^{t_i} + \sum_{k=1}^{n_x}(A)^{n_x-k}B\Delta\mathbf{u}^{t_i+k-1} + \sum_{k=1}^{n_x}(A)^{n_x-k}E\mathbf{w}^{t_i+k-1}. \tag{6.27}$$

This equation is not exact, it is only an approximation of the exact nonlinear evolution equation (6.10), valid when both $\Delta\mathbf{x}^t$ and $\Delta\mathbf{u}^t$ are sufficiently small for all times $t = t_i, \cdots, t_f - 1$, as discussed in section 5.3.1. The linearization (5.39) on which equation (6.27) is based is valid for arbitrary $\Delta\mathbf{u}^t$. However, since the perturbation $\Delta u_m^t$ is defined as the change in $x_{i_m}^t$ due to the control action, its magnitude is limited by nonlinearities to the same range $\delta x$ as the local deviation $\Delta x_i^t$ from the target state. Therefore, the control sequence should satisfy both equation (6.27) and the restriction

$$|\Delta u_m^t| < \delta x, \quad m = 1, 2, \quad t = t_i, \cdots, t_f - 1. \tag{6.28}$$

Taking $\Delta\mathbf{x}^{t_i} = \Delta\mathbf{x}^{t_f} = \mathbf{0}$ (the initial and final states coincide with the target state) equation (6.27) can be rewritten as

$$\mathbf{z} = -\sum_{k=1}^{n_x}(A)^{n_x-k}E\mathbf{w}^{t_i+k-1} = \mathbf{0} + \sum_{k=1}^{n_x}\sum_{m=1}^{2}(A)^{n_x-k}\mathbf{b}_m\,\Delta u_m^{t_i+k-1}, \tag{6.29}$$

which is formally equivalent to the problem of finding the feedback sequence bringing the system from the initial state $\Delta\mathbf{x}_i = \mathbf{0}$ to the final state $\Delta\mathbf{x}_f = \mathbf{z}$ in $n_x$ steps in the absence of noise.

Again we assume that the process noise $\mathbf{w}^t$ is represented by a vector whose components $w_i^t$ are independent random variables uniformly distributed in the interval $[-\sigma_w, \sigma_w]$. Noise is amplified roughly by a factor of $\lambda$ per iteration, where $\lambda$ is the largest eigenvalue (6.17) of the Jacobian ($\lambda = \alpha$ for $\epsilon \leq 0.5$ and $\lambda = (1 - 4\epsilon)\alpha$ for $\epsilon > 0.5$). As a consequence, the left-hand side of equation (6.29) can also be represented as a vector with random components $z_i$ distributed in the interval $[-\beta\sigma_w, \beta\sigma_w]$, where

$$\beta = \sum_{t=0}^{n_x-1} |\lambda|^t \approx \frac{|\lambda|^{n_x}}{|\lambda| - 1}. \tag{6.30}$$

It could be argued that for the control to suppress any sequence of random perturbations $\mathbf{w}^t$, every term $(A)^{n_x-k}\mathbf{b}_m\,\Delta u_m^{t_i+k-1}$ on the right-hand side of equation (6.29) should be of the same order of magnitude as the "worst case" amplified noise $\mathbf{z}$. The vector $\mathbf{b}_m\,\Delta u_m^{t_i+k-1}$ represents local perturbation $\delta x_{i_m}^t = \Delta u_m^{t_i+k-1}$ introduced at the site $i_m$ at time $t = t_i + k - 1$, while the matrix $(A)^{n_x-k}$ describes the propagation of that perturbation throughout the lattice. According to the structure of the matrix $A$, local perturbation at site $i_m$ affects the dynamics of the remote site $j$ only after propagating a distance $l = |i_m - j|$ in time $\Delta t = l$, decaying (or being amplified) by a factor of $\alpha\epsilon$ per iteration. Consequently, the state of site $j$ at time $t_f$ will be affected by control $\Delta u_m^t$ applied only at times $t_i, \cdots, t_i + n_x - l - 1$. The perturbation applied at $t = t_i + n_x - l - 1$ is amplified the least and, therefore, one obtains the following order of magnitude relation

$$\delta x = O\left((\alpha\epsilon)^{-l}\beta\sigma_w\right). \tag{6.31}$$

Due to the periodic boundary condition, $0 \leq l \leq n_x/2$. For weak coupling, $\epsilon < |\alpha|^{-1}$, the propagating perturbation *decays* exponentially in magnitude, so the strength of feedback is ultimately determined by the largest distance the signal has to travel, and we should take $l = n_x/2$ in (6.31). On the contrary, for strong coupling, $\epsilon \geq |\alpha|^{-1}$, the propagating perturbation is *amplified* and, therefore, suppressing local noise requires

the strongest feedback, setting $l = 0$.

On the other hand, $\delta x$ can be estimated by equating the magnitude of the linear term with the magnitude of the next nonlinear term in the Taylor expansion of the local map function:

$$f(\bar{x} + \delta x, a) = f(\bar{x}, a) + \kappa(\delta x + \mu(\delta x)^2 + \cdots). \tag{6.32}$$

For instance, the logistic map (6.14) gives $\delta x \sim \mu^{-1} = 2\bar{x} - 1 = 1 - 2a^{-1}$. As a result, we obtain the following estimate on the size of the controllable domain for an arbitrary coupled map lattice with the quadratic nonlinearity:

$$\bar{n}_x^{(1)}(\sigma_w) = -\frac{\ln(\mu\sigma_w) + \ln(\xi)}{\ln(\zeta)}, \tag{6.33}$$

which is rather similar to the estimates obtained by Auerbach [28] and Aranson *et al.* [67] for the lattice with asymmetric coupling. Parameters $\xi$ and $\zeta$ in (6.33) are defined thus: $\xi = (|\lambda| - 1)^{-1}$, while $\zeta = |\lambda||\alpha\epsilon|^{-1/2}$ for $\epsilon < |\alpha|^{-1}$ and $\zeta = |\lambda|$ for $\epsilon \geq |\alpha|^{-1}$. We should note that the estimate obtained for $|\alpha| = 2$ in [14] was derived in the assumption of strong local instability, $|\alpha| \gg 1$, and (6.33) reduces to it in the limit $\mu = 1$ and $\xi = 1$.

Another method for the calculation of $\bar{n}_x(\sigma_w)$ was proposed by Egolf and Socolar [68], who suggested to use the actual feedback gain matrix $K$ to obtain more precise results for a specific control scheme. As we have seen in section 5.3.2, when a linear system is perturbed by the noise of amplitude $\sigma_w$, one can estimate the average deviation from the target trajectory as $\sigma_x = \nu\sigma_w$, where $\nu$ is the noise amplification factor defined by (5.45). Regarding the nonlinearity as the additional source of noise, one can instead write

$$\sigma_x = \nu(\sigma_w^2 + \sigma_{xx}^2)^{1/2}, \tag{6.34}$$

where $\sigma_{xx}$ is the error resulting from ignoring the effect of nonlinear terms in equation (5.39). For a coupled map lattice with the quadratic nonlinearity one obtains $\sigma_{xx} = \mu\sigma_x^2$ and thus

$$\sigma_x^2 = \nu^2(\sigma_w^2 + \mu^2\sigma_x^4). \tag{6.35}$$

This is a quadratic equation in $\sigma_x^2$ which has solutions only when

$$\nu \leq \bar{\nu}(\sigma_w) = (2\mu\sigma_w)^{-1/2}, \tag{6.36}$$

thus determining the critical noise amplification factor. For $\nu > \bar{\nu}(\sigma_w)$ the effect of nonlinear terms can no longer be ignored and the control scheme breaks down. In principle, one can stop here and numerically evaluate the length of the system at which $\nu = \bar{\nu}(\sigma_w)$, thus obtaining the required functional dependence $\bar{n}_x(\sigma_w) = n_x(\bar{\nu}(\sigma_w))$ for a specific $K$.

However, making one more step allows one to easily extract the analytic dependence on the strength of noise. It can be argued that for any $K$ the noise amplification factor depends exponentially on the length of the system

$$\nu = \chi\eta^{n_x}, \tag{6.37}$$

where both $\chi$ and $\eta$ are functions of the system parameters $\alpha$ and $\epsilon$ and the feedback gain matrix $K$. Substituting (6.36) into (6.37) yields the final result in the form similar to equation (6.33):

$$\bar{n}_x^{(2)}(\sigma_w) = -\frac{\ln(\mu\sigma_w) + \ln(2\chi^2)}{\ln(\eta^2)}. \tag{6.38}$$

Two important conclusions can be drawn from this result. First of all, even though the length $\bar{n}_x$ does depend on a particular choice of the feedback gain, this dependence is rather weak, because it is attenuated by the logarithmic function, so that the obtained estimate is valid for any typical feedback gain that stabilizes the system. Second, the dependence on the strength of noise is also logarithmic and weak; however, the magnitude of $\sigma_w$ is that crucial parameter that ultimately determines the scale for the length $\bar{n}_x$ and, consequently, the minimal density of pinning sites $\rho$.

The maximal length of the system that can actually be stabilized by the linear-quadratic control method with two pinning sites placed at the boundaries can be obtained numerically by choosing the target state as the initial condition and monitoring the evolution of the closed-loop system in the presence of process noise $\mathbf{w}^t$ of amplitude $\sigma_w$, applying feedback calculated using the formula (5.37) with $Q = I$ and

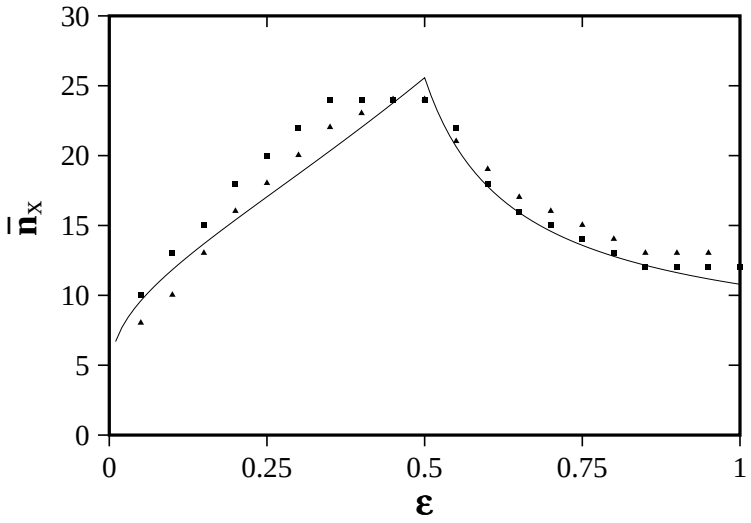


Figure 6.10: The largest length of the lattice which can be stabilized with two pinning sites using state feedback control: theoretical estimates $\bar{n}_x^{(1)}$ (solid line) and $\bar{n}_x^{(2)}$ (triangles), and numerical results (squares) obtained with the process noise of amplitude $\sigma_w = 10^{-8}$ as functions of coupling $\epsilon$ for $a = 4.0$.

$R = 0$. As seen from figure 6.5.2, this length is quite large for a moderate level of noise and is rather close to the values where the controllability breaks down according to (6.33). The agreement between the numerical results and theoretical estimates (6.33) and (6.38) is not perfect, although it is surprisingly good taking into account the order of magnitude arguments used in the derivations. The choice of the noise level was motivated by the need to separate the effect of the deviations $\sigma_{xx}$ introduced by the nonlinearity from the precision of numerical calculations $\sigma_n = O(10^{-16})$ in the evaluation of the feedback gain. Since, according to (6.34), $\sigma_w/\sigma_{xx} = O(1)$ when linear control breaks down, one needs $1 \gg \sigma_w \gg \sigma_n$, so $\sigma_w = 10^{-8}$ was taken here (as opposed to $\sigma_w = 10^{-14}$ used in [14]).

As expected, the minimal density of pinning sites is reduced substantially by replacing equally spaced single pinnings with equally spaced paired pinnings. For the uniform steady target state S1T1, $a = 4.0$ and $\epsilon = 0.4$, for example, the estimate (6.33) gives $\rho_2 = 2/n_d = 1/11$ for the noise level $\sigma_w = 10^{-8}$ (the actual value of $1/12$ is even lower as seen from figure 6.5.2). If single pinnings are used instead, equation (6.19) demands $\rho_1 = 1/n_d = 1/2$ even in the absence of noise, which is much higher than $\rho_2$.

### 6.5.3 Output Feedback

Finally, consider the output feedback control of the target state S1T1. Let us assume that the state of the system cannot be determined directly. Instead it has to be reconstructed using the measurements at the pinnings, i.e., using the time series of the lattice variables $x^t_{i_1}$ and $x^t_{i_2}$. As we noted in section 6.4, this setup dictates that $C = B^\dagger$ in (5.69). To avoid unnecessarily complicating the problem we also assume that the measurements are perfect, $\mathbf{v}^t = \mathbf{0}$.

In order to estimate $\bar{n}_x$ with these assumptions we will need to exploit both the controllability and the observability conditions. First, the state of the system has to be reconstructed using $n_x$ consecutive measurements of the variables at the pinning sites. However, because of the nonzero process noise the reconstructed state will deviate from the actual state. Arguments similar to the ones used in deriving (6.31) allow one to estimate the order of magnitude of the reconstruction error at a lattice site with distance $l$ to the closest pinning:

$$\delta\tilde{x}_l = O\left((\alpha\epsilon)^{-l}\beta\sigma_w\right). \tag{6.39}$$

Since the reconstruction error $\delta\tilde{x}_l$ is substantially larger than the strength of noise $\sigma_w$, the former has to be substituted for the latter in (6.31) yielding

$$\delta x = O\left((\alpha\epsilon)^{-2l}\beta^2\sigma_w\right). \tag{6.40}$$

Eventually, we obtain the following estimate of the maximal size:

$$\bar{n}^{(3)}_x(\sigma_w) = -\frac{\ln(\mu\sigma_w) + \ln(\xi^2)}{2\ln(\zeta)} \approx \frac{\bar{n}^{(1)}_x(\sigma_w)}{2}, \tag{6.41}$$

i.e., one half of the size of the lattice that can be stabilized using state feedback. This result can be understood intuitively: when output feedback is used, a signal in the system has to travel twice the distance in twice the time, first from a remote lattice site to the pinnings, carrying information about the state of the system, and then back in the form of feedback. This is effectively equivalent to doubling the size of the lattice, hence the factor of one half.

The same result can be obtained using the noise amplification factor. Observing that, according to our assumptions $A^\dagger = A$, $\hat{R} = 0$, and $\hat{Q} = (\sigma_w^2/3)EE^\dagger$, we conclude that the filter gain and the feedback gain calculated for $R = 0$ and $Q = qEE^\dagger$ are directly related[1], $\hat{K} = K^\dagger$, as are the solutions of the respective Riccati equations, $S = P$. Therefore, the evolution equation (5.61) for the reconstruction error reduces to

$$\Delta\tilde{\mathbf{x}}^{t+1} = (A - BK)^\dagger \Delta\tilde{\mathbf{x}}^t + E\mathbf{w}^t. \tag{6.42}$$

Comparing (6.42) with the evolution equation (5.42) for the closed-loop system, we conclude that the noise amplification factor of the filter is equal to that of the controller, $\tilde{\nu} = \nu$. Since both the process noise and the deviation caused by nonlinear terms are amplified first by the filtering and then by the feedback, (6.34) has to be modified to read

$$\sigma_x = \tilde{\nu}\nu(\sigma_w^2 + \sigma_{xx}^2)^{1/2}, \tag{6.43}$$

with the subsequent change in the condition determining when the linear control breaks down:

$$\bar{\nu}(\sigma_w) = (2\mu\sigma_w)^{-1/4}. \tag{6.44}$$

Substituting this result into (6.37) yields

$$\bar{n}_x^{(4)}(\sigma_w) = -\frac{\ln(\mu\sigma_w) + \ln(2\chi^4)}{2\ln(\eta^2)} \approx \frac{\bar{n}_x^{(3)}(\sigma_w)}{2}. \tag{6.45}$$

We compare the theoretical predictions (6.41) and (6.45) with the actual numerical results for the CML subjected to the noise of amplitude $\sigma_w = 10^{-8}$ in figure 6.5.3. The target state S1T1 is stabilized using output feedback control (5.70), where the feedback gain $K$ is calculated using (5.37) with $Q = I$ and $R = 0$ and the filter gain is set to $\hat{K} = K^\dagger$. Once again we conclude that, similarly to the state feedback case, the numerical results are in very good agreement with the theoretical estimates based on the assumption that the breakdown of linear control is caused by the interplay between the stochasticity and the nonlinearity of the evolution equation (6.10).

A comment should be made regarding the placement of sensors on the lattice. We

[1] This is a general result: as long as $A = A^\dagger$ and $C = B^\dagger$, taking $\hat{K} = K^\dagger$ guarantees that the filter is stable even if the feedback gain $K$ is not optimal.

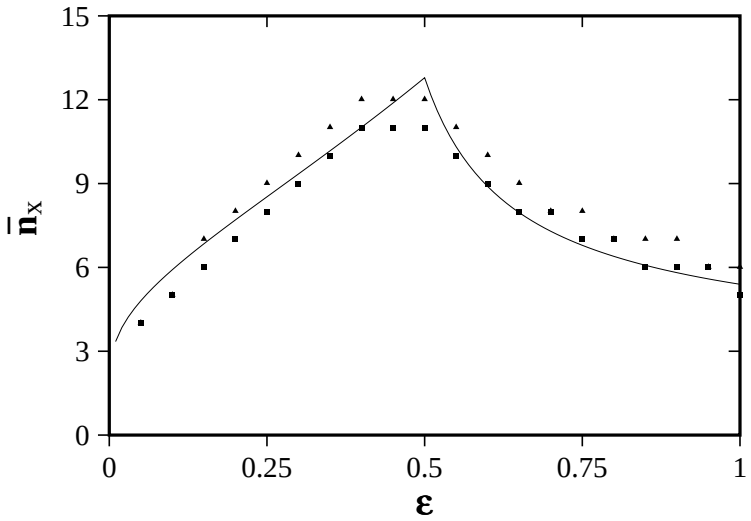


Figure 6.11: The largest length of the lattice which can be stabilized with two pinning sites using output feedback control: theoretical estimates $\bar{n}_x^{(3)}$ (solid line) and $\bar{n}_x^{(4)}$ (triangles) and numerical results (squares) obtained with the process noise of amplitude $\sigma_w = 10^{-8}$ as functions of coupling $\epsilon$ for $a = 4.0$. The measurement errors were assumed to be negligible.

have already established that the pinning control is most sensitive to the state of the system at sites furthest from the pinnings. It is, therefore, advantageous to place the sensors as far from the actuators as possible. In particular, in case of control at the boundaries the optimal location for the sensors is the middle of the lattice. This turns out to be a rather general result which cannot be explained by either the observability or the controllability condition alone, only by their interaction.

# Chapter 7 Conclusions

Reviewing the results obtained in this thesis we see that the problem of controlling chaos in symmetric systems in general, and spatiotemporal chaos in extended systems in particular, can be split into three major parts: symmetry analysis, system identification (if the model equations are not available *a priori*), and controller synthesis. The first part consists of analyzing how the symmetry related degeneracies of evolution operators affect the control algorithm. The results of this analysis are then used in the second part to obtain symmetry preserving model equations describing the local dynamics of the system in the vicinity of the target state. Finally, in the third part the model equations and the structure of the controller determined in the first part are used to find the optimal feedback driving the system towards the target state.

The first and the most important conclusion of our theoretical analysis can be summarized thus: if the system under consideration is symmetric, as are most of extended chaotic systems, it cannot be considered generic with respect to conventional chaos control techniques, and its symmetry properties should be understood prior to constructing a control scheme, even if the symmetry is only approximate. The failure to observe the restrictions imposed by the symmetry on the structure of the measured output signal will usually prevent the experimental reconstruction of the system dynamics. Similarly, an inappropriate choice of control parameters will result in weak controllability and, as a result, extreme sensitivity to noise, or even worse, complete loss of control.

From the practical point of view, the main result of the symmetry analysis is that the minimal number of independent control parameters required for control, as well as the minimal number of independent scalar observables required for the reconstruction of local dynamics, can typically be determined without any knowledge of the evolution equations governing the dynamics of the system. One only needs to know the symmetry properties, such as spatial and temporal periodicity, of the target state, and

the structural symmetry of the dynamical equations, which in the case of extended chaotic systems is often uniquely defined by the geometry of the underlying physical space. One should, however, realize that this typical pattern does not apply to all symmetric systems without exception. The dynamical equations might, in principle, be symmetric with respect to transformations unrelated to "geometrical" symmetries, such as rotational, reflectional, or translational invariance. Additional "nonphysical" symmetries can also be introduced as a result of the linearization procedure.

A number of comments have to be made regarding accidental degeneracies. We found that when accidental degeneracies are present, restrictions obtained using symmetry considerations alone provide only the necessary conditions for controllability. In particular, one obtains a lower bound on the minimal number of control parameters. Exact determination of that number in this case requires additional information about the structure of the Jacobian matrix, which can be gathered using experimental reconstruction. On the other hand, experimental reconstruction itself is only possible, if there is an adequate number of independent scalar observables. This number, however, is similarly undetermined. In practice, though, one rarely has to worry about such complications, since accidental degeneracies are not common and unlikely to be a problem for most actual experimental systems. Besides, an estimate for the minimal number of observables and control parameters can always be easily obtained using combinatorial arguments. Also, one should be careful in equating the minimal number of observables or control parameters with the highest degeneracy of the Jacobian matrix, especially if this degeneracy is at least partially accidental. It can be argued that accidental degeneracies between eigenvalues from the same irreducible invariant subspace typically will not increase the dimensionality of the respective eigenspace and, therefore will not lead to additional degeneracy in the local dynamics.

We also established that it is not enough to find an adequate number of control parameters (or observables). These control parameters (observables) have to satisfy certain conditions. In particular, perturbation of the control parameters should completely break the dynamical symmetry. The more strict independence condition is specific to each target trajectory and, on the one hand, requires the knowledge of the system's response to variation of different control parameters (which can be obtained

experimentally, if necessary), but, on the other hand, allows one to choose the minimal set of control parameters systematically, avoiding trial and error search. For example, in case of extended dynamical systems with local feedback the independence condition usually imposes restrictions on the mutual arrangement of pinning sites, while the number of pinning sites is determined by the number of control parameters.

The conventional approach to system identification has to be modified in the presence of symmetries. In particular, in order to preserve not only the topology of the original attractor, but also the symmetry of the original dynamical equations, one has to use a number of simultaneously measured observables, which have to be the components of an equivariant vector function of the actual state of the system. The restrictions on the output can be relaxed somewhat in the case of local reconstruction in the vicinity of some target trajectory. However, even then a number of independent observables should be used instead of just a single one, as long as the symmetry of the target state is nontrivial, leading to the increase in the dimension of the embedding space. Otherwise, the conventional approach carries over with minor modifications.

A number of more specific conclusions can be made concerning extended chaotic systems. The analysis of the simplified model system containing the defining features of a general spatially extended dynamical system suggests that the localized control of spatiotemporal chaos, which assumes that the system is monitored and perturbed at a number of distinct spatial locations (pinnings), is quite convenient not only from the theoretical point of view (this approach significantly simplifies the analysis of the interaction between the system and the controller), but also from the practical point of view. Indeed, we have argued that in the experimental setting it is usually much easier to both apply feedback and extract information about the system locally, which is crucial for practical implementation of control methods based on this approach. Besides, as we have learned from the study of the model system, localized control is quite effective in stabilizing a variety of unstable periodic orbits. Equally important from the practical standpoint, one can track target trajectories as system parameters slowly change, or switch between different trajectories by changing feedback *without* changing either the density or the location of pinnings.

We determined that in order to make the target state controllable, the pinning

sites should be arranged properly. Choosing this arrangement in accordance with the underlying symmetries of the system affords a significant reduction of the complexity with simultaneous increase in the flexibility of the control algorithm, allowing it to control target states with arbitrary spatiotemporal properties, while at the same time requiring a smaller density of pinnings per unit volume of the system. Generally speaking, the pinning sites should be arranged such that there are no uncontrollable normal modes. For instance, in case of systems with translational and reflectional invariance, the pinnings *should not* be arranged in a periodic array. One particular arrangement deserves special attention. We determined that, if the noise is sufficiently weak, or the system size is sufficiently small, even highly symmetric spatially extended systems can be controlled by dynamically adjusting the boundary conditions. This can be considered as a "nonintrusive" control that requires minimal modification of the controlled system and can be implemented rather easily in a variety of applications.

The density of pinning sites required to achieve control depends on many factors. Perhaps surprisingly, although there is a minimal *number* of pinning sites, their minimal *density* is not bounded from below — in the absence of noise an extended system of arbitrary size can, in principle, be controlled using the number of pinning sites equal to the minimal number of control parameters, which is determined by the symmetry properties alone. (In practice certain restrictions appear due to the fact that the volume of the basin of attraction shrinks exponentially with increasing size of the system.) However, when noise appears, the minimal density of pinning sites depends on the strength of noise (as well as parameters of the system and the type of feedback control method used). Generally, strongly chaotic and weakly coupled systems will require a higher density of pinning sites than weakly chaotic and strongly coupled systems. Conversely, the maximum level of noise tolerated by control depends on the density (and mutual arrangement) of pinnings and increases with the density of pinnings.

This brings us to the final ingredient of a general control algorithm applicable to extended spatiotemporally chaotic systems — the feedback control method. As a rule, practical considerations call for more than just stabilization of a target trajectory

with desired properties. Additional and very significant benefits can be obtained by maximizing the domain of attraction in the deterministic case or by minimizing the noise amplification factor in the stochastic case. Both of these goals call for optimal feedback control. In fact, the numerical results obtained indicate that compared with conventional chaos control techniques, optimal control techniques are able to tolerate higher levels of noise and have shorter transient periods when the system wanders throughout the chaotic attractor before being captured by linear control in the vicinity of the target trajectory. The difference in performance becomes especially significant for large and weakly coupled extended chaotic systems. As a result, by using optimal feedback control one can considerably reduce the density of pinnings, thus simplifying the issue of practical implementation.

Summarizing, we can suggest the following sequence of steps in constructing a control scheme for an experimental extended chaotic system. First the symmetry properties of the system and the target state should be analyzed. The results of this analysis should be used to determine the number and mutual arrangement of sensors and actuators. The locations of the actuators should not necessarily coincide with the locations of the sensors, as was assumed in the analysis of the model system. In fact, it is usually undesirable to place the sensors at or close to the actuators. If the symmetry is too low to determine the spatial structure of the controller completely, additional information about the structure of the system Jacobian should be gathered using trial and error experimental reconstruction. The time series measurement of the sensors' output should then be used for local reconstruction of the system dynamics in the vicinity of the target state using the delay coordinate embedding. Finally, the optimal feedback should be found based on the above information using either the linear-quadratic or the worst case control technique.

# Bibliography

[1] C. Lee, J. Kim, D. Bobcock and R. Goodman, Phys. Fluids, **9**, 1740 (1997).

[2] A. Pentek, J. B. Kadtke, and Z. Toroczkai, Phys. Lett. A **224**, 85 (1996).

[3] V. Petrov, M. F. Crowley, and K. Showalter, Physica D **84**, 12 (1995).

[4] A. Garfinkel, M. L. Spano, W. L. Ditto, and J. N. Weiss, Science, **257**, 1230 (1992).

[5] S. J. Schiff, K. Jerger, D. H. Duong, T. Chang, M. L. Spano, and W. L. Ditto, Nature, **370**, 615 (1994).

[6] A. Hjelmfelt and J. Ross, J. Phys. Chem. **98**, 1176 (1994).

[7] M. E. Bleich, D. Hochheiser, J. V. Moloney, and J. E. S. Socolar, Phys. Rev. E **55**, 2119 (1997).

[8] C. Lourenco and A. Babloyantz, Int. J. Neu. Sys, **7**, 507 (1996).

[9] V. Petrov, M. J. Crowley, and K. Showalter, Phys. Rev. Lett. **72**, 2955 (1994).

[10] M. Ding, W. Yang, V. In, W. L. Ditto, M. L. Spano, and B. Gluckman, Phys. Rev. E **53**, 4334 (1996).

[11] J. Warncke, M. Bauer, and W. Martienssen, Europhys. Lett. **25**, 323 (1994).

[12] M. A. Rhode, J. Thomas, and R. W. Rollins, Phys. Rev. E **54**, 4880 (1996).

[13] R. O. Grigoriev and M. C. Cross, Phys. Rev. E **57**, 1550 (1998).

[14] R. O. Grigoriev, M. C. Cross, and H. G. Schuster, Phys. Rev. Lett. **79**, 2795 (1997).

[15] G. Hu and Z. Qu, Phys. Rev. Lett. **72**, 68 (1994).

[16] G. Hu and K. He, Phys. Rev. Lett. **71**, 3794 (1993).

[17] F. J. Romeiras, C. Grebogi, E. Ott, and W. P. Dayawansa, Physica D **58**, 165 (1992).

[18] V. Petrov, E. Mihaliuk, S. K. Scott, and K. Showalter, Phys. Rev. E **51**, 3988 (1995).

[19] E. Tziperman, H. Scher, S. E. Zebiak, and M. A. Cane, Phys. Rev. Lett. **79**, 1034 (1997).

[20] L. Ljung, *System Identification — Theory for the User* (Prentice-Hall, Englewood Cliffs, NJ, 1984).

[21] V. Petrov, S. Metens, P. Borckmans, G. Dewel, and K. Showalter, Phys. Rev. Lett. **75**, 2895 (1995).

[22] D. Battogtokh, A. Preusser, and A. Mikhailov, Physica D **106**, 327 (1997).

[23] P. Parmananda, M. Hildebrand, and M. Eiswirth, Phys. Rev. E **56**, 239 (1997).

[24] M. E. Bleich and J. E. S. Socolar, Phys. Rev. E **54**, R17 (1996).

[25] K. Pyragas, Phys. Lett. A **170**, 421 (1992).

[26] W. Lu, D. Yu, and R. G. Harrison, Phys. Rev. Lett. **76**, 3316 (1996).

[27] L. Kocarev, U. Parlitz, T. Stojanovski, and P. Jajić, Phys. Rev. E **56**, 1238 (1997).

[28] D. Auerbach, Phys. Rev. Lett. **72**, 1184 (1994).

[29] P. Chossat and M. Golubitsky, SIAM J. Math. Anal. **19**, 1259 (1988).

[30] P. Chossat and M. Golubitsky, Physica D **32**, 423 (1988).

[31] M. Golubitsky, I. Stewart, and D. G. Schaeffer, *Singularities and Groups in Bifurcation Theory* (Springer-Verlag, New York, 1988).

[32] M. J. Field and M. Golubitsky, *Symmetry in Chaos: A Search for Pattern in Mathematics, Art, and Nature* (Oxford Univ. Press, Oxford, 1992).

[33] N. H. Packard, J. P. Crutchfield, J. D. Farmer, and R. S. Shaw, Phys. Rev. Lett. **45**, 712 (1980).

[34] F. Takens, in *Dynamical Systems and Turbulence*, edited by D. Rand and L. S. Young (Springer-Verlag, Berlin, 1981).

[35] J.-C. Roux, R. H. Simoyi, and H. L. Swinney, Physica D **8** 257 (1983).

[36] G. Gouesbet and J. Maquet, Physica D **58**, 251 (1992).

[37] G. Rowlands and J. C. Sprott, Physica D **58**, 251 (1992).

[38] G. Fairweather, *Finite Element Galerkin Methods for Differential Equations* (Marcel Dekker, New York, 1978).

[39] G. Nitsche and U. Dressler, Physica D **58**, 153 (1992).

[40] D. P. Lathrop and E. J. Kostelich, Phys. Rev. A **40**, 4028 (1989).

[41] K. Pawelzik and H. G. Schuster, Phys. Rev. A **43**, 1808 (1991).

[42] E. J. Kostelich, Physica D **58**, 138 (1992).

[43] D. S. Broomhead and G. P. King, Physica D **20**, 217 (1986).

[44] E. Bacry, J. F. Muzy, and A. Arneodo, J. Stat. Phys. **70**, 635 (1993).

[45] I. Triandaf and I. B. Schwartz, Phys. Rev. E **56**, 204 (1997).

[46] E. Barreto and C. Grebogi, Phys. Rev. E **52**, 3553 (1995).

[47] M. Locher and E. R. Hunt, Phys. Rev. Lett. **79**, 63 (1997).

[48] J.-P. Eckmann and D. Ruelle, Rev. Mod. Phys. **57**, 617 (1985).

[49] G. P. King and I. Stewart, Physica D **58**, 216 (1992).

[50] J. E. Rubio, *The Theory of Linear Systems* (Academic Press, New York, 1971).

[51] K. Zhou, J. C. Doyle, and K. Glover, *Robust and Optimal Control* (Prentice Hall, New Jersey, 1995).

[52] J. P. Elliott and P. G. Dawber, *Symmetry in Physics* (The Macmillan Press Ltd., London, 1979).

[53] J. F. Lindner and W. L. Ditto, Appl. Mech. Rev. **48**, 795 (1995).

[54] E. Ott, C. Grebogi, and J. A. Yorke, Phys. Rev. Lett. **64**, 1196 (1990).

[55] W. L. Ditto, S. N. Rauseo, and M. L. Spano, Phys. Rev. Lett. **65**, 3211 (1990).

[56] J. Starret and R. Tagg, Phys. Rev. Lett. **74**, 1974 (1995).

[57] E. R. Hunt, Phys. Rev. Lett. **67**, 1953 (1991).

[58] R. Roy, T. W. Murphy, T. D. Maier, Z. Gills, and E. R. Hunt, Phys. Rev. Lett. **68**, 1259 (1992).

[59] R. F. Stengel, *Stochastic Optimal Control: Theory and Application* (J. Wiley, New York, 1986).

[60] J. J. Hench and A. J. Laub, IEEE Trans. Auto Contr. **39**, 1197 (1994).

[61] L. M. Pecora and T. L. Carrol, Phys. Rev. Lett. **64**, 821 (1990).

[62] G. Grassi and S. Mascolo, IEEE Trans. Circuits Syst. **44**, 1011 (1997).

[63] G. E. Dullerud and S. G. Lall, *A new approach for analysis and synthesis of time varying systems*, in Proc. 1997 IEEE/CDC.

[64] H. K. Khalil, *Nonlinear systems* (Prentice Hall, New Jersey, 1996).

[65] K. Kaneko, Prog. Theor. Phys. **72**, 480 (1984).

[66] Y. S. Kwon, S. W. Ham, and K. K. Lee, Phys. Rev. E **55**, 2009 (1997).

[67] I. Aranson, D. Golomb, and H. Sompolinsky, Phys. Rev. Lett. **68**, 3495 (1992).

[68] D. A. Egolf and J. E. S. Socolar, Phys. Rev. E **57**, 5091 (1998).